E-ISSN: 3062-3227

INTERVENTIONAL CARDIOLOGY PERSPECTIVES

OFFICIAL JOURNAL OF THE SOCIETY OF CARDIOVASCULAR INTERVENTIONS

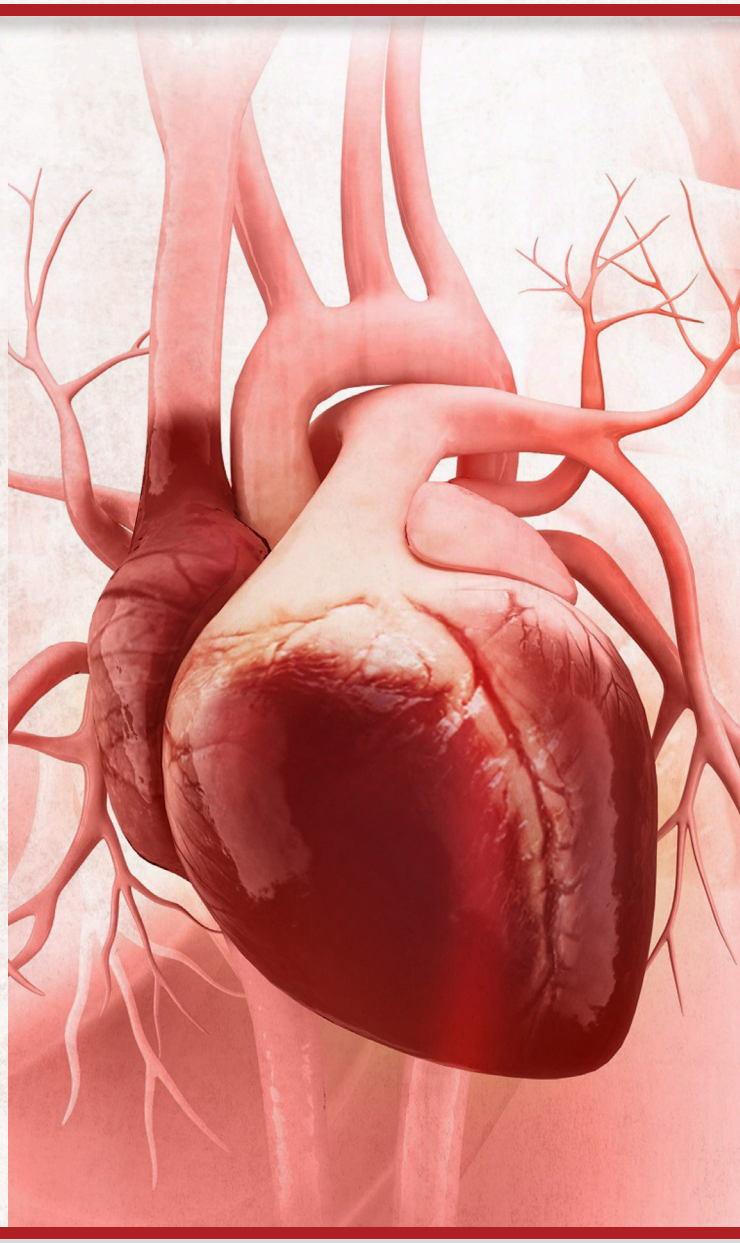

Society Of Cardiovascular INTERVENTIONS

galenos

VOLUME: 1 ISSUE: 2 AUGUST 2025

INTERVENTIONAL CARDIOLOGY PERSPECTIVES

VOLUME: 1 | ISSUE: 2 | AUGUST 2025

EDITORIAL BOARD

Please refer to the journal's webpage (**https://www.intcarper.com/**) for **"Editorial Policy"** and **"Instructions to Authors"**.

The editorial and publication process of the **Interventional Cardiology Perspectives** are shaped in accordance with the guidelines of the **ICMJE, WAME, CSE, COPE, EASE**, and **NISO**. The journal is in conformity with the Principles of Transparency and Best Practice in Scholarly Publishing. The journal is published online.

Owner: Society of Cardiovascular Interventions

Responsible Manager: Harun Kundi

Publisher Contact
Address: Molla Gürani Mah. Kaçamak Sk. No: 21/1 34093 İstanbul, Türkiye
Phone: +90 (530) 177 30 97 / +90 (539) 307 32 03
E-mail: info@galenos.com.tr/yayin@galenos.com.tr
Web: www.galenos.com.tr
Publisher Certificate Number: 14521

Publication Date: August 2025
E-ISSN: 3062-3227
International scientific journal published quarterly.

INTERVENTIONAL CARDIOLOGY PERSPECTIVES

VOLUME: 1 | ISSUE: 2 | AUGUST 2025

CONTENTS

INTERVENTIONAL CARDIOLOGY PERSPECTIVES

Inter Cardio Pers 2025;1(2):38-39

DOI: 10.4274/intercardiopers.2025.2025.070825

EDITORIAL

Interventional Cardiology: A Field of Continuous Transformation

İsmail Doğu Kılıç

Department of Cardiology, Pamukkale University Faculty of Medicine, Denizli, Türkiye

INTRODUCTION

Interventional cardiology (IC) continues to evolve rapidly—marked by relentless innovation, continuous adaptation, and a commitment to advancing the boundaries of patient care. In the coronary field, recent years have seen remarkable progress, particularly in lesion preparation and modification techniques, enabling the management of increasingly complex coronary pathology. Intravascular imaging modalities are now more widely available, offering higher resolution and improved usability across multiple platforms. Concurrently, advancements in plaque characterization are ongoing. With the refinement of microcatheters, guidewires, and adjunctive technologies—and perhaps most notably, the growing global expertise in chronic total occlusion recanalization—more operators are successfully treating occlusions that were previously deemed intractable. Drug-coated balloons exemplify this spirit of innovation. Originally validated in the treatment of in-stent restenosis, Drug-coated balloons offer a stent-free therapeutic option. More recently, their promising application in *de novo* coronary lesions[1] has opened new avenues, potentially signaling a paradigm shift in coronary intervention strategy.

The structural heart disease domain is experiencing a parallel transformation. Transcatheter aortic valve replacement, once limited to patients deemed high-risk or inoperable, has now touched the lives of many. A growing body of evidence supports its expanding use in patients at lower surgical risk.[2,3] Transcatheter edge-to-edge repair for mitral and tricuspid regurgitation is becoming increasingly commonplace. Importantly, these advances represent just a fraction of ongoing innovation. Despite that the existing devices continue to undergo refinement, novel technologies targeting the mitral, tricuspid, and pulmonary valves are progressing through preclinical development and early clinical trials.[4]

However, innovation in IC extends beyond catheters and valves. As in all facets of medicine—and indeed, daily life—digital technologies and artificial intelligence (AI) are increasingly being integrated into our field. These tools are beginning to transform imaging, diagnostics, and clinical decision-making.[5] AI-powered platforms now assist in procedural planning, whereas machine learning algorithms analyze intracoronary imaging and physiological data to offer real-time procedural guidance. Simulators enhanced by AI are improving IC training and education. Together, these advancements hold immense potential to improve procedural precision, efficiency, and ultimately, patient outcomes.[5-7] We now stand at the threshold of an era in which AI could aid in predicting procedural success, optimizing device selection, and personalizing care. Nonetheless, the promise of AI also brings new challenges. A recent study revealed that although interventional cardiologists generally have a positive outlook on AI, many feel underprepared to incorporate it into their practice. Only a small fraction currently use it in daily clinical workflows.[8] This indicates that acquiring AI competency may soon become an essential part of our professional skillset—akin to learning new interventional techniques or devices. Notably, some AI systems have already demonstrated the ability to pass IC exams. Although they still perform below IC fellows—particularly on questions requiring interpretation or nuanced clinical reasoning[9]—their ability to generate sophisticated responses is remarkable.[10] In a field defined by rapid change, it would be shortsighted to underestimate the transformative potential of AI. Crucially, AI is not here to replace clinicians, but to augment their capabilities. The future likely lies in human–AI collaboration rather than competition.[11] However, when that future arrives—which may be sooner than anticipated—it will demand that we lead with the irreplaceable human elements of care: empathy, clinical intuition, and the doctor–patient relationship. These humanistic aspects will remain essential to delivering high-quality, patient-centered care.[12] At the same time, the introduction of AI raises important ethical and regulatory considerations. Issues of data privacy, algorithmic bias, responsibility for AI-supported decisions, and the need for rigorous and transparent validation frameworks are pressing.[12,13] These concerns will continue to shape discussions around the safe and effective implementation of AI in cardiovascular medicine.

Address for Correspondence: İsmail Doğu Kılıç MD, Department of Cardiology, Pamukkale University Faculty of Medicine, Denizli, Türkiye
E-mail: idogukilic@yahoo.com **ORCID ID:** orcid.org/0000-0002-5270-3897

Publication Date: 11.08.2025

Cite as: Kılıç İD. Interventional cardiology: a field of continuous transformation. *Inter Cardio Pers.* 2025;1(2):38-39

In conclusion, the dynamic evolution of IC is both exhilarating and challenging. While we navigate the influx of novel devices, techniques, and digital tools, we must also address the complex questions they raise. This dual reality underscores the importance of lifelong learning, multidisciplinary collaboration, and ethical foresight. As the field continues to transform, our most valuable asset will be our willingness to evolve-to lead with responsibility, to embrace innovation with discernment, and to help shape the future of patient care.

REFERENCES

1. Giacoppo D, Saucedo J, Scheller B. Coronary drug-coated balloons for de novo and in-stent restenosis indications. *J Soc Cardiovasc Angiogr Interv.* 2023;2:100625.
2. Reardon MJ, Van Mieghem NM, Popma JJ, et al; SURTAVI Investigators. Surgical or transcatheter aortic-valve replacement in intermediate-risk patients. *N Engl J Med.* 2017;376:1321-1331.
3. Mack MJ, Leon MB, Thourani VH, et al.; PARTNER 3 Investigators. Transcatheter Aortic-Valve Replacement in Low-Risk Patients at Five Years. N Eng*l J Med.* 2023;389:1949-1960.
4. Ktenopoulos N, Katsaros O, Apostolos A, et al. Emerging transcatheter therapies for valvular heart disease: focus on mitral and tricuspid valve procedures. *Life (Basel).* 2024;14:842.
5. Khelimskii D, Badoyan A, Krymcov O, Baranov A, Manukian S, Lazarev M. AI in interventional cardiology: innovations and challenges. *Heliyon.* 2024;10:e36691.
6. Sule AA, Poh KK, Srinivasan DK. Role of ChatGPT in interventional cardiology. *Singapore Med J*. Epub ahead of print.
7. Aminorroaya A, Biswas D, Pedroso AF, Khera R. Harnessing artificial intelligence for innovation in interventional cardiovascular care. *J Soc Cardiovasc Angiogr Interv.* 2025;4(3Part B):102562.
8. Alexandrou M, Rempakos A, Mutlu D, et al. Interventional cardiologists' perspectives and knowledge towards artificial intelligence. *J Invasive Cardiol.* 2024;36.
9. Alexandrou M, Mahtani AU, Rempakos A, et al. Performance of ChatGPT on ACC/SCAI Interventional Cardiology Certification simulation exam. *JACC Cardiovasc Interv.* 2024;17:1292-1293.
10. Yavuz YE, Kahraman F. Evaluation of the prediagnosis and management of ChatGPT-4.0 in clinical cases in cardiology. *Future Cardiol.* 2024;20:197-207.
11. Mittal M, Forbes Technology Council. AI vs. developers: a future of collaboration, not competition. Last Accessed Date: 26.07.2025. Available from: https://www.forbes.com/councils/forbestechcouncil/2025/05/20/ai-vs-developers-a-future-of-collaboration-not-competition/
12. Lata K, Rooney C, Tukaye D, Velagaleti R, Tariq A. Governing the unbound: SCAI's role in the future of artificial intelligence. *J Soc Cardiovasc Angiogr Interv.* 2025;4(3 Part B):102517.
13. Biondi-Zoccai G, D'Ascenzo F, Giordano S, et al. Artificial intelligence in cardiology: general perspectives and focus on interventional cardiology. *Anatol J Cardiol.* 2025;29:152-163.

INTERVENTIONAL CARDIOLOGY PERSPECTIVES

Inter Cardio Pers 2025;1(2):40-43

DOI: 10.4274/intercardiopers.2025.2025-5-1

REVIEW

Left Ventricular Pseudoaneurysm Formation in the Context of Acute Myocardial Infarction: A Perspective Review of the Mechanistic and Clinical Implications

Kenan Yalta, Uğur Özkan, Nilay Solak, Emirhan Çakır, Gizem Ayyıldız, Fatih Kardaş, Murat Gök

Department of Cardiology, Trakya University Faculty of Medicine, Edirne, Türkiye

ABSTRACT

Background: Coronary slow flow (CSF) is a frequently observed angiographic and clinical condition linked to various complications, including stable and unstableangina pectoris, acute coronary syndromes, hypertension, and potentially fatal arrhythmias. Semaphorin 4D (Sema4D), a recently identified type 1 transmembrane glycoprotein, has been implicated in processes such as inflammation, oxidative stress, atherosclerosis, and angiogenesis. Elevated Sema4D levels have been documented in individuals with atrial fibrillation, acute coronary syndrome, and heart failure.

Aim: This study aimed to assess the association between Sema4D levels and both the presence and severity of CSF.

Study Design: Cross-sectional observational study.

Methods: The study comprised 79 patients diagnosed with CSF and 81 healthy control subjects. Serum levels of Sema4D were measured, and coronary flow was assessed using the thrombolysis in myocardial infarction frame count (TFC) method.

Results: Sema4D concentrations were significantly higher in the CSF group compared to the control group ($p<0.001$). Notably, Serum4D levels showed a positive correlation with high-sensitivity C-reactive protein ($r=073$, $p<0.001$), mean TFC ($r=088$, $p<0.001$), and the neutrophil-to-lymphocyte ratio ($r=0.37$, $p<0.001$).

Conclusion: Sema4D may serve as a biomarker associated with CSF and could aid in identifying patients with CSF-related unstable angina.

Keywords: Acute myocardial infarction, intramyocardial hemorrhage, left ventricular pseudoaneurysm, myocardial rupture, percutaneous closure

INTRODUCTION

Left ventricular pseudoaneurysm (LV-PSA) formation in the context of acute myocardial infarction (AMI) has been regarded as a rare but potentially fatal entity, particularly in cases of a missed diagnosis.[1,2] Structurally, this form of LV-PSA has been attributed to a subtle myocardial rupture, usually in the posterobasal (or inferior) segment, which leads to the evolution of a blood-containing pericardial sac with a narrow neck.[2] In this perspective paper, we attempted to underscore certain aspects of LV-PSA in the context of AMI, as detailed below:

First, LV-PSAs can exhibit atypical presentation patterns, challenging conventional diagnostic expectations. As such, cardiologists must remain open-minded, avoiding preconceived notions or stereotypical assumptions about this potentially fatal condition. Awareness of unusual clinical manifestations is essential in real-world practice.[1] LV-PSAs may occur in atypical locations, including the apex, may appear exceptionally large, and critically, may lead to unexpected complications, such as stroke.[1]

Second, LV-PSA, mechanistically, may be regarded as a form of free wall rupture in patients with AMI. Therefore, the potential mechanisms and temporal characteristics of myocardial rupture should be considered in the categorization of various scenarios in these patients. Free wall rupture in the post-AMI setting is a highly fatal complication, possibly presenting with one of the following clinical scenarios, largely depending on the severity of the rupture (Figure 1):

1. Cardiac arrest (due to the complete drainage of intraventricular blood into the thoracic cavity),[2]

2. Pericardial effusion (without or with tamponade)

3. LV-PSA.[2]

Temporally, free wall rupture mostly commonly occurs in the subacute phase of AMI, typically resulting from progressive erosion of the infarcted segment (called histopathological type-2 myocardial rupture). In rare cases, it may present acutely within the first 24 h of AMI, particularly in patients with intramyocardial hemorrhage (IMH) (called histopathological type-1 myocardial rupture). Even more

Address for Correspondence: Kenan Yalta MD, Department of Cardiology, Trakya University Faculty of Medicine, Edirne, Türkiye
E-mail: kyalta@gmail.com, akenanyalta@trakya.edu.tr **ORCID ID:** orcid.org/0000-0001-5966-2488

Cite as: Yalta K, Özkan U, Solak N, et al. Left ventricular pseudoaneurysm formation in the context of acute myocardial infarction: a perspective review of the mechanistic and clinical implications. *Inter Cardio Pers*. 2025;1(2):40-43

Received: 02.05.2025
Accepted: 21.07.2025
Publication Date: 11.08.2025

rarely, free wall rupture can complicate a pre-existing true aneurysm in the post-recovery phase, corresponding to histopathological type-3 myocardial rupture.[2-4] Among these, type-1 rupture is more frequently associated with cardiac tamponade and sudden cardiac arrest, whereas LV-PSAs typically develop as a sequel of type-2 myocardial rupture.[2-4] An overview of the histopathological types of myocardial free wall rupture in the context of AMI is presented in Table 1.

Third, LV-PSAs, in addition to the classical symptoms, including dyspnea and angina, may present with atypical symptoms, such as persistent cough, hiccup (due to diaphragmatic irritation), dysphagia, and dizziness (possibly due to enhanced Bezold-Jarish reflex).[2] These symptoms may be more likely in the setting of huge aneurysms and should therefore alert the clinician to fully explore the potential of LV-PSA in the post-AMI setting.

Fourth, as mentioned earlier, certain LV-PSA patterns[1] may surprisingly emerge in the acute phase of AMI (possibly due to a type-1 rupture), potentially highlighting their interesting temporal features along with the potential role of IMH in their evolution.[2] Several risk factors have been associated with the occurrence of IMH, including delayed myocardial reperfusion [with percutaneous coronary intervention (PCI) or thrombolysis], elevated glucose levels at the time of admission, smoking, and anterior AMI.[5] In this context, every effort should be made to prevent and/or manage the risk factors for IMH evolution (if any).[5] Particularly, early reperfusion with PCI and a strict control of blood glucose level should be given critical importance in the prevention of IMH.[5] Importantly, late-stage thrombolytic therapy should be avoided, as it significantly increases the risk of IMH.[2] Early LV-PSAs resulting from IMH may manifest with a secondary rise in troponin levels, either due to the rupture itself[2] or, more rarely, due to a coronary or cerebral embolism[6-8] originating from LV-PSA thrombus, or a combination of these mechanisms.

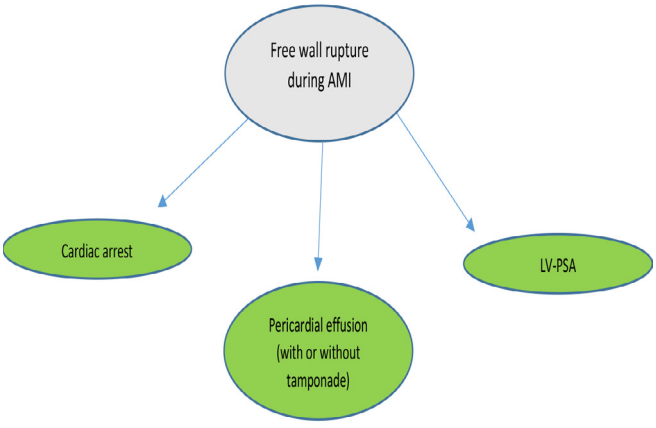

Figure 1. Clinical scenarios in the setting of AMI-related free wall rupture
AMI: Acute myocardial infarction, LV-PSA: Left ventricular pseudoaneurysm

Table 1. Histopathological types of free wall rupture in the setting of AMI[2-4]

Type-1	Free wall rupture (due to an intramural hematoma) arising within the first 24 hours of AMI
Type-2	Free wall rupture (due to the erosion of the infarct tissue) arising during the subacute stage of AMI
Type-3	Free wall rupture (secondary to the erosion of a left ventricular true aneurysm) arising in the late stage of AMI

AMI: Acute myocardial infarction

Fifth, advanced diagnostic tests, including cardiac magnetic resonance imaging (MRI) and computed tomography (CT), have proved useful in several cardiovascular disorders, particularly in challenging cases.[9,10] Similarly, cardiac MRI and CT might uncover further aspects of LV-PSA and the accompanying signs, such as IMH and absolute differentiation from true aneurysms or rare variants, including pseudo-pseudo aneurysms, thereby conferring higher diagnostic sensitivity and specificity relative to echocardiogram.[2,11-14] Therefore, we strongly advocate that any AMI patient with echocardiographic findings highly suggestive of an LV-PSA should undergo further evaluation with cardiac MRI or CT for definitive characterization.

Sixth, surgical excision has been considered as a routine management strategy of LV-PSAs owing to the extremely high risk of secondary late rupture (and sudden death) with medical therapy alone.[2,14] On the other hand, although surgical excision has been the primary management strategy in such cases, successful percutaneous closure has been previously reported in select patients using a variety of devices such as Amplatzer occluder, vascular plugs, and coil embolization.[14-17] In this context, percutaneous closure has been mostly recommended in patients at a high surgical risk.[14] However, patient eligibility (such as anatomical factors) for percutaneous closure has been the fundamental factor in this context.[14] Although percutaneous closure has been considered relatively safe compared to surgery, certain complications may arise. A systematic review of published cases (involving the analysis of outcomes for 71 patients) reported a complication rate of 9.9% following percutaneous closure (the reported complications included coil loss, residual leak, neurological deficits, and mechanical compression, all of which could be managed successfully).[14] On follow-up, a mortality rate of 8.5% was determined, largely attributable to diverse clinical conditions.[14] Interestingly, conservative management was previously reported in the context of high-risk features for radical management strategies.[14,18] The general recommendations and pitfalls regarding the management of LV-PSAs[14-17] are summarized in Table 2. Notably, LV-PSAs, in addition to being encountered in the post-AMI setting, may arise as a complication of cardiac surgery, chest trauma, or infections.[14] However, the management strategies of LV-PSAs are generally similar in such conditions.[14]

Finally, every effort should be made to prevent aneurysm rupture until definitive management can be implemented. It is well established that areas of micro- or macro-bleeding increase tissue fragility, thereby highlighting the risk of rupture, particularly in vulnerable conditions such as aortic dissection. This vulnerability may similarly apply to the setting of LV-PSAs. In the post-AMI setting, patients are often on heparin therapy for various clinical indications. However, the use of protamine for rapid heparin reversal following the diagnosis of an LV-PSA remains controversial. While protamine is routinely employed during interventional procedures, such as in cases of coronary perforation

Table 2. General recommendations and pitfalls regarding the management of LV-PSAs[14-18]

Further evaluation of LV-PSA and co-existing complications (including aneurysmal thrombus formation) through advanced imaging modalities (CT, MRI, TEE, three-dimensional echocardiogram, etc.).
Consider surgery as the first-line management strategy in all cases (particularly in the setting of urgent or emergent clinical presentation).
Consider percutaneous intervention in surgically high-risk patients or previous sternotomy with suitable LV-PSA anatomical features [narrow neck (mostly <10-12 mm), absence of cavitary thrombus].
Consider using occluder devices and vascular plugs in moderate-to-large aneurysms and coil embolization in small to moderate aneurysms. Avoid using occluder devices at sites where impingement on other cardiac structures (including bioprosthetic valves, coronary arteries, etc.) seems likely.
Percutaneous intervention may be performed through antegrade (through major veins, transapical or direct puncture of the chest wall and aneurysm) or retrograde (through major arteries) routes, largely depending on the aneurysm location, technical feasibility, and operator experience.
Consider oversizing the VSD occluder device by 5-6 mm (relative to the aneurysmal neck diameter) due to potential enlargement in the neck diameter, hypermobility, etc. In general, a cut-off oversizing value of 3.3 mm or an oversizing ratio of 1.6 is highly recommended for occluder devices.
Following the deployment of occluder devices, the partial persistence of unidirectional flow from the LV cavity to the LV-PSA cavity may result in a progressive increase in the aneurysm diameter, potentially leading to late rupture. During the intervention, this should be tested and avoided, if possible, before the device is released.
Re-evaluate anatomical and clinical features in case of failed percutaneous closure. Consider reintervention or surgery accordingly.
Consider conservative management in select cases with extremely high surgical risk and unsuitable anatomical features, particularly in the presence of small to moderate (<30 mm) and asymptomatic aneurysms.

LV-PSA: Left ventricular pseudoaneurysm, CT: Computed tomography, MRI: Magnetic resonance imaging, TEE: Transesophageal echocardiogram, VSD: Ventricular septal defect, LV: Left ventricle

or access site hemostasis.[19] However, its use has been associated with serious thrombotic complications, including stent thrombosis, intrapericardial thrombus formation (which can hinder pericardial drainage), and peripheral ischemic events.[19] In cases of established LV-PSA, many clinicians choose to discontinue anticoagulation, primarily out of concern for secondary aneurysm rupture.[18] Nevertheless, long-term anticoagulation has been reported as a relatively safe option in conservatively managed, late-onset LV-PSAs.[18] Conversely, withholding anticoagulation may predispose to thrombus formation within the aneurysmal sac,[18] potentially leading to life-threatening embolic events. Based on the limited literature available and our expert opinion, we recommend that protamine use for rapid heparin reversal, along with the discontinuation of anticoagulation may be the preferred strategy just before the emergent or urgent surgical management of high-risk LV-PSAs (extremely huge ones or those leading to severe symptoms or hemodynamic compromise, etc.) to avoid postsurgical hemorrhagic complications. In the context of planned elective interventions (surgical or percutaneous) for lenient LV-PSAs, withholding protamine and the continuation of anticoagulation until the day of intervention may be the preferred strategy for the prevention of thromboembolic complications. However, in rare instances where LV-PSA is diagnosed within the first 24 h of an AMI admission (and hence, LV-PSA might be potentially attributable to a type-1 rupture due to an IMH), protamine administration and the discontinuation of anticoagulation (in an attempt to mitigate IMH propagation and secondary aneurysm rupture) may be the preferred strategy, irrespective of the existing LV-PSA features.

CONCLUSION

In summary, LV-PSAs following AMI may present with atypical features in terms of their location (involvement of segments other than the posterobasal segment), temporal evolution (emergence in the very early or late phase), and morphological characteristics (for instance, presentation with a relatively broad neck mimicking a true aneurysm).[1,2] Advanced imaging modalities may thus be necessary to avoid a missed or delayed diagnosis of LV-PSAs,[2,11-13] particularly in the setting of atypical presentation patterns. Therefore, a high index of suspicion is thus critical for the timely recognition and management of this potentially fatal complication.[2] Protamine use and continuation or discontinuation of anticoagulant therapy should be tailored in accordance with the clinical features and management type in this context.[19] Finally, although surgery has been the preferred strategy for the management of LV-PSAs, percutaneous closure may also be considered in select cases based on previous reports suggesting high procedural success.[14-18]

Authorship Contributions: Surgical and Medial Practices: K.Y., U.Ö., E.Ç., F.K., M.G., Concept: K.Y., U.Ö., N.S., F.K., Design: K.Y., U.Ö., E.Ç., E.Ç., G.A., M.G., Data Collection or Processing: K.Y., U.Ö., N.S., Analysis or Interpretation: K.Y., U.Ö., G.A., Literature Search: K.Y., U.Ö., Writing: K.Y., U.Ö., E.Ç.

Conflict of Interest: No conflict of interest was declared by the authors.

Financial Disclosure: The authors declared that this study received no financial support.

REFERENCES

1. Şaşmaz Mİ, Demir B, Uçar M, Avci A. Huge pseudoaneursym presenting with silent myocardial infarction and stroke. *Anatol J Cardiol*. 2024;28:24-25.
2. Yalta K. Mechanical complications and cardiogenic shock in the setting of acute myocardial infarction: diagnostic perspectives. *Turkiye Klinikleri J Cardiol-Special Topics*. 2016;9:16-26.
3. Jones BM, Kapadia SR, Smedira NG, et al. Ventricular septal rupture complicating acute myocardial infarction: a contemporary review. *Eur Heart J*. 2014;35:2060-2068.
4. Becker AE, van Mantgem JP. Cardiac tamponade. A study of 50 hearts. *Eur J Cardiol*. 1975;3:349-358.
5. Yang YX, Zhou F, Wen T, Li WJ. Deciphering the enigma of İntramyocardial hemorrhage following reperfusion therapy in acute ST-segment elevation

myocardial infarction: a comprehensive exploration from mechanisms to therapeutic strategies. *Cardiol Rev.* 2024;30.

6. Yalta K, Gurdogan M, Ozturk C, Yalta T. MINOCA? Takotsubo syndrome? Or both? Pitfalls, clues and indications for advanced modalities in the differential diagnosis. *Kardiol Pol*. 2022;80:1282-1283.
7. Yildiz M, Ashokprabhu N, Shewale A, Pico M, Henry TD, Quesada O. Myocardial infarction with non-obstructive coronary arteries (MINOCA). *Front Cardiovasc Med.* 2022;9:1032436.
8. Yaghi S, Chang AD, Ricci BA, et al. Early elevated troponin levels after ischemic stroke suggests a cardioembolic source. *Stroke.* 2018;49:121-126.
9. Yalta K, Madias JE, Kounis NG, et al. Takotsubo syndrome: an international expert consensus report on practical challenges and specific conditions (part-1: diagnostic and therapeutic challenges). *Balkan Med J.* 2024;41:421-441.
10. Yalta K, Madias JE, Kounis NG, et al. Takotsubo syndrome: an international expert consensus report on practical challenges and specific conditions (part-2: specific entities, risk stratification and challenges after recovery). *Balkan Med J*. 2024;41:442-457.
11. Flavian A, Carta F, Thuny F, et al. Cardiac MRI in the diagnosis of complications of myocardial infarction. *Diagn Interv Imaging*. 2012;93:578-585.
12. Mousavi N, Buksak R, Walker JR, et al. Left ventricular pseudoaneurysm: the role of multimodality cardiac imaging. *Can J Cardiol*. 2009;25:389.
13. Basso C, Corbetti F, Silva C, et al. Morphologic validation of reperfused hemorrhagic myocardial infarction by cardiovascular magnetic resonance. *Am J Cardiol.* 2007;100:1322-1327.
14. Yuan SM. Percutaneous closure of left ventricular pseudoaneurysm. *Postepy Kardiol Interwencyjnej*. 2022;18:101-110.
15. Al-Hijji MA, Guerrero M, Rihal CS, Eleid MF. Transapical percutaneous closure of rapidly expanding post-surgical left ventricular outflow tract pseudoaneurysm. *Catheter Cardiovasc Interv.* 2019;94:859-862.
16. Clift P, Thorne S, de Giovanni J. Percutaneous device closure of a pseudoaneurysm of the left ventricular wall. *Heart.* 2004;90:62.
17. Moriarty J, Harris TJ, Vorobiof G, Kwon M, Aboulhosn J. Direct percutaneous repair of left ventricular pseudoaneurysm via transthoracic deployment of a ventricular septal defect closure device. *Tex Heart Inst J*. 2015;42:362-366.
18. Zachwyc J, Kobusiak-Prokopowicz M, Guziński M, Kuliczkowski W. An unusual long-term follow-up of a patient with a left ventricular pseudoaneurysm after myocardial infarction. *Kardiol Pol.* 2024;82:239-240.
19. Danek BA, Kearney KE, Chung CJ, et al. The contemporary role of protamine in the cardiac catheterization laboratory. *Catheter Cardiovasc Interv*. 2023;102:111-120.

INTERVENTIONAL CARDIOLOGY PERSPECTIVES

Inter Cardio Pers 2025;1(2):44-51

DOI: 10.4274/intercardiopers.2025.2025-2-8

ORIGINAL ARTICLE

Evaluation of the Relationship Between Semaphorin 4D Levels and the Coronary Slow Flow Phenomenon

Hüseyin Altuğ Çakmak[1], Özlem Karakurt[2], Selçuk Kanat[2], Kübra Çiğdem Pekkoç-Uyanık[3]

[1]Department of Cardiology, Haliç University Faculty of Medicine, İstanbul, Türkiye

[2]Clinic of Cardiology, University of Health Sciences Türkiye, Bursa High Education Training and Research Hospital, Bursa, Türkiye

[3]Department of Medical Biology, Haliç University Faculty of Medicine, İstanbul, Türkiye

ABSTRACT

Background: Coronary slow flow (CSF) is a frequently observed angiographic and clinical condition linked to various complications, including stable and unstableangina pectoris, acute coronary syndromes, hypertension, and potentially fatal arrhythmias. Semaphorin 4D (Sema4D), a recently identified type 1 transmembrane glycoprotein, has been implicated in processes such as inflammation, oxidative stress, atherosclerosis, and angiogenesis. Elevated Sema4D levels have been documented in individuals with atrial fibrillation, acute coronary syndrome, and heart failure.

Aim: This study aimed to assess the association between Sema4D levels and both the presence and severity of CSF.

Study Design: Cross-sectional observational study.

Methods: The study comprised 79 patients diagnosed with CSF and 81 healthy control subjects. Serum levels of Sema4D were measured, and coronary flow was assessed using the thrombolysis in myocardial infarction frame count (TFC) method.

Results: Sema4D concentrations were significantly higher in the CSF group compared to the control group ($p<0.001$). Notably, Serum4D levels showed a positive correlation with high-sensitivity C-reactive protein ($r=073$, $p<0.001$), mean TFC ($r=088$, $p<0.001$), and the neutrophil-to-lymphocyte ratio ($r=0.37$, $p<0.001$).

Conclusion: Sema4D may serve as a biomarker associated with CSF and could aid in identifying patients with CSF-related unstable angina.

Keywords: Semaphorin 4D, coronary slow flow, inflammation, biomarker, TIMI frame count

INTRODUCTION

Coronary slow flow (CSF), a commonly observed angiographic and clinical finding, is characterized by delayed forward movement of contrast medium to the distal segments of a specific coronary artery during coronary angiography, in the absence of obstructive coronary artery disease, coronary vasospasm, acute myocardial infarction, coronary ectasia, connective tissue disorders, coronary embolism, heart failure, or myocardial and valvular disease.[1] The incidence of CSF varies widely, ranging from 1% to 7% of all coronary angiographic procedures.[1] CSF can present with a variety of clinically significant manifestations and complications, including acute coronary syndromes, stable and unstable angina pectoris, hypertension, and potentially fatal arrhythmias, such as sudden cardiac death.[1-4] Although the primary risk factors and underlying pathophysiological mechanisms of CSF remain unclear, several contributing processes have been proposed, including small-vessel disease, endothelial dysfunction, marked inflammation, subclinical atherosclerosis, and abnormal flow patterns in the epicardial coronary arteries.[5-9]

Semaphorin 4D (Sema4D), also known as CD100, belongs to the class 4 semaphorin family. It is a type 1 transmembrane glycoprotein with a molecular weight of 150 kDa. Sema4D is broadly expressed by various cell types, including endothelial cells, platelets, B and T lymphocytes, monocytes, and neutrophils. Its primary receptors are Plexin-B1 and CD72.[10,11] Sema4D has been identified as a key pathophysiological factor involved in numerous biological processes such as chronic inflammation, immune system development and maturation, atherosclerosis, angiogenesis, osteogenesis, neurogenesis, and tumor formation and progression.[12-16] Elevated Sema4D levels have been observed in patients with heart failure and chronic atrial fibrillation (AF) when compared with healthy individuals. These findings suggest that Sema4D may play a significant role in the onset and progression of these conditions.[14] Moreover, a study by Xiang et al.[17] demonstrated a significant and independent positive association between Sema4D levels and left atrial diameter in chronic AF. Additionally, Can et al.[18] reported that Sema4D may serve as a potential marker for predicting recurrence in patients with paroxysmal AF (PAF) who have undergone catheter ablation.

Address for Correspondence: Hüseyin Altuğ Çakmak, MD, PhD, FESC, FACC, Department of Cardiology, Haliç University Faculty of Medicine, İstanbul, Türkiye

E-mail: altugcakmak@hotmail.com **ORCID ID:** orcid.org/0000-0002-5101-1928

Cite as: Çakmak HA, Karakurt Ö, Kanat S, Pekkoç-Uyanık KÇ. Evaluation of the relationship between Semaphorin 4D levels and the coronary slow flow phenomenon. *Inter Cardio Pers.* 2025;1(2):44-51

Received: 22.02.2025
Accepted: 18.05.2025
Publication Date: 11.08.2025

As there are no existing studies in the literature examining the association between Sema4D and CSF, this study was undertaken to address that gap. It also represents the first attempt to clarify the role of Sema4D in the pathogenesis of CSF. Furthermore, the study aimed to explore the relationship between Sema4D and established inflammatory markers in the context of stable angina pectoris.

METHODS

Study Population

This study was designed as a cross-sectional observational investigation. A total of 1,762 consecutive patients who underwent coronary angiography between November 2019 and May 2021 at a high-volume training and research hospital were considered for inclusion. These procedures were performed due to symptoms, clinical and physical examination findings, or evidence of myocardial ischemia identified through exercise stress testing or noninvasive imaging modalities such as myocardial perfusion scintigraphy or stress echocardiography. Based on coronary angiography findings, the study population was divided into two groups. The patient group included 79 consecutive individuals with angiographically confirmed normal coronary artery anatomy who exhibited slow coronary flow in the absence of atherosclerotic coronary artery disease. The control group consisted of 81 randomly selected subjects who had undergone coronary angiography and were found to have both anatomically normal coronary arteries and normal coronary flow, including appropriate myocardial blush and clearance. The control group selection was performed independently by three experienced invasive cardiologists who were blinded to the purpose of the study.

Patients in both study groups presented with typical chest pain or angina-equivalent symptoms and had positive findings on either an exercise stress test or noninvasive imaging modalities, including myocardial perfusion imaging, stress echocardiography, or coronary computed tomographic angiography. Demographic, clinical, and laboratory data for all participants were documented by cardiologists at the time of cardiac catheterization. Moreover, all subjects underwent 12-lead surface electrocardiography and two-dimensional (2D) transthoracic echocardiography prior to the coronary angiography procedure. Echocardiographic assessments were conducted using a Vivid S5 system (GE Healthcare, WI, USA) equipped with a 1.7/3.4-MHz phased-array transducer, with patients positioned in the left lateral decubitus posture. These evaluations were performed to assess left ventricular structure and function, including ejection fraction, and were independently carried out by two non-invasive cardiologists who were blinded to the study outcomes. Left ventricular ejection fraction (LVEF) was calculated using Simpson's biplane method of disks based on 2D images obtained from the apical four- and two-chamber views.

Smoking was defined as regular cigarette use, either in the past or concurrently, prior to or during the study period. Diagnoses of hypertension, hyperlipidemia, and diabetes mellitus were made in accordance with current relevant clinical guidelines.[19-21] A documented history of these conditions and/or the sue of antihypertensive, lipid-lowering, or antidiabetic medications, including insulin, was considered indicative of the corresponding disease in this study. Renal function was assessed by calculating the glomerular filtration rate using both plasma creatinine levels and the Cockcroft-Gault formula.[19] Furthermore, height and weight were measured for all participants, and body mass index was calculated by dividing body weight in kilograms by the square of height in meters (kg/m^2).

In this study, CSF was defined angiographically by the following criteria: (a) absence of obstructive epicardial coronary artery disease, (b) delayed antegrade passage of contrast medium resulting in distal vessel opacification consistent with either thrombolysis in myocardial infarction (TIMI)-2 flow or a corrected TIMI frame count >27 frames, and (c) delayed distal vessel opacification in at least one epicardial coronary artery. Participants who were using vasoactive medications before or during the study underwent a 3-day "washout" period prior to coronary angiography to minimize potential interference with study outcomes.

The main exclusion criteria for this study included moderate to severe valvular heart disease, a history of chronic ischemic heart disease or previous percutaneous coronary intervention or coronary artery bypass grafting, acute coronary syndromes, heart failure with reduced or mid-range ejection fraction, cardiomyopathies, congenital structural heart disease, moderate to left ventricular hypertrophy, peripheral vascular disease, stroke, myopericarditis, active infections, chronic obstructive pulmonary disease, pulmonary hypertension, recent trauma or major surgery within the past 3 months, cardiac syndrome X, acute or chronic renal or hepatic dysfunction, pheochromocytoma, hematologic disorders, thyroid dysfunction, acute or chronic inflammatory diseases, malignancy, autoimmune diseases, and the use of specific medications that may influence blood viscosity or platelet structure and function, such as antiplatelet or anticoagulant agents, corticosteroids, immunosuppressive drugs, and statins.

Participants were eligible for inclusion if they were between 18 and 80 years of age and capable of providing written informed consent, which was a mandatory requirement for enrollment. The study was conducted in accordance with the principles of the Declaration of Helsinki and was approved by the Haliç University Ethics Committee (approval no: 64, date: 30.03.2022).

Coronary Angiography Procedure

Coronary angiography was carried out by two experienced interventional cardiologists who were blinded to the study results. The procedure was performed via either the femoral or radial artery using the standard Judkins technique and a monoplane cine angiography system. Coronary images were captured at a frame rate of 30 frames per second in both right and left oblique views, utilizing cranial and caudal angulations. All participants received the nonionic contrast agent iopromide (Ultravist 370, Schering AG, Berlin, Germany) during the procedure. Coronary blood flow was quantitatively assessed using the TIMI frame count (TFC) method by three experienced interventional cardiologists who were blinded to the study data. The intra- and interobserver coefficients of variation (CV) were 3.6% and 6.4%, respectively.

In this method, the number of cine frames required for the contrast agent to reach predefined distal coronary landmarks in the left anterior descending (LAD) artery, left circumflex (LCX) artery, and right coronary

artery (RCA) was measured and recorded. The initial frame was defined as the frame in which the concentrated contrast dye completely filled the width of the proximal coronary artery lumen, touching both edges and advancing distally beyond that point. The final frame was identified as the frame when the leading edge of the contrast first reached the distal landmark. The TFC for each artery was calculated by subtracting the initial frame from the final frame. The predefined distal landmarks were the distal bifurcation of the LAD, commonly referred to as the "moustache," for the LCX, and the first branch of the posterolateral artery for the RCA. Since the LAD is longer than the LCX and RCA, its TFC is naturally higher; therefore, the corrected TIMI frame count (cTFC) for the LAD was obtained by dividing its TFC by 1.7. The mean TFC for each participant was calculated by adding the TFC values for the LAD, LCX, and RCA and dividing the sum by three. According to a previous study,[22] the standard corrected mean values for normal coronary artery visualization were 36.2±2.6 frames for the LAD, 22.2±4.1 for the LCX, and 20.4±3 frames for the RCA. Moreover, the corrected mean TFC (cTFC) for the LAD was reported as 21.1±1.5 frames.[22] In the present study, participants with a TFC exceeding the previously reported normal range by more than two standard deviations (SD) in any of the LAD or LCX arteries or RCA were classified as having CSF.

Experimental Method

Blood samples were collected from the antecubital veins of all participants by venipuncture early in the morning after 12 h of fasting and prior to the coronary angiography procedure. Samples were collected into vacuum tubes containing ethylenediaminetetraacetic acid as an anticoagulant. Serum was immediately separated by centrifugation at 3,000 g for 15 min and stored at -80 °C until analysis. Routine hematological, coagulation, and biochemical tests were performed on the same day as blood collection. Hematological parameters were measured using a Coulter LH 780 Hematology Analyzer (Beckman Coulter Ireland, Inc., Mervue, Galway, Ireland). Serum high-sensitivity C-reactive protein (hs-CRP) was measured at admission by enzyme-linked immunosorbent assay (ELISA) using commercial kits (Hitachi 917 analyzer, Boehringer Mannheim, Germany). Biochemical parameters, including fasting blood glucose and lipid profiles, were analyzed using an Abbott Diagnostics C8000i autoanalyzer (Abbott, Germany) with commercial reagents. Low-density lipoprotein (LDL) cholesterol was calculated using Friedewald's formula for samples with triglyceride levels ≤400 mg/dL. The neutrophil-to-lymphocyte ratio (NLR), platelet-to-lymphocyte ratio (PLR), and monocyte-to-lymphocyte ratio (MLR) were determined by dividing the absolute counts of neutrophils, platelets, and monocytes by the absolute lymphocyte count, respectively.

Serum Sema4D levels were measured using a commercial ELISA kit according to the manufacturer's instructions (intra-assay CV <8%; inter-assay CV <10%; Nepenthe Research Technology Laboratory, Cat. No: NE010156601, Gebze-Kocaeli, Türkiye). The assay's sensitivity range for Sema4D concentrations was 0.31-20 ng/mL. All samples were analyzed in duplicate, and the mean values were used for subsequent analyses.

Statistical Analysis

The Kolmogorov-Smirnov test was applied to assess whether the study variables followed a normal distribution. Continuous variables with normal distribution were expressed as mean±SD, while non-normally distributed continuous variables were presented as medians. Categorical variables were reported as frequencies and/or percentages (%). Differences between the two groups were analyzed using Student's t-test for normally distributed continuous variables and the Mann-Whitney U test for non-normally distributed continuous variables. Chi-squared or Fisher's exact tests were used for categorical variables. Correlation analyses between variables employed either Spearman or Pearson correlation tests, depending on the distribution of the data. Receiver operating characteristic (ROC) curve analysis was conducted to assess the diagnostic value of Sema4D, hs-CRP, NLR, PLR, and MLR in distinguishing patients with CSF in any of the three coronary arteries from those with normal coronary blood flow. Moreover, multiple linear regression analysis was used to identify significant independent predictors of Sema4D levels. A two-sided p value <0.05 was considered statistically significant, with a type 1 error rate of 5%. Standardized β coefficients and 95% confidence intervals (CI) were reported. Statistical analyses were performed using IBM Statistical Package for the Social Sciences statistics for Windows, version 21.0 (Armonk, NY, USA).

RESULTS

A total of 160 participants were included in this study, with 79 patients in the CSF group (53.1% male) and 81 subjects in the coronary normal blood flow (CNF) group (40.7% male). The baseline demographic and clinical characteristics of both groups are summarized in Table 1. No significant differences were found between the groups except for systolic blood pressure, hypertension, smoking history, hyperlipidemia, family history, and antiplatelet drug use, all of which were higher in the CSF group compared to the control group (p<0.001). LVEF was similar between the groups (p=0.948). Serum Sema4D levels were significantly elevated in the CSF group compared to the CNF group (7.78±0.87 vs. 4.23±0.88; p<0.001) (Figure 1).

Baseline laboratory parameters for the groups are presented in Table 2. Levels of hs-CRP, LDL, total cholesterol, and the NLR were significantly higher in the CSF group than in controls (p<0.001). In contrast, lymphocyte counts were significantly lower in the CSF group (p=0.03). Other laboratory values showed no significant differences between the two groups (all p values >0.05).

As expected, patients with CSF showed significantly higher cTFC values compared to those in the CNF group (Table 3). Among the CSF patients, 56 (71.0%) exhibited slow flow in all 3 coronary vessels, 12 patients (15.1%) had slow flow in 2 vessels, and 11 patients (13.9%) had slow flow in 1 vessel. When analyzing CSF distribution by affected coronary artery, the RCA was the most frequently involved vessel, affecting 48 patients (60.7%). The TFC values for the LAD, LCX, and RCA, as well as the mean TFC, were all significantly higher in the CSF group compared to the CNF group (all p values <0.001).

Correlation analysis was conducted to assess the relationship between Sema4D and established inflammatory markers in patients with CSF. Sema4D showed a significant positive correlation with the NLR (r=0.37, p<0.001), hs-CRP (r=0.73, p<0.001), and mean TFC (r=0.88, p<0.001) (Figure 2). Moreover, strong correlations were found between Sema4D and the TFC for the Cx (r=0.80, p<0.001), LAD (r=0.84, p<0.001), and RCA (r=0.88, p<0.001).

Table 1. Baseline demographic, clinical, and laboratory features of the CSF and control groups

	CSF (n=79)	CNF (n=81)	p value
Age, y	58.30±11.21	60.11±9.82	0.27
Gender (F/M), n	37/42	48/33	0.11
DM, n (%)	19 (24%)	14 (17%)	0.29
HT, n (%)	61 (77%)	17 (21%)	**<0.001**
Hyperlipidemia, n (%)	41 (51%)	13 (16%)	**<0.001**
Smoking, n (%)	58 (73%)	14 (17%)	**<0.001**
Family history, n (%)	35 (44%)	15 (18%)	**<0.001**
Antiplatelet, n (%)	44 (55%)	13 (16%)	**<0.001**
Beta-blocker, n (%)	46 (58%)	54 (66%)	0.27
Calcium channel blocker, n (%)	8 (10%)	3 (3%)	0.10
ACE inhibitors/ARB, n (%)	19 (24%)	9 (11%)	0.05
SBP, mmHg	142.09±24.6	124.38±14.01	**<0.001**
DBP, mmHg	88±15.04	70.37±10.04	**<0.001**
LVEF, %	59.68±4.19	59.20±4.16	0.948
GFR, (mL/min/1.73 m^2)	128.45±5.80	130.25±6.30	0.455
Hemoglobin, g/dL	13.91±1.69	13.91±1.69	0.13
Neutrophil, x10^3	4,414±1,297	4,468±1,415	0.80
Lymphocyte, x10^3	2,395±696	2,170±665	**0.03**
Neutrophil/lymphocyte, ratio	2.66±0.90	1.99±0.66	**<0.001**
Total cholesterol, mg/dL	168.58±32.72	143.74±26.51	**<0.001**
LDL, mg/dL	133.56±43.68	114.44±33.77	**0.002**
HDL, mg/dL	44.82±8.06	45.69±10.81	0.56
TG, mg/dL	138.42±7.15	134±5.88	0.31
hs-CRP, mg/dL	2.62±0.36	1.60±0.32	<0.001
Semaphorin 4D, ng/mL	7.78±0.87	4.23±0.88	<0.001

Values are expressed as means±standard deviation or number (%), as appropriate; statistically significant values are highlighted in bold.
F/M: Female/male, ACE: Angiotensin-converting enzyme, ARB: Angiotensin receptor blocker, CNF: Coronary normal flow, CSF: Coronary slow flow, DBP: Diastolic blood pressure, DM: Diabetes mellitus, HT: Hypertension, HDL: High-density lipoprotein, hs-CRP: High-sensitivity C-reactive protein, LDL: Low-density lipoprotein, LVEF: Left ventricular ejection fraction, TC: Total cholesterol, TG: Triglyceride, SBP: Systolic blood pressure, GFR: Glomerular filtration rate

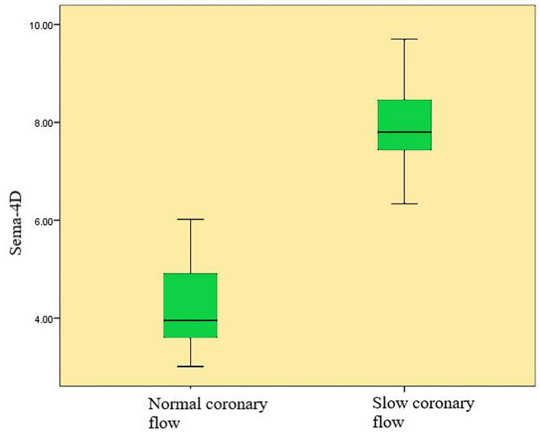

Figure 1. Sema4D levels in patients with the CSF and CNF
Sema4D: Semaphorin 4D, CSF: Coronary slow flow, CNF: Coronary normal flow

Multiple linear regression analysis revealed that NLR and the TFC for Cx and RCA were significant predictors of Sema4D levels in patients with CSF ($p<0.002$, $p<0.027$, and $p<0.001$, respectively; model $R^2=0.81$, $p<0.001$) (Table 4).

A ROC analysis was conducted to examine the potential of Sema4D in predicting CSF. The areas under the curve (AUCs) were utilized to assess the diagnostic accuracy of serum Sema4D in distinguishing patients with CSF in at least one coronary artery from those with normal CNF (Figure 3). The discrimination ability was very high (AUC=0.990, 95% CI: 0.98-1.00; $p<0.001$). Using a cut-off value of 5.79 ng/mL for Sema4D, CSF presence could be predicted with 97.1% sensitivity and 95.4% specificity. The negative predictive value was 95.0%, and the positive predictive value was 97.3%.

DISCUSSION

This study showed a strong link between elevated Sema4D levels and the presence and severity of CSF in patients undergoing coronary

Table 2. Comparison of angiographic features between the CSF and CNF groups

	CSF (n=79)	CNF (n=81)	p value
TFC, LCX	18.17±1.99	31.78±3.99	**<0.001**
TFC, RCA	17.49±1.93	33.83±4.08	**<0.001**
TFC, LAD (corrected)	17.81±1.81	33.32±3.92	**<0.001**
TFC, mean	17.82±1.15	32.98±2.64	**<0.001**

Values are expressed as means±standard deviation or number (%), as appropriate; statistically significant values are highlighted in bold.
CNF: Coronary normal flow, CSF: Coronary slow flow, LAD: Left anterior descending artery, LCX: Left circumflex artery, RCA: Right coronary artery, TFC: Thrombolysis in myocardial infarction frame count

Table 3. Correlation analysis of Sema4D levels with inflammatory and neurohormonal markers in patients with CSF

	r	p
Lymphocyte count	0.16	**0.03***
NLR	0.27	**<0.001***
TC (mg/dL)	0.28	**<0.001***
LDL (mg/dL)	0.13	0.09
TG (mg/dL)	0.194	**0.014****
hs-CRP	0.73	**<0.001***
TFC, LCX	0.80	**<0.001***
TFC, RCA	0.88	**<0.001***
TFC, LAD	0.84	**<0.001***
TFC, mean	0.88	**<0.001***
SBP, mmHg	0.72	**0.032**
DBP, mmHg	0.68	**0.045**
Family history	0.20	**0.011****
Smoking	0.43	**<0.001****
Hypertension	0.48	**<0.001****
Hyperlipidemia	0.23	**0.002****
Antiplatelet drug	0.33	**<0.001****

*Pearson correlation coefficient, **Spearman correlation coefficient.
Correlation coefficient (r); CSF: Coronary slow flow, DBP: Diastolic blood pressure, hs-CRP: High-sensitivity C-reactive protein, NLR: Neutrophil-to-lymphocyte ratio; LDL: Low-density lipoprotein, TC: Total cholesterol, TFC: Thrombolysis in myocardial infarction frame count, TG: Triglyceride, SBP: Systolic blood pressure, Sema4D: Semaphorin 4D

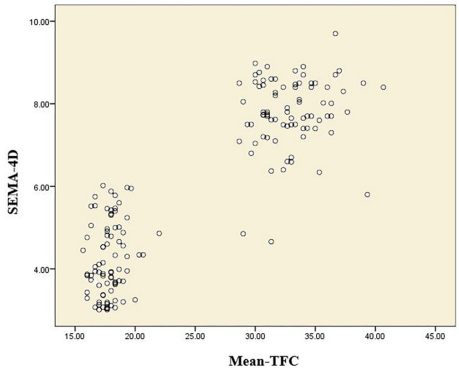

Figure 2. Correlation between serum Sema4D levels and mean TFC
Sema4D: Semaphorin 4D, TFC: Thrombolysis in myocardial infarction frame count

angiography for stable angina pectoris. Sema4D levels were also significantly correlated with inflammatory and oxidative stress markers, including hs-CRP and NLR. The degree of CSF, as measured by the mean TFC, was significantly associated with Sema4D levels. Additionally, Sema4D emerged as a novel and valuable biomarker in clinical settings for patients with stable angina pectoris, demonstrating strong diagnostic performance with high sensitivity and specificity in distinguishing patients with CSF in at least one coronary artery from healthy individuals.

Previous studies have identified smoking, hypertension, hyperlipidemia, male gender, obesity, and metabolic syndrome as major risk factors.[1] However, the precise underlying pathophysiological mechanisms and causes of CSF remain unclear. In line with prior research, our study found higher rates of hypertension, hyperlipidemia, and smoking in the CSF group compared to those with normal coronary flow.

The CSF phenomenon shares risk factors similar to those of atherosclerosis. Possible pathophysiological mechanisms involved in the development of CSF include endothelial dysfunction, chronic severe inflammation, oxidative stress, widespread atherosclerosis, vasomotor dysfunction in the microvasculature, small-vessel disease, and increased platelet count and/or activity.[1-4] Intravascular ultrasound studies have previously demonstrated the important roles of both epicardial coronary artery disease and microvascular dysfunction in the onset and progression of CSF.[23] De Bruyne et al.[24] highlighted the strong connection between abnormal slow flow in coronary arteries and atherosclerotic heart disease, which results from chronic severe inflammation, oxidative stress, free radical damage, and endothelial dysfunction, even without angiographically visible lesions.

Endothelial injury and dysfunction caused by inflammation, oxidative stress, and free radical damage may contribute to CSF development.[1-4] Various inflammatory markers, including paraoxonase, malondialdehyde, erythrocyte superoxide dismutase, visfatin, hs-CRP, NLR, and PLR, have been reported to be significantly associated with the presence of CSF in previous studies.[25-27] Consistent with these findings, our study found elevated levels of hs-CRP, interleukin-6,[28] and NLR in the CSF group compared to the CNF group. Moreover, Sema4D, identified as a novel inflammatory marker, was also shown to be increased in patients with CSF. A significant positive correlation was detected between Sema4D, hs-CRP, and NLR in patients with CSF.

CSF can be a significant cause of transient myocardial hypoperfusion, abnormal results on exercise stress tests, and impaired ventricular wall motion and function in patients with CNF who have stable

Table 4. Multiple linear regression analysis identifying independent predictors of Sema4D levels in patients with CSF

	Univariate		Multivariate	
	OR (CI 95%)	**p value**	**OR (CI 95%)**	**p value**
NLR	0.642 (0.292-0.992)	<0.001	-0.330 (-0.536-0.123)	0.002
TFC, RCA	0.200 (0.183-0.216)	<0.001	0.134 (0.089-0.179)	<0.001
TFC, LCX	0.211 (0.187-0.236)	<0.001	0.047 (0.005-0.089)	0.027
Lymphocyte count	0.000 (0.000-0.001)	0.034		
TC	0.018 (0.008-0.027)	<0.001		
TG	0.010 (0.002-0.018)	0.011		
hs-CRP	2.354 (2.011-2.698)	<0.001		
Family history	1.007 (0.354-1.661)	0.003		
Smoking	1.857 (1.300-2.413)	<0.001		
Hypertension	2.060 (1.526-2.594)	<0.001		
Hyperlipidemia	1.189 (0.550-1.827)	<0.001		
Antiplatelet drug	1.478 (0.870-2.086)	<0.001		
TFC, mean	0.222 (0.203-0.241)	<0.001		
TFC, LAD	0.200 (0.180-0.220)	<0.001		

Statistically significant values are highlighted in bold. Adjusted R^2, 0.81; p value <0.001.
CSF: Coronary slow flow, hs-CRP: High-sensitivity C-reactive protein, NLR: Neutrophil-to-lymphocyte ratio, LDL: Low-density lipoprotein, TC: Total cholesterol, TFC: Thrombolysis in myocardial infarction frame count, TG: Triglyceride, SBP: Systolic blood pressure, CI: Confidence interval, OR: Odds ratio

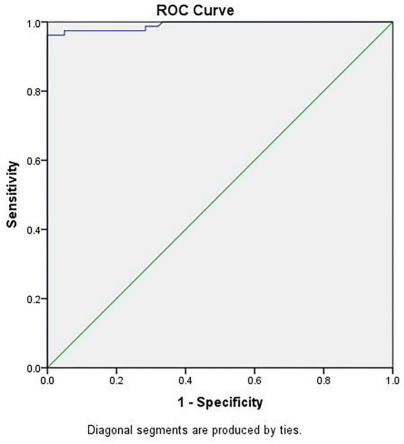

Figure 3. Receiver operating characteristic curve analysis to distinguish patients with CSF from those with CNF
CSF: Coronary slow flow, CNF: Coronary normal flow, ROC: Receiver operating characteristic

angina pectoris that is resistant to optimal medical treatment.[1,2] It may also contribute to various major adverse cardiovascular events (MACE), including stable angina pectoris, acute coronary syndromes, life-threatening arrhythmias, and sudden cardiac death.[1-4] Although the prognostic importance of CSF has been examined in multiple studies, the findings have been inconsistent. While some observational studies suggested a benign prognosis, others identified an association between CSF and MACE.[29,30] Nonetheless, the precise pathophysiological mechanisms linking CSF to MACE remain unclear.

Sema4D plays a role in inflammation, oxidative stress, atherosclerosis, and angiogenesis, potentially contributing to disease development and progression. Previous studies have reported associations between Sema4D and AF, heart failure, and coronary artery disease.[17,30,31] Willner et al.[32] found that Sema4D levels were elevated and correlated with N-terminal pro-brain natriuretic peptide in cases of acute heart failure. Lu et al.[30] also observed similar findings in heart failure patients, with the highest levels seen in those with diabetes. Moreover, Gong et al.[31] reported a link between Sema4D and coronary artery disease, noting increased levels particularly in patients with acute myocardial infarction. In this study, Sema4D was identified as an independent risk factor for developing coronary artery disease.[31] Furthermore, Xiang et al.[17] demonstrated a connection between elevated serum Sema4D levels and the presence of AF, especially in the non-paroxysmal group, highlighting Sema4D as a key independent risk factor for atrial remodeling. Consistent with Xiang et al.,[17] Can et al.[18] reported increased Sema4D levels in patients with PAF. They also investigated the relationship between Sema4D levels and AF recurrence following catheter ablation, finding significantly higher Sema4D levels in the non-ablation PAF group compared to patients who underwent ablation.[18] Moreover, Sema4D level showed a significant positive correlation with both hs-CRP and the NLR in PAF.[18]

Since no previous studies have shown a connection between Sema4D and CSF, we explored and identified this significant relationship in the present study. Furthermore, for the first time, we demonstrated an association between Sema4D and well-known inflammatory and oxidative markers such as hs-CRP and NLR in patients with CSF, highlighting an important role of Sema4D in the pathophysiology of CSF. These results indicate that elevated Sema4D levels may contribute to the presence and progression of inflammation, oxidative stress, and

endothelial and vasomotor dysfunction-key mechanisms involved in the development of CSF. Moreover, significant positive correlations were observed between Sema4D levels and the mean TFC, as well as the TFC values of all three coronary arteries, suggesting a potential role of Sema4D in the progression and severity of atherosclerosis leading to CSF. Our study also demonstrated, via ROC analysis, that Sema4D serves as a significant independent predictor for the presence of CSF. Sema4D appears to promote the secretion and activation of various pro-inflammatory cells, oxidative markers, and cytokines, triggering vascular inflammation, remodeling, and vasomotor dysfunction-particularly in endothelial and smooth muscle cells-which may accelerate the onset and progression of CSF. Overall, the main findings of this study support the idea that Sema4D may be involved in various coronary pathologies and that its levels can be detected through blood tests in clinical practice. This increase in Sema4D may be associated with chronic endothelial inflammation and oxidative stress in CSF.

Study Limitations

The present study has several limitations. First, it was conducted at a single center and was non-randomized, which may introduce selection bias. Second, the sample size was relatively small. Nevertheless, we were able to show a strong association between Sema4D level and both the presence and extent of CSF. Third, the potential coexistence of non-obstructive coronary artery disease and CSF could not be assessed due to the absence of data on atherosclerotic characteristics and coronary plaque burden, which could be assessed by intravascular ultrasonography-a technique not routinely used in clinical practice. Finally, the study's cross-sectional design meant there were no short- or medium-term follow-up data on MACEs.

CONCLUSION

This study demonstrated a statistically significant correlation between elevated serum Sema4D levels and the presence and extent of CSF in patients with stable angina pectoris who underwent coronary angiography. Furthermore, Sema4D was found to be associated with well-known inflammatory markers such as hs-CRP and NLR in this condition. Sema4D may have a critical role in the development and progression of coronary atherosclerosis, which can manifest as isolated CSF. To clarify this relationship, further large-scale, multicenter clinical studies are needed. Sema4D shows promise as a biomarker for identifying the presence and extent of CSF in patients with stable angina.

Acknowledgment: We express our gratitude to the patients and healthy control subjects who took part in this study.

Presented in: This study was presented as an oral presentation at the 38th National Cardiology Congress. The abstract was published in The Anatolian Journal of Cardiology, TSC abstracts/orals, november 10-13, 2022, Anatol J Cardiol. 2022;26(Suppl 1):S1-S177.

Ethics Committee Approval: The study was conducted in accordance with the principles of the Declaration of Helsinki and was approved by the Haliç University Ethics Committee (approval no: 64, date: 30.03.2022).

Informed Consent: Consent form was filled out by all participants.

Authorship Contributions: Concept: H.A.Ç., Design: H.A.Ç., Data Collection or Processing: H.A.Ç., Ö.K., S.K., Analysis or Interpretation: S.K., K.Ç.P-U., Literature Search: Ö.K., K.Ç.P-U., Writing: H.A.Ç., K.Ç.P-U.

Conflict of Interest: No conflict of interest was declared by the authors.

Financial Disclosure: The authors declared that this study received no financial support.

REFERENCES

1. Wang X, Nie SP. The coronary slow flow phenomenon: characteristics, mechanisms and implications. *Cardiovasc Diagn Ther*. 2011;1:37-43.
2. Horjeti B, Goda A. Acute ischemia manifestation in a patient with coronary slow flow phenomenon. *J Electrocardiol*. 2012;45:277-279.
3. Wozakowska-Kapłon B, Niedziela J, Krzyzak P, Stec S. Clinical manifestations of slow coronary flow from acute coronary syndrome to serious arrhythmias. *Cardiol J*. 2009;16:462-468.
4. Saya S, Hennebry TA, Lozano P, Lazzara R, Schechter E. Coronary slow flow phenomenon and risk for sudden cardiac death due to ventricular arrhythmias: a case report and review of literature. *Clin Cardiol*. 2008;31:352-355.
5. Tambe AA, Demany MA, Zimmerman HA, Mascarenhas E. Angina pectoris and slow flow velocity of dye in coronary arteries--a new angiographic finding. *Am Heart J*. 1972;84:66-71.
6. Mosseri M, Yarom R, Gotsman MS, Hasin Y. Histologic evidence for small-vessel coronary artery disease in patients with angina pectoris and patent large coronary arteries. *Circulation*. 1986;74:964-972.
7. Sezgin AT, Sigirci A, Barutcu I, et al. Vascular endothelial function in patients with slow coronary flow. *Coron Artery Dis*. 2003;14:155-161.
8. Cin VG, Pekdemir H, Camsar A, et al. Diffuse intimal thickening of coronary arteries in slow coronary flow. *Jpn Heart J*. 2003;44:907-919.
9. Kalay N, Aytekin M, Kaya MG, et al. The relationship between inflammation and slow coronary flow: increased red cell distribution width and serum uric acid levels. *Turk Kardiyol Dern Ars*. 2011;39:463-468.
10. Kumanogoh A, Kikutani H. Semaphorins and their receptors: novel features of neural guidance molecules. *Proc Jpn Acad Ser B Phys Biol Sci*. 2010;86:611-620.
11. Tasaka G, Negishi M, Oinuma I. Semaphorin 4D/Plexin-B1-mediated M-Ras GAP activity regulates actin-based dendrite remodeling through Lamellipodin. *J Neurosci*. 2012;32:8293-8305.
12. Suzuki K, Kumanogoh A, Kikutani H. Semaphorins and their receptors in immune cell interactions. *Nat Immunol*. 2008;9:17-23.
13. Basile JR, Barac A, Zhu T, Guan KL, Gutkind JS. Class IV semaphorins promote angiogenesis by stimulating Rho-initiated pathways through plexin-B. *Cancer Res*. 2004;64:5212-5224.
14. Zhang Y, Feng E, Xu Y, et al. Serum Sema4D levels are associated with lumbar spine bone mineral density and bone turnover markers in patients with postmenopausal osteoporosis. *Int J Clin Exp Med*. 2015;8:16352-16357.
15. Chapoval SP, Vadasz Z, Chapoval AI, Toubi E. Semaphorins 4A and 4D in chronic inflammatory diseases. *Inflamm Res*. 2017;66:111-117.

16. Kato S, Kubota K, Shimamura T, et al. Semaphorin 4D, a lymphocyte semaphorin, enhances tumor cell motility through binding its receptor, plexinB1, in pancreatic cancer. *Cancer Sci*. 2011;102:2029-2037.
17. Xiang L, You T, Chen J, Xu W, Jiao Y. Serum soluble semaphorin 4D is associated with left atrial diameter in patients with atrial fibrillation. *Med Sci Monit*. 2015;21:2912-2917.
18. Can V, Cakmak HA, Vatansever F, et al. Assessment of the relationship between semaphorin4D level and recurrence after catheter ablation in paroxysmal atrial fibrillation. *Biomarkers*. 2021;26:468-476.
19. Williams B, Mancia G, Spiering W, et al. 2018 ESC/ESH Guidelines for the management of arterial hypertension. *Eur Heart J*. 2018;39:3021-3104.
20. Mach F, Baigent C, Catapano AL, et al. 2019 ESC/EAS Guidelines for the management of dyslipidaemias: lipid modification to reduce cardiovascular risk. *Eur Heart J*. 2020;41:111-188.
21. Cosentino F, Grant PJ, Aboyans V, et al. 2019 ESC Guidelines on diabetes, pre-diabetes, and cardiovascular diseases developed in collaboration with the EASD. *Eur Heart J*. 2020;41:255-323.
22. Yang SB, Cui Y, Hou JJ, Zhang H, Pei XY, Wang Y. Assessment of the relationship between plasma fibrinogen-to-albumin ratio and slow coronary flow phenomenon in patients without obstructive coronary artery disease. *BMC Cardiovasc Disord*. 2023;23:540.
23. Pekdemir H, Polat G, Cin VG, et al. Elevated plasma endothelin-1 levels in coronary sinus during rapid right atrial pacing in patients with slow coronary flow. *Int J Cardiol*. 2004;97:35-41.
24. De Bruyne B, Fearon WF, Pijls NH, et al. Fractional flow reserve-guided PCI for stable coronary artery disease. *N Engl J Med*. 2014;371:1208-1217.
25. Yildiz A, Gur M, Yilmaz R, et al. Association of paraoxonase activity and coronary blood flow. *Atherosclerosis*. 2008;197:257-263.
26. Enli Y, Turk M, Akbay R, et al. Oxidative stress parameters in patients with slow coronary flow. *Adv Ther*. 2008;25:37-44.
27. Cakmak HA, Aslan S, Yalcin AA, et al. Relationship between serum visfatin levels and coronary slow-flow phenomenon. *Herz*. 2015;40:921-928.
28. Li JJ, Qin XW, Li ZC, et al. Increased plasma C-reactive protein and interleukin-6 concentrations in patients with slow coronary flow. *Clin Chim Acta*. 2007;385:43-47.
29. Li JJ, Wu YJ, Qin XW. Should slow coronary flow be considered as a coronary syndrome? *Med Hypotheses*. 2006;66:953-956.
30. Lu Q, Dong N, Wang Q, et al. Correction: increased levels of plasma soluble Sema4D in patients with heart failure. *PLoS One*. 2019;14:e0214894.
31. Gong H, Lyu X, Li S, Chen R, Hu M, Zhang X. sSema4D levels are increased in coronary heart disease and associated with the extent of coronary artery stenosis. *Life Sci*. 2019;219:329-335.
32. Willner N, Goldberg Y, Schiff E, Vadasz Z. Semaphorin 4D levels in heart failure patients: a potential novel biomarker of acute heart failure? *ESC Heart Fail*. 2018;5:603-609.

INTERVENTIONAL CARDIOLOGY PERSPECTIVES

Inter Cardio Pers 2025;1(2):52-58

DOI: 10.4274/intercardiopers.2025.2025-6-2

ORIGINAL ARTICLE

Outcomes and Predictors of Amputation After Endovascular Revascularization in Diabetic Foot Disease with Peripheral Artery Involvement

Cuma Süleymanoğlu[1], Adem Kıdık[2], Zeynettin Kaya[3], Volkan Çamkıran[4]

[1]Clinic of Cardiology, Osmaniye State Hospital, Osmaniye, Türkiye

[2]Clinic of Internal Medicine, Osmaniye State Hospital, Osmaniye, Türkiye

[3]Clinic of Cardiology, Anatolia Hospital, Antalya, Türkiye

[4]Clinic of Cardiology, Medical Park Göztepe Hospital, İstanbul, Türkiye

ABSTRACT

Background: Peripheral arterial disease (PAD) is significantly more prevalent in diabetic populations and is a major contributor to non-traumatic lower limb amputations.

Aim: This study assesses outcomes of percutaneous revascularization in diabetic PAD patients, comparing clinical characteristics between those who underwent amputation and those who did not.

Study Design: A single center retrospective observational study.

Methods: The study was conducted on 100 diabetic PAD patients undergoing endovascular revascularization between March 2023 and April 2024. Clinical classifications and laboratory parameters [hemoglobin A1c (HbA1c), renal function, C-reactive protein, low-density lipoprotein] were analyzed at baseline and 6 months.

Results: Amputation occurred in 15 patients (15%). These patients had significantly higher HbA1c (10.5 vs. 8.8, $p<0.001$), creatinine (1.52 vs. 0.89, $p<0.001$), and lower estimated glomerular filtration rate (47 vs. 89, $p<0.001$). PAD severity scores (Rutherford, Fontaine, Wagner, WIfI, TASC II) were all significantly higher in the amputation group. Receiver operating characteristic (ROC) analysis showed Wagner classification had the best predictive value (area under the ROC curve 0.982).

Conclusion: Advanced PAD in diabetics correlates with worse metabolic control and renal dysfunction. Early diagnosis and revascularization are critical to avoid amputation.

Keywords: Peripheral artery disease, interventional cardiology, below-the-knee intervention, diabetic foot

INTRODUCTION

Individuals with diabetes mellitus (DM) have a substantially elevated lifetime risk—approximately tenfold—of developing cardiovascular disease compared to the general population.[1] Cardiovascular complications account for about 77% of diabetes-related hospitalizations in the United States.[2]

Peripheral artery disease (PAD), a form of atherosclerotic occlusion affecting the arteries of the lower extremities, is a common and serious complication among diabetic patients.[3] Atherosclerosis obliterans is the leading cause of chronic arterial blockage in the lower limbs, particularly in those over 35 years of age.[4] Importantly, nearly half of diabetic patients with foot ulcers also have PAD,[5] and non-healing foot ulcers are among the most frequent concerns in this group. The incidence of PAD is estimated to be two to four times higher in individuals with diabetes compared to those without,[6] and diabetes is present in roughly 20-30% of patients diagnosed with PAD.[7] An estimated 15% of diabetic individuals will develop a foot ulcer during their lifetime,[6] and PAD is identified in up to 90% of diabetic patients who undergo major limb amputation.[8] Diabetes is, in fact, the most common cause of non-traumatic lower limb amputations, with rates of major amputation being 5-10 times greater than those in non-diabetic individuals.[9]

Address for Correspondence: Cuma Süleymanoğlu MD, Clinic of Cardiology, Osmaniye State Hospital, Osmaniye, Türkiye
E-mail: j92sulaiman@gmail.com **ORCID ID:** orcid.org/0000-0002-0108-2824

Cite as: Süleymanoğlu C, Kıdık A, Kaya Z, Çamkıran V. Outcomes and predictors of amputation after endovascular revascularization in diabetic foot disease with peripheral artery involvement. *Inter Cardio Pers*. 2025;1(2):52-58

Received: 04.06.2025
Accepted: 21.07.2025
Publication Date: 11.08.2025

Vascular disease in diabetes is predominantly macrovascular in nature, resulting from atherosclerosis, rather than being caused by microvascular arteriolar obstruction.[10] This distinction holds clinical importance, as macrovascular disease is often responsive to revascularization procedures. Nevertheless, diabetes also induces microvascular dysfunction through autonomic neuropathy (neuroischemia), which leads to capillary hypoperfusion and compromised collateral blood flow.[11] Furthermore, endothelial dysfunction and reduced nitric oxide-mediated vasodilation contribute to the worsening of ischemic injury.[12] In diabetic patients, PAD typically presents at a younger age, advances more quickly, and frequently affects long, distal segments of the arterial system.[7]

Multiple classification systems are used to assess the severity of PAD and guide treatment strategies. The Fontaine and Rutherford systems are commonly used for clinical staging.[13] In the Fontaine classification, stage 1 corresponds to asymptomatic disease, stage 2a to claudication occurring beyond 100 m; stage 2b to claudication within 100 meters; stage 3 to rest pain; and stage 4 to ulceration or gangrene—stages 3 and 4 are categorized as critical limb ischemia (CLI). The Wagner classification is typically applied to grade the severity of diabetic foot ulcers,[14] while the TASC II classification provides anatomical stratification of aortoiliac and femoropopliteal lesions.[15]

This study evaluated diabetic patients with PAD who underwent percutaneous revascularization. We compared those who eventually underwent limb amputation during follow-up with those who did not, emphasizing clinical parameters and potential predictors of limb salvage versus limb loss.

METHODS

This retrospective study was carried out in the Clinic of Cardiology at Osmaniye State Hospital over a 1-year period, from March 2023 to April 2024. The objective was to evaluate the outcomes of 100 endovascular revascularization procedures performed in patients with ischemic diabetic foot.

Patient Selection and Ethical Approval

Patients were referred from the diabetic foot clinic as confirmed cases of DM, diagnosed based on the criteria established by the American Diabetes Association, and presented with ischemic foot lesions. Informed consent was obtained from all participants after a thorough explanation of the procedure and possible complications. The study received ethical approval from the Osmaniye State Hospital Ethical Committee (decision number: 254426875, date: 19.09.2024).

Diagnostic Evaluation

All patients underwent Doppler ultrasonography to localize, visualize, and assess the hemodynamic characteristics of arterial lesions. Evaluations included gray-scale imaging, color Doppler mapping, power Doppler, and pulsed-wave Doppler to assess blood flow.

Conventional angiography was performed in all cases. Percutaneous transluminal angioplasty was carried out on one or more infrapopliteal arteries—preferably targeting the artery supplying the ulcer—when critical stenosis or occlusion was identified. For patients with associated superficial femoral artery (SFA) involvement, SFA angioplasty was performed during the same session.

Medical Management

All patients received comprehensive medical treatment for cardiovascular risk factors. Perioperative management included the following:

- Surgical debridement of necrotic tissue,

- Glycemic control using insulin therapy,

- Administration of broad-spectrum antibiotics,

- Antiplatelet therapy with aspirin (100 mg/day) and/or clopidogrel (75 mg/day).

For patients with elevated creatinine levels (>1.1 mg/dL), a renal protection strategy was implemented, which included intravenous hydration and oral N-acetylcysteine (600 mg twice daily) starting the day before the procedure. Metformin was discontinued 2 days prior to angiography and resumed afterward. Dialysis was initiated in patients who developed renal failure following the procedure. Blood urea nitrogen and serum creatinine were routinely assessed prior to angioplasty.

Interventional Procedure

All procedures were conducted under local anesthesia. The primary approach involved an anterograde puncture of the ipsilateral common femoral artery (CFA) using a 6F introducer sheath. In select cases, a contralateral CFA puncture with a crossover technique was employed. Angiographic evaluation utilized a nonionic contrast agent (iodixanol), digital subtraction angiography, and multiple oblique and lateral views of the foot to ensure optimal visualization.

Lesions were traversed using 0.014", 0.018", or 0.035" guidewires. For total occlusions, true lumen recanalization was the first-line approach, using dedicated coronary or peripheral guidewires. If this was unsuccessful, a subintimal technique was used.

Balloon angioplasty commenced with predilation using low-profile balloons, followed by inflation of peripheral balloons selected according to a 1:1 artery-to-balloon diameter and ratio and the length of the lesion, with inflation maintained for 3 minutes. No stents were deployed in any of the interventions. Intravenous heparin (70 IU/kg) was administered following guidewire advancement. In cases of vessel spasm, a bolus of 0.1-0.2 mg intra-arterial nitroglycerin was administered. Hemostasis at the puncture site was achieved with manual compression.

Statistical Analysis

All statistical analyses were conducted using IBM Statistical Package for the Social Sciences statistics for Windows, version 25.0 (IBM Corp., Armonk, NY, USA). The distribution of continuous variables was assessed visually through histograms and Q-Q plots. Descriptive statistics are reported as mean±standard deviation for variables with normal distribution, median (interquartile range, 25^{th}-75^{th} percentile) for variables without normal distribution, and frequency (percentage) for categorical variables.

Group comparisons were made using the Student's t-test for normally distributed continuous variables and the Mann-Whitney U test for those not normally distributed. Categorical variables were analyzed using the chi-squared test, Fisher's exact test, or the Fisher-Freeman-Halton test, depending on the context.

Receiver operating characteristic (ROC) curve analysis was used to assess the predictive value of clinical and laboratory variables for amputation. Optimal cut-off points were identified by maximizing Youden's index. A two-sided p value of <0.05 was considered statistically significant.

RESULTS

The study included 100 patients, consisting of 62 males and 38 females, with a mean age of 60.46±9.43 years (range, 40-80 years). Major lower extremity amputation was performed in 15 patients (15.0%). No in-hospital deaths were recorded.

There were no statistically significant differences in age or sex between the amputation and non-amputation groups.

Clinical Classifications and Disease Severity

Patients who underwent amputation had significantly more severe disease, as indicated by the following:

Rutherford classification: Grade 3/category 5 and grade 3/category 6 were significantly more prevalent in the amputation group (p<0.001).

Fontaine classification: Grade 4 occurred significantly more often in the amputation group (p<0.001).

Wagner classification: Grade 4 was significantly more frequent among patients who underwent amputation (p<0.001).

WIfI (Wound, Ischemia, and foot Infection) classification: Grade 3 was significantly more common in the amputation group (p<0.001).

TASC II classification: Type D lesions were significantly more prevalent in the amputation group (p<0.001).

Diabetes-related and Baseline Characteristics

The duration of DM was significantly longer in the amputation group (p=0.011), and a previous history of amputation was also significantly more frequent in this group (p<0.001).

There were no statistically significant differences between the groups in terms of smoking status, hypertension, or history of coronary artery disease.

Procedural Characteristics

Combined below- and above-knee interventions were significantly more common in patients who underwent amputation (p<0.001). Additionally, the amount of contrast agent used was significantly greater in this group (p<0.001). Balloon diameter and inflation time (3 minutes in all cases) did not differ significantly between the groups.

Renal Function and Contrast-induced Nephropathy

Baseline serum creatinine levels were significantly higher (p<0.001), and estimated glomerular filtration rate (eGFR) was significantly lower (p<0.001) in the amputation group. An increase in creatinine levels occurred in six patients (6.0%), and two patients (2.0%) required temporary hemodialysis. Although the frequency of creatinine elevation was significantly greater in the amputation group (p<0.001), the requirement for hemodialysis did not significantly differ between the groups.

Metabolic and Inflammatory Markers

Patients in the amputation group exhibited significantly poorer glycemic and lipid control:

- Baseline hemoglobin A1c (HbA1c) (p=0.001) and 6-month HbA1c (p=0.002) levels were elevated.

- Baseline low-density lipoprotein (LDL) (p<0.001) and 6-month LDL (p=0.002) levels were also higher.

- Baseline C-reactive protein (CRP) (p<0.001) and 6-month CRP (p<0.001) levels were significantly increased.

No significant differences were found between the groups regarding baseline or 6-month hemoglobin levels (Table 1).

Predictive Value of the Clinical Classification Systems

All five classification systems—Rutherford, Fontaine, Wagner, WIfI, and TASC II—were statistically significant predictors of amputation (each with p<0.001).

Among these:

- Rutherford, Fontaine, and Wagner classifications demonstrated the highest sensitivity (100.0%) and negative predictive value (NPV) (100.0%), indicating strong reliability in excluding amputation risk in lower-grade cases.

- Wagner classification showed the highest specificity (96.47%), accuracy (97.0%), and positive predictive value (PPV) (83.33%), making it the most effective tool for predicting limb loss in this cohort.

- Wagner classification also achieved the highest area under the ROC curve (AUC) [AUC=0.982, 95% confidence interval (CI): 0.959-1.000], indicating excellent diagnostic accuracy (Table 2).

Predictive Value of the Baseline Laboratory Parameters

Baseline levels of creatinine (p<0.001), eGFR (p<0.001), HbA1c (p=0.001), LDL (p<0.001), and CRP (p<0.001) were all statistically significant predictors of major limb amputation.

Among these markers:

- HbA1c and CRP showed the highest sensitivity (100.0%) and NPV (100.0%), indicating strong utility in ruling out amputation risk when values are within normal limits.

- eGFR demonstrated the highest specificity (92.94%), accuracy (91.0%), and PPV (66.67%), supporting its usefulness in identifying patients at higher risk.

- CRP achieved the largest (AUC=0.944, 95% CI: 0.897-0.990), reflecting excellent discriminative power for predicting limb loss (Figures 1, 2 and, Table 3).

Table 1. Summary of variables by amputation status

		Amputation		
	Total (n=100)	**No (n=85)**	**Yes (n=15)**	**p**
Age	60.46±9.43	60.82±9.22	58.40±10.61	0.361†
Sex				
Male	62 (62.00%)	54 (63.53%)	8 (53.33%)	0.644#
Female	38 (38.00%)	31 (36.47%)	7 (46.67%)	
Rutherford classification				
Grade 1/category 3	22 (22.00%)	22 (25.88%)	0 (0.00%)	**<0.001¶**
Grade 2/category 4	34 (34.00%)	34 (40.00%)	0 (0.00%)	
Grade 3/category 5	25 (25.00%)	18 (21.18%)	7 (46.67%)	
Grade 4/category 6	19 (19.00%)	11 (12.94%)	8 (53.33%)	
Fontaine classification				
Grade 2b	22 (22.00%)	22 (25.88%)	0 (0.00%)	**<0.001#**
Grade 3	34 (34.00%)	34 (40.00%)	0 (0.00%)	
Grade 4	44 (44.00%)	29 (34.12%)	15 (100.00%)	
Wagner classification				
Grade 0	20 (20.00%)	20 (23.53%)	0 (0.00%)	**<0.001¶**
Grade 1	26 (26.00%)	26 (30.59%)	0 (0.00%)	
Grade 2	21 (21.00%)	21 (24.71%)	0 (0.00%)	
Grade 3	15 (15.00%)	15 (17.65%)	0 (0.00%)	
Grade 4	18 (18.00%)	3 (3.53%)	15 (100.00%)	
Grade 5	0 (0.00%)	0 (0.00%)	0 (0.00%)	
WIfI classification system				
Grade 0	0 (0.00%)	0 (0.00%)	0 (0.00%)	**<0.001#**
Grade 1	41 (41.00%)	41 (48.24%)	0 (0.00%)	
Grade 2	34 (34.00%)	31 (36.47%)	3 (20.00%)	
Grade 3	25 (25.00%)	13 (15.29%)	12 (80.00%)	
TASC II classification				
Type A	24 (24.00%)	24 (28.24%)	0 (0.00%)	**<0.001¶**
Type B	24 (24.00%)	24 (28.24%)	0 (0.00%)	
Type C	28 (28.00%)	24 (28.24%)	4 (26.67%)	
Type D	24 (24.00%)	13 (15.29%)	11 (73.33%)	
Smoking	72 (72.00%)	59 (69.41%)	13 (86.67%)	0.222§
Duration of diabetes, years	8 (7-9)	8 (6-9)	9 (8-9)	**0.011‡**
Comorbidity				
Hypertension	28 (28.00%)	26 (30.59%)	2 (13.33%)	0.293¶
Coronary artery disease	48 (48.00%)	38 (44.71%)	10 (66.67%)	
Both	24 (24.00%)	21 (24.71%)	3 (20.00%)	
Prior amputation	23 (23.00%)	10 (11.76%)	13 (86.67%)	**<0.001§**
Location of the intervention				
Below knee	65 (65.00%)	63 (74.12%)	2 (13.33%)	**<0.001#**
Below and above the knee	35 (35.00%)	22 (25.88%)	13 (86.67%)	
Amount of contrast substance, cc	26 (24-28)	24 (24-28)	28 (28-30)	**<0.001‡**

Table 1. Continued

		Amputation		
	Total (n=100)	**No (n=85)**	**Yes (n=15)**	**p**
Size of the balloon				
2.0 mm	44 (44.00%)	38 (44.71%)	6 (40.00%)	
2.5 mm	31 (31.00%)	24 (28.24%)	7 (46.67%)	0.325¶
3.0 mm	25 (25.00%)	23 (27.06%)	2 (13.33%)	
Balloon inflation time per lesion				
3 min	100 (100.00%)	85 (100.00%)	15 (100.00%)	N/A
Creatinine	0.93 (0.74-1.14)	0.89 (0.72-1.00)	1.52 (1.21-1.64)	**<0.001**‡
eGFR	87.5 (67-97)	89 (79-97)	47 (42-53)	**<0.001**‡
Increase in the creatinine	6 (6.00%)	1 (1.18%)	5 (33.33%)	**<0.001**§
Hemodialysis	2 (2.00%)	1 (1.18%)	1 (6.67%)	0.279§
HbA1c				
Baseline	9.25 (8.15-10.55)	8.8 (8.1-10.5)	10.5 (9.8-11.7)	**0.001**‡
6th month	8.35 (7.55-9.2)	8.0 (7.4-9.1)	9.2 (8.7-10.0)	**0.002**‡
LDL				
Baseline	124.5 (104-144)	121 (102-139)	157 (143-162)	**<0.001**‡
6th month	89 (79.5-93.5)	88 (79-93)	92 (89-101)	**0.002**‡
CRP, mg/L				
Baseline	7 (4-18)	7 (4-10)	27 (24-31)	**<0.001**‡
6th month	4 (2-5.5)	4 (2-5)	7 (5-8)	**<0.001**‡
Hemoglobin, g/dL				
Baseline	13.07±0.85	13.04±0.81	13.18±1.05	0.572†
6th month	12.74±0.88	12.71±0.90	12.89±0.78	0.484†

Descriptive statistics are expressed as mean±standard deviation for continuous variables with normal distribution, median (25th-75th percentile) for non-normally distributed continuous variables, and frequency (percentage) for categorical variables.
†Student's t-test, ‡Mann-Whitney U test, #chi-squared test, §Fisher's exact test, ¶Fisher-Freeman-Halton test, N/A: Not applicable, eGFR: Estimated glomerular filtration rate, HbA1c: Hemoglobin A1c, LDL: Low-density lipoprotein, CRP: C-reactive protein

Table 2. Predictive performance of clinical classification systems and ROC curve analysis for amputation

Classification	**Rutherford**	**Fontaine**	**Wagner's**	**WIfI**	**TASC II**
Cut-off	Grade 3	Grade 4	Grade 4	Grade 3	Type D
Sensitivity	100.00%	100.00%	100.00%	80.00%	73.33%
Specificity	65.88%	65.88%	96.47%	84.71%	84.71%
Accuracy	71.00%	71.00%	97.00%	84.00%	83.00%
PPV	34.09%	34.09%	83.33%	48.00%	45.83%
NPV	100.00%	100.00%	100.00%	96.00%	94.74%
AUC (95% CI)	0.856 (0.780-0.931)	0.829 (0.749-0.910)	0.982 (0.959-1.000)	0.872 (0.793-0.950)	0.865 (0.789-0.942)
p	**<0.001**	**<0.001**	**<0.001**	**<0.001**	**<0.001**

ROC: Receiver operating characteristic, PPV: Positive predictive value, NPV: Negative predictive value, AUC: Area under the ROC curve, CI: Confidence interval

Table 3. Predictive performance of baseline laboratory parameters and ROC curve analysis for amputation

Measurement, baseline	Creatinine	eGFR	HbA1c	LDL	CRP
Cut-off	>1.20	≤55	>9.4	>133	>11
Sensitivity	80.00%	80.00%	100.00%	93.33%	100.00%
Specificity	88.24%	92.94%	60.00%	69.41%	78.82%
Accuracy	87.00%	91.00%	66.00%	73.00%	82.00%
PPV	54.55%	66.67%	30.61%	35.00%	45.45%
NPV	96.15%	96.34%	100.00%	98.33%	100.00%
AUC (95% CI)	0.887 (0.798-0.975)	0.896 (0.807-0.985)	0.771 (0.674-0.869)	0.864 (0.787-0.941)	0.944 (0.897-0.990)
p	<0.001	<0.001	0.001	<0.001	<0.001

ROC: Receiver operating characteristic, PPV: Positive predictive value, NPV: Negative predictive value, AUC: Area under the ROC curve, CI: Confidence interval, eGFR: Estimated glomerular filtration rate, HbA1c: Hemoglobin A1c, LDL: Low-density lipoprotein, CRP: C-reactive protein

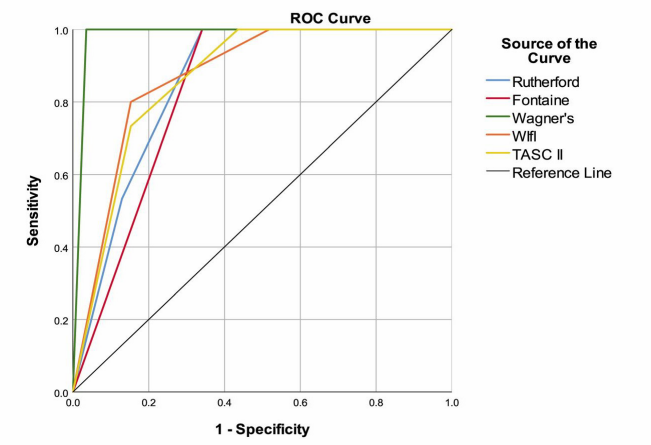

Figure 1. ROC curves for clinical classification systems. ROC curves illustrating the predictive accuracy of the Wagner, Rutherford, Fontaine, WIfI, and TASC II classifications for amputation in patients with diabetic peripheral artery disease

ROC: Receiver operating characteristic

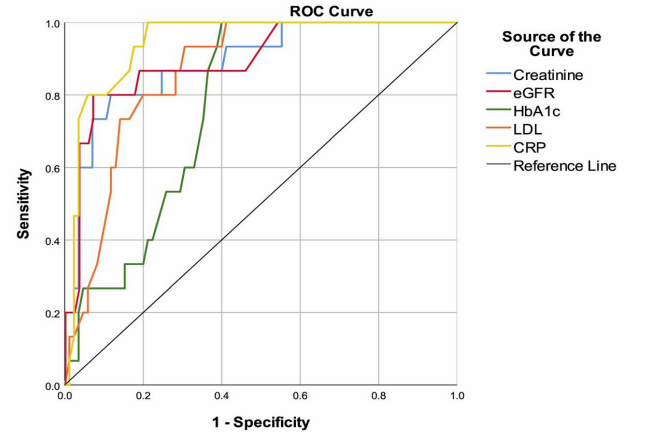

Figure 2. ROC curves for baseline laboratory parameters. ROC curves depicting the predictive performance of baseline laboratory values (HbA1c, creatinine, eGFR, CRP, LDL) for amputation in patients with diabetic peripheral artery disease

ROC: Receiver operating characteristic, eGFR: Estimated glomerular filtration rate, HbA1c: Hemoglobin A1c, LDL: Low-density lipoprotein, CRP: C-reactive protein

DISCUSSION

This study evaluated 100 patients with diabetic PAD who underwent percutaneous revascularization, among whom 15 required major amputation during follow-up. Demographic characteristics and comorbid conditions were comparable between the amputation and non-amputation groups, with the exception of diabetes duration, which was significantly longer in those who underwent amputation.

Inadequate glycemic control, as indicated by elevated baseline and 6-month HbA1c levels, was also significantly linked to a higher risk of amputation. This observation is consistent with earlier studies showing that poor diabetes control and prolonged disease duration are associated with a greater incidence and severity of diabetes-related complications, including PAD.[16,17] These findings emphasize the essential role of maintaining tight glycemic control to reduce the risk of limb-threatening ischemia.

Renal dysfunction was significantly more pronounced in the amputation group, as indicated by higher baseline creatinine levels and lower eGFR. This finding suggests that PAD severity may reflect broader systemic target organ damage, including renal impairment. The greater volume of contrast agent used during revascularization procedures in this group likely corresponds to more extensive and complex arterial disease, which may contribute to additional kidney injury. As a result, this group exhibited a higher rate of contrast-induced nephropathy, demonstrated by a significant postprocedural increase in creatinine and a greater, though not statistically significant, requirement for hemodialysis.

The study also demonstrated that clinical and anatomical severity scores—specifically the Rutherford, Fontaine, Wagner, WIfI, and TASC II classifications—were significantly higher in patients who underwent amputation. These scoring systems proved to be valuable predictors of amputation risk, highlighting the critical importance of early diagnosis and prompt treatment of PAD to prevent progression to CLI and eventual limb loss.

Collectively, these findings underscore PAD as a serious complication of DM, closely linked to both the duration and severity of the disease, as well as to damage in other target organs. The relationship among poor glycemic control, advanced vascular disease, and declining renal

function highlights the need for integrated management approaches that address all contributing factors.

Finally, the results indicate that patients with advanced PAD should be closely monitored for renal function, particularly when undergoing contrast-enhanced endovascular interventions, to minimize the risk of additional kidney injury and enhance overall clinical outcomes.

Study Limitations

This study has several limitations. First, its retrospective nature may introduce selection bias and restrict the ability to draw causal inferences. Although the sample size was sufficient, it was relatively small and sourced from a single center, which may limit the broader applicability of the results. Furthermore, follow-up was limited to 6 months, and extended observation would be beneficial to assess the long-term durability of revascularization and outcomes such as recurrent ischemia or mortality.

Future research should include prospective, multicenter studies with larger patient populations and longer follow-up periods to confirm these findings. Further investigation into the role of emerging endovascular techniques, adjunct pharmacologic therapies, and integrated multidisciplinary care models in reducing amputation rates among patients with diabetic PAD may help refine treatment approaches.

CONCLUSION

This study shows that diabetic patients with PAD undergoing endovascular revascularization remain at considerable risk for limb amputation, especially those with prolonged diabetes duration, poor glycemic control, advanced PAD classification scores, and compromised renal function. Early detection, effective diabetes management, and close monitoring of kidney function are essential to enhance limb salvage and overall outcomes. These findings highlight the importance of a multidisciplinary approach in the management of diabetic PAD to prevent progression to critical ischemia and the need for amputation.

Ethics Committee Approval: The study received ethical approval from the Osmaniye State Hospital Ethical Committee (decision number: 254426875, date: 19.09.2024).

Informed Consent: Informed consent was obtained from all participants after a thorough explanation of the procedure and possible complications.

Authorship Contributions: Concept: C.S., Design: C.S., Data Collection or Processing: C.S., A.K., Analysis or Interpretation: V.Ç., Literature Search: Z.K., Writing: C.S., Z.K.

Conflict of Interest: No conflict of interest was declared by the authors.

Financial Disclosure: The authors declared that this study received no financial support.

REFERENCES

1. Fan W. Epidemiology in diabetes mellitus and cardiovascular disease. *Cardiovasc Endocrinol*. 2017;6:8-16.
2. Leon BM, Maddox TM. Diabetes and cardiovascular disease: epidemiology, biological mechanisms, treatment recommendations and future research. *World J Diabetes*. 2015;6:1246-1258.
3. Simon F, Oberhuber A, Floros N, Düppers P, Schelzig H, Duran M. Pathophysiology of chronic limb ischemia. *Gefasschirurgie*. 2018;23:13-18.
4. Aronow WS. Peripheral arterial disease of the lower extremities. *Arch Med Sci*. 2012;8:375-388.
5. Wukich DK, Shen W, Raspovic KM, Suder NC, Baril DT, Avgerinos E. Noninvasive arterial testing in patients with diabetes: a guide for foot and ankle surgeons. *Foot Ankle Int*. 2015;36:1391-1399.
6. Akkus G, Sert M. Diabetic foot ulcers: a devastating complication of diabetes mellitus continues non-stop in spite of new medical treatment modalities. *World J Diabetes*. 2022;13:1106-1121.
7. Thiruvoipati T, Kielhorn CE, Armstrong EJ. Peripheral artery disease in patients with diabetes: epidemiology, mechanisms, and outcomes. *World J Diabetes*. 2015;6:961-969.
8. Humphries MD, Brunson A, Hedayati N, Romano P, Melnkow J. Amputation risk in patients with diabetes mellitus and peripheral artery disease using statewide data. *Ann Vasc Surg*. 2016;30:123-131.
9. Costa WJT, Penha-Silva N, Bezerra IMP, et al. Analysis of diabetes mellitus-related amputations in the state of Espírito Santo, Brazil. *Medicina*. 2020;56:287.
10. Cade WT. Diabetes-related microvascular and macrovascular diseases in the physical therapy setting. Phys Ther. 2008;88:1322-1335.
11. Nukada H. Ischemia and diabetic neuropathy. *Handb Clin Neurol*. 2014;126:469-487.
12. Tabit CE, Chung WB, Hamburg NM, Vita JA. Endothelial dysfunction in diabetes mellitus: molecular mechanisms and clinical implications. *Rev Endocr Metab Disord*. 2010;11:61-74.
13. Hardman RL, Jazaeri O, Yi J, Smith M, Gupta R. Overview of classification systems in peripheral artery disease. *Semin Intervent Radiol*. 2014;31:378-388.
14. Morbach S, Müller E, Reike H, et al. Dieser Beitrag ist eine aktualisierte version des beitrags: Diabetisches Fußsyndrom. *Diabetologie*. 2017;12(Suppl 2):181-189.
15. Jaff MR, White CJ, Hiatt WR, et al. An update on methods for revascularization and expansion of the TASC lesion classification to include below-the-knee arteries: a supplement to the inter-society consensus for the management of peripheral arterial disease (TASC II). *Vasc Med*. 2015;20:465-478.
16. Memon R, Levitt D, Munir K, et al. Knowledge of hemoglobin A1c and glycemic control in an urban population. *Cureus*. 2021;13:13995.
17. Jude EB, Oyibo SO, Chalmers N, Boulton AJ. Peripheral arterial disease in diabetic and nondiabetic patients: a comparison of severity and outcome. *Diabetes Care*. 2001;24:1433-1437.

INTERVENTIONAL CARDIOLOGY PERSPECTIVES

Inter Cardio Pers 2025;1(2):59-66

DOI: 10.4274/intercardiopers.2025.2025-3-4

ORIGINAL ARTICLE

Association Among Levels of Troponin and Inflammatory Biomarkers at Admission with SARS-CoV-2 Disease Severity and Recent Cardiac Injury Detected Using Cardiac Magnetic Resonance Imaging

Mikail Yarlıoğlueş[1], Damla Yalçınkaya Öner[1], Hasan Yiğit[2], Uğur Bozkurt[1], Sani Namık Murat[1]

[1]Clinic of Cardiology, University of Health Sciences Türkiye, Ankara Training and Research Hospital, Ankara, Türkiye

[2]Clinic of Radiology, University of Health Sciences Türkiye, Ankara Training and Research Hospital, Ankara, Türkiye

ABSTRACT

Background: Troponin and select inflammation biomarkers are associated with Coronavirus disease-2019 (COVID-19) severity and intensive care unit (ICU) admissions related to cardiac injury. However, cardiac magnetic resonance imaging (CMRI) remains the gold standard for detecting myocardial involvement.

Aim: This study aimed to determine whether troponin levels at admission are associated with clinical severity and CMRI-confirmed cardiac injury.

Study Design: A prospective, observational cohort study involving 51 recovered COVID-19 patients, categorized into ICU (n=16) and non-ICU (n=35) groups, and assessed 4-6 weeks postdischarge.

Methods: Blood samples were collected during hospital admission to ascertain the levels of high-sensitivity cardiac troponin T (hs-cTnT), C-reactive protein (CRP), procalcitonin, neutrophil-to-lymphocyte ratio (NLR), D-dimer, ferritin, and systemic immune-inflammation index (SII). Patients also underwent electrocardiography (ECG), transthoracic echocardiography (TTE), and CMRI. Group differences were analyzed statistically, and receiver operating characteristic (ROC) curve analysis assessed biomarker predictive performance for ICU admission and cardiac injury.

Results: ICU patients had considerably greater levels of inflammatory biomarkers and hs-cTnT ($p<0.05$). The ROC curve analysis revealed that hs-cTnT, NLR, D-dimer, ferritin, CRP, and SII levels predicted ICU admission ($p<0.05$). ECG and TTE findings were comparable between the groups. On CMRI, non-ischemic fibrosis was observed to be more prevalent in ICU patients ($p=0.03$). ROC curve revealed that hs-cTnT and SII levels predicted CMRI-detected cardiac injury ($p<0.05$).

Conclusion: The troponin and SII levels at admission were associated with disease severity and CMRI-confirmed cardiac injury, even in the presence of normal echocardiographic findings. Both markers may help predict ICU necessity and serious cardiac involvement.

Keywords: COVID-19, clinical severity, cardiac injury, biomarkers, MRI

INTRODUCTION

Coronavirus disease-2019 (COVID-19), caused by Severe acute respiratory syndrome-Coronavirus-2 (SARS-CoV-2), has continued to spread globally since its emergence in 2019. Despite primarily affecting the respiratory tract, cardiovascular (CV) manifestations have become increasingly significant in terms of mortality and morbidity.[1,2] A review article examining the relationship between COVID-19 and CV involvement found that myocardial injury occurred in over a quarter of critically ill patients, either during the acute phase or as the disease severity progressed.[3]

Multiple biomarkers have been associated with COVID-19 severity and intensive care unit (ICU) admissions.[4-6] Patients with elevated high-sensitivity cardiac troponin I (cTnI), cardiac troponin T (cTnT), creatine kinase-myocardial band (CK-MB), dimerized plasma fragment (D-dimer), C-reactive protein (CRP), and interleukin-6 (IL-6) have been linked to a higher risk of developing severe disease or requiring ICU admission due to cardiac injury.[7-9]

Although several biomarkers can predict cardiac injury, cardiac magnetic resonance imaging (CMRI) remains the gold standard for detecting myocardial involvement.[10] Recovered COVID-19 patients exhibited elevated rates of cardiac involvement on CMRI, with even

Address for Correspondence: Damla Yalçınkaya Öner MD, Clinic of Cardiology, University of Health Sciences Türkiye, Ankara Training and Research Hospital, Ankara, Türkiye

E-mail: damlaykaya@gmail.com **ORCID ID:** orcid.org/0000-0002-8047-389X

Cite as: Yarlıoğlueş M, Yalçınkaya Öner D, Yiğit H, Bozkurt U, Murat SN. Association among levels of troponin and inflammatory biomarkers at admission with SARS-CoV-2 disease severity and recent cardiac injury detected using cardiac magnetic resonance imaging. *Inter Cardio Pers*. 2025;1(2):59-66

Received: 03.03.2025
Accepted: 11.05.2025
Epub: 11.07.2025
Publication Date: 11.08.2025

higher prevalence observed in more severe cases.[11,12] This study aimed to investigate the association between admission troponin levels, clinical severity, and CMRI-confirmed cardiac injury.

MATERIALS AND METHODS

Study Population and Design

This single-center, prospective, observational cohort study included patients diagnosed with COVID-19 on reverse transcription-polymerase chain reaction (RT-PCR). Patients over 18 years of age with a positive RT-PCR test who required in-hospital follow-up either in COVID-19 clinics or COVID-19 ICU were included. In COVID-19 clinics, patients with characteristic COVID-19-related symptoms and a respiratory rate (RR) >24 beats per minute or an oxygen saturation (SpO_2) <93% were monitored. ICU admission criteria included the following: dyspnea and respiratory distress, RR ≥30/min, ratio of arterial oxygen partial pressure to fractional inspired oxygen (PaO_2/FiO_2) 300, elevated oxygen requirement, SpO_2 <90% or PaO_2 <70 mmHg despite 5 L/min oxygen therapy, hypotension (systolic blood pressure <90 mmHg or a drop in systolic blood pressure of more than 40 mmHg and mean arterial pressure <65 mmHg), tachycardia (>100 beats/min), acute kidney damage, impaired liver function tests, development of acute organ dysfunction (confusion, acute bleeding diathesis, etc.), immunosuppression, troponin elevation, arrhythmia, lactate >2 mmol, and skin disorders such as capillary return disorder and cutis marmaratus existence. The study excluded those under the age of 18 years, those who did not need in-hospital follow-up (RR under 24/minute, SpO_2 above 93%, and absence of bilateral diffuse (>50%) involvement on lung imaging), those with contraindications for CMRI, and those who did not volunteer.

Between November 2020 and March 2021, we enrolled 70 patients with COVID-19 who required in-hospital follow-up. The study participants were examined in two separate groups. Group 1 (n=24) contained patients who needed COVID-19 ICU follow-up, and group 2 (n=46) included patients who did not require ICU and were monitored in the COVID-19 clinics. Of these patients, four died and eight declined to participate in the study. Following their discharge, 58 patients who recovered and survived COVID-19 were monitored. Patients were deemed to have recovered if their symptoms subsided and their inflammatory markers returned to normal while their swab test findings were negative. CMRI appointments were scheduled for all participants, typically 4-6 weeks following discharge. Finally, our study population consisted of 51 patients (group 1, n=16 and group 2, n=35) after excluding those lost to follow-up (n=4) and those unable to undergo CMRI for any reason (n=3). Transthoracic echocardiogram (TTE), CMRI, and electrocardiogram (ECG) were performed concurrently on all 51 participants. Figure 1 presents the study flow diagram.

This study was conducted in accordance with the principles of the Declaration of Helsinki and was approved by the Local Ethical Committee of the Ankara Training and Research Hospital, Ankara, Türkiye (approval number: 485/2020, date: 15.01.2021). Approval for the study was obtained from the Scientific Research Platform of the Ministry of Health in Türkiye. Written informed consent was obtained from each patient after providing detailed information regarding the

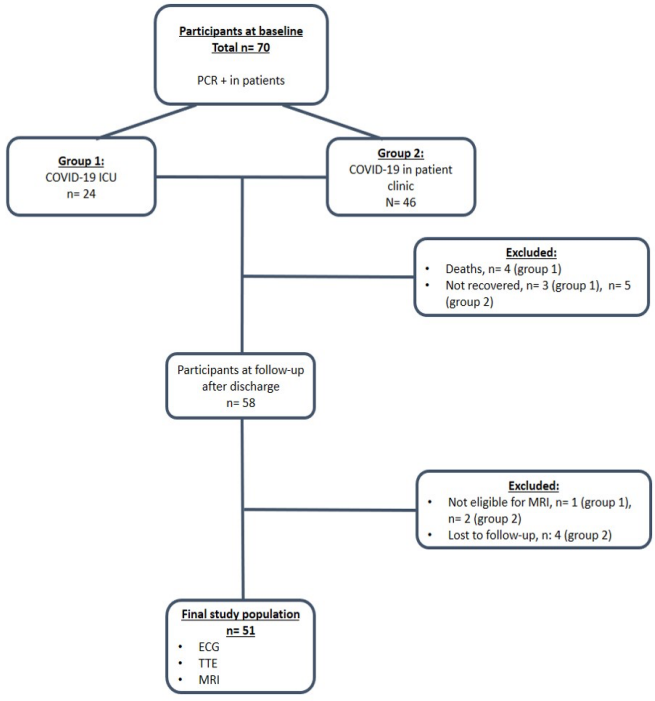

Figure 1. Flow diagram of the study population
PCR: Polymerase chain reaction, COVID-19: Coronavirus disease-2019, ICU: Intensive care unit, MRI: Magnetic resonance imaging, ECG: Electrocardiography, TTE: Transthoracic echocardiography

study. Patients or the public were not involved in the design, conduct, reporting, or dissemination plans of this study.

Data Collection and Analysis

Demographic data (sex, age, and body mass index) and clinical information, including the presence of hypertension, diabetes mellitus, hyperlipidemia, coronary artery disease, heart failure, cerebrovascular disease, chronic kidney disease, chronic obstructive pulmonary disease, history of smoking, and COVID-19 RT-PCR results, were obtained from the electronic medical records and medical history forms. Initial symptoms, vital signs, and treatment administered were recorded during the in-hospital follow-up. ECG, TTE, and CMRI were performed concurrently after discharge and were evaluated by specialists in the relevant field.

Cardiac Magnetic Resonance Imaging

CMRI was performed using a 1.5 Tesla MR system (Magnetom Aera, Siemens Healthineers) with an 18-channel phased-array torso surface coil. To synchronize with the cardiac cycle, vectorcardiography was employed, and breath-hold imaging for image acquisition. Blood samples were collected while the patients were on the CMRI table, immediately before the scan, to determine hematocrit levels required for extracellular volume (ECV) calculation.

The CMRI protocol comprised static axial balanced steady-state free precession (b-SSFP) and half-Fourier acquisition single-shot turbo spin echo images beginning from the supra-aortic level and encompassing the entire heart and cine long-axis and short-axis images of both

ventricles and the left ventricular (LV) outflow tract obtained using the b-SSFP sequence. T2-weighted short-tau inversion recovery and late gadolinium enhancement (LGE) images were acquired in both long-axis and short-axis planes. For LGE imaging, a phase sensitive inversion-recovery sequence was performed ten minutes after administering gadolinium-based contrast material at a dose of 0.15 mmol/kg; TI scout software was used to determine the optimal inversion time. T2 mapping, native precontrast, and postcontrast T1 mapping sequences were added to the protocol and acquired at the same long-axis and short-axis image planes. An optimized modified look-locker inversion recovery sequence was employed for T1 mapping, acquired with a 5(3)3 scheme before contrast administration and a 4(1)3(1)2 scheme after contrast. For T2 mapping, a T2-prepared b-SSFP sequence was utilized.

Image analyses were performed on a remote diagnostic workstation (Leonardo Syngo MR E11, Siemens Healthineers) by a radiologist with 13 years of experience in CMRI. The radiologist was blinded to the participants' data when assessing the CMRI images. Cardiac analysis software (Argus; Siemens Healthineers) was used for routine cardiac measurements and functional assessment. T2-weighted short-tau inversion-recovery sequences and T2 maps were used to determine the presence of focal or global myocardial edema. Myocardial damage was assessed using both precontrast native T1 maps and postcontrast T1 maps. Pre- and post-contrast T1 and T2 times were measured using a region of interest (ROI) from focal myocardial lesions, and the ECV was calculated for these lesions. Furthermore, the mean native T1 and T2 times were ascertained with an ROI positioned in the lesion-free areas of the septal wall in all patients, and the mean myocardial ECV volume was calculated. The normal ranges of T1 and T2 times for our scanner were previously established in healthy volunteers, in accordance with the consensus statement of the Society for Cardiovascular Magnetic Resonance.

Transthoracic Echocardiography

Echocardiography was performed using a standard imaging system (Vivid S60N, GE Healthcare) equipped with a 1.5- to 4-MHz phased-array transducer. Quantitative measurements followed the American Society of Echocardiography guidelines.[13] All measurements for each participant were performed by the same specialist. The researchers were blinded to the participants' data when analyzing the TTE images. All assessments were performed with the participant in the left lateral decubitus position. LV volumes and LV ejection fraction (LVEF) were measured based on the modified two-dimensional biplane Simpson's method from apical 2 and 4-chamber views. LV end diastolic and LV end-systolic diameters were calculated using the Teichholz method from the parasternal long-axis view. Mitral inflow E and A wave velocities were assessed using pulsed wave (PW) Doppler from the apical four-chamber view, and the E/A ratio was calculated. The E' wave velocity was measured using PW tissue Doppler at the lateral mitral annulus, and the E/e' ratio was calculated. Right ventricular (RV) functioning was assessed using tricuspid annular plane systolic excursion (TAPSE) and tricuspid S' velocity. TAPSE and tricuspid S' velocity were measured through the apical four-chamber view using M-mode echocardiography and PW tissue Doppler at the lateral tricuspid annulus, respectively. The peak tricuspid regurgitation velocity was measured, while the systolic pulmonary artery pressure was evaluated using the modified Bernoulli equation.

Laboratory Findings

Blood samples were collected from patients upon hospital admission, within the first 24 hours after onset of their symptoms. Sample-giving time was defined as the interval between the onset of symptoms and the time of blood sampling. Routine blood tests included: complete blood count; serum biochemical tests [renal and liver function, creatinine kinase, glomerular filtration rate (mL/min/1.73 m^2), aspartate aminotransferase (units/L), alanine aminotransferase (units/L), and albumin levels (g/dL)]; inflammatory biomarkers [CRP, mg/dL, procalcitonin (PCT), ng/mL and ferritin, ng/mL]; coagulation biomarkers (D-dimer, ng/mL and fibrinogen, mg/dL); and cardiac biomarkers [high-sensitive cTnT (hs-cTnT, ng/L) and CK-MB, ng/mL]. Standardized test kits for hs-cTnT assay were used to process blood samples (Roche Diagnostics Cobas e411). The local laboratory cut-off value for detectable hs-cTnT was greater than 3 ng/L, with levels exceeding the 99th percentile (13.9 ng/L) considered significantly elevated. Hematological indices were measured using a SYSMEX XN-3000 automated hematology analyzer. Additionally, creatinine, serum electrolytes, and detailed liver function tests were performed utilizing a Roche Diagnostics Cobas 8000 modular analyzer. The neutrophil-to-lymphocyte ratio (NLR) represents the NLR, while the systemic immune-inflammation index (SII) is calculated as the ratio of platelet count to NLR.

Statistical Analysis

The post-hoc power analysis indicated that our study had a 91% power with an alpha value of 0.05, as calculated using a network software (https://clincalc.com/stats/Power.aspx). All statistical analyses were performed using the Statistical Package for the Social Sciences (SPSS) program (version 22.0; SPSS, Chicago, Illinois, USA). The Kolmogorov-Smirnov test was utilized to ascertain the distribution characteristics of the data. Normally distributed data are presented as mean±standard deviation, while the non-normally distributed data are presented as median (interquartile range). Categorical variables were compared using the chi-square test or Fisher's exact test. Results are presented as percentages. The independent sample t-test was used to evaluate the parametric scale variables, and the Mann-Whitney U test was used to analyze the non-parametric scale variables. Receiver operating characteristic (ROC) curve analysis was performed to establish the cut-off value of biomarkers for predicting the need for ICU and the presence of recent cardiac injury on CMRI. The optimal binning procedure was applied to these variables to reduce the cardinality of continuous and distinct data. A p value less than 0.05 was considered statistically significant.

RESULTS

Among the study population, 25 patients (49%) were infected with SARS-CoV-2 variants, including the alpha variant [n=16, (31%)], beta [n= 5, (10%)], and delta variants [n=4, (8%)]. Table 1 summarizes the baseline characteristics.

Table 1. Basal characteristics, clinical characteristics, and laboratory parameters of study group patients

Variables	All patients (n=51)	Group 1 (n=16)	Group 2 (n=35)	p value
Patient characteristics				
Age, years	53.1±12.7	56.8±11.6	51.3±10.6	0.077
Male, (n, %)	23 (45)	9 (56)	14 (40)	0.21
BMI	28 (24.8-32)	27.5 (24.8-29.2)	27.9 (24.8-30.3)	**0.022**
Hypertension, (n, %)	21 (41)	7 (44)	14 (40)	0.52
Diabetes mellitus, (n, %)	15 (29)	5 (31)	10 (28)	0.54
Hyperlipidemia, (n, %)	7 (14)	1 (6)	6 (17)	0.28
Current smoker, (n, %)	8 (16)	1 (6)	7 (20)	0.2
Prior history of CAD (n, %)	7 (14)	3 (19)	4 (11)	0.38
Prior history of stroke, (n, %)	1 (2)	0	1 (3)	0.68
Heart failure, (n, %)	1 (2)	1 (6)	0	0.31
CKD, (n, %)	5 (10)	1 (6)	4 (11)	0.5
COPD, (n, %)	5 (10)	3 (19)	2 (6)	0.17
Vital signs at rest				
SBP, mmHg	122.12±16.1	121.8±14.5	122.43±16.8	0.76
DBP, mmHg	74.1±.9.7	71.7±9.2	72.7±9.8	0.42
Heart rate (beats/minute)	80.29±13.6	81.1±20.2	78±12.2	0.19
Respiratory rate	19.82±4.7	23±6.7	19.8±2.5	**0.003**
Oxygen saturation level	88.18±11	76.21±14.7	90.2±1.9	**<0.001**
Temperature ≥38 °C, (n, %)	19 (33)	8	11	0.20
Initial symptoms				
Cough, (n, %)	29 (57)	8 (50)	21 (6)	0.35
Respiratory distress, (n, %)	27 (53)	12 (75)	15 (43)	**0.03**
Myalgia, (n, %)	24 (49)	8 (50)	17 (48)	0.58
Chest discomfort, (n, %)	10 (20)	1 (6)	9 (26)	0.10
Palpitation, (n, %)	7 (14)	2 (12)	5 (14)	0.62
Treatments				
Antivirals, (n, %)	50 (98)	16 (100)	34 (97)	0.68
Antibiotics, (n, %)	19 (37)	13 (81)	6 (17)	**<0.001**
IV steroids, (n, %)	32 (63)	15 (94)	17 (48)	**0.002**
Anticoagulants, (n, %)	50 (98)	16 (100)	34 (97)	0.68
Supplemental oxygen				
Nasal cannula, (n, %)	15 (29)	6 (37)	9 (26)	0.29
Reservoir mask, (n, %)	16 (31)	10 (62)	6 (17)	**0.002**
NIMV/high flow rate, (n, %)	10 (20)	10 (62)	0	**<0.001**
IMV, (n, %)	0	0	0	-
Initial laboratory measurements				
Sample collection time and hours	17 (7-23)	16 (6-23)	18 (8-23)	0.69
WBC, $\times 10^6$/L	6.43 (4.86-8.87)	8.2 (6.9-12.5)	5.31 (4-8.4)	**<0.001**
Neutrophil, $\times 10^9$/L	4.46 (3.16-7)	7 (4.82-10.63)	3.53 (2.97-7.13)	**<0.001**
Lymphocyte, $\times 10^9$/L	1.12 (0.73-1.37)	0.98 (0.69-1.4)	1.14 (0.71-1.37)	0.16
NLR	4.1 (2.5-9)	9.35 (3.87-15)	3.7 (2.97-7.13)	**0.001**
Creatine kinase, U/L	0.92±0.46	1.0±0.74	0.93±0.35	0.69
GFR (mL/min/1.73 m^2)	87.2±24.8	82.3±29.5	87.4±24.4	0.69
AST, U/L	25 (18-40)	26.5 (23.92-63.25)	30 (18.75-37.75)	**0.031**
ALT, U/L	23 (14-35)	27.4 (15.5-49.5)	25.5 (17.32-36.75)	**0.043**
Albumin, g/dL	4 (3.6-4.6)	3.2 (2.98-3.75)	4 (3.77-4.35)	**<0.001**
hs-cTnT, ng/L	5.24 (3-14.8)	23 (15.5-85.1)	4.67 (3-9.4)	**<0.001**
CK-MB, ng/mL	1.66 (0.92-2.6)	2 (1-6.2)	1.24 (0.82-2.51)	0.11
Procalcitonin, ng/mL	0.082 (0.05-0.12)	0.11 (0.09-0.33)	0.07 (0.039-0.13)	**<0.001**
D-dimer, ng/mL	490 (280-1330)	1315 (632-2832)	485 (352.5-1080)	**0.002**
Ferritin, ng/mL	387 (123-1000)	973 (403-1265)	337.5 (108-715)	**<0.001**
Fibrinogen, mg/dL	565±187.3	590.5±183.2	593.6±154.5	0.61
CRP, mg/dL	41.35 (12-114.6)	116.7 (41.1-202.1)	50.65 (17.2-98.8)	**0.011**
SII	684 (442.7-966.1)	874 (680.8-1191.9)	570 (387.2-936.2)	**0.024**

BMI: Body mass index, CAD: Coronary artery disease, CKD: Chronic kidney disease, COPD: Chronic obstructive pulmonary disease, NYHA: New York Heart Association, SBP: Systolic blood pressure, DBP: Diastolic blood pressure, NIMV: Non-invasive mechanical ventilation, IMV: Invasive mechanic ventilation, WBC: White blood cell count, NLR: Neutrophil-to-lymphocyte ratio, AST: Aspartate aminotransferase, ALT: Alanine aminotransferase, hs-cTnT: High-sensitivity troponin T, CK-MB: Creatinine kinase myocardial bind, CRP: C-reactive protein, SII: Systemic immune-inflammation index

Group 1 patients experienced more respiratory distress as an initial symptom than group 2 patients. Group 1 patients exhibited higher RR, lower SpO_2 levels, and higher supplemental oxygen requirements than group 2 patients, consistent with the more pronounced respiratory distress. All patients received antiviral therapy. In the ICU arm, the requirement for antibiotics and intravenous steroids during hospitalization exceeded what would typically be anticipated given the disease severity.

Systemic inflammation markers, such as CRP and PCT levels, were significantly higher in group 1 patients. NLR, a crucial predictor of COVID-19 severity, was significantly higher in ICU patients. D-dimer and ferritin levels were also significantly higher in group 1. The SII, which has previously been proven to indicate COVID-19 severity, was significantly higher in group 1 patients. Hs-cTnT levels were significantly higher in group 1 compared to group 2 patients.

The ROC curve was used to determine the predictive value of hs-cTnT, NLR, D-dimer, ferritin, CRP, SII levels, and ICU admission (Supplementary Figure 1). The diagnostic accuracy of each of the significantly distinct biochemical markers was validated by the area under the curve (AUC). The hs-cTnT ROC curve for ICU admission prediction had an AUC of 0.91; the optimal cut-off value was 12.48 ng/L, with a 98% sensitivity and 87% specificity [95% confidence interval (CI): 0.83-0.98, p<0.001]. ICU admission was predicted by an NLR >3.2 with 81% sensitivity and 62% specificity [AUC=0.79 (95% CI: 0.64-0.93), p=0.001]. The optimal cut-off values for D-dimer, ferritin, and CRP to predict ICU admission were 660 ng/mL with a sensitivity of 75% and specificity of 75% [AUC=0.76 (95% CI: 0.62-0.91), p=0.002]; 294 ng/mL, with a 93% sensitivity and 52% specificity [AUC=0.81 (95% CI: 0.69-0.93), p=0.001]; 45.95 mg/dL with a 75% sensitivity and 68% specificity [AUC=0.72 (95% CI: 0.56-0.88), p=0.011], respectively. ICU admission was predicted by SII >683.2 with a 78% sensitivity and a 65% specificity [AUC=0.70 (95% CI: 544-852), p=0.02]. We also evaluated fibrinogen and CK-MB levels; however, no significant threshold values were identified for predicting ICU admission.

Table 2 details the TTE and CMRI features of the study groups. On TTE, LVEF and RV systolic functions were comparable between groups. CMRI data revealed that functional parameters were similar for both

Table 2. Electrocardiographic, transthoracic echocardiographic, and cardiac magnetic resonance imaging findings of study group patients

Variables	All patients	Group 1	Group 2	p value
Echocardiographic findings				
LVEF, %	59.1±7.8	60.3±6	56.9±9	0.77
LVED diameter = mm	49±7	51±7	50±10	0.42
RVED diameter = mm	30±3	33±9	30±4	0.64
PASP, mmHg	28.4±9	29.3±5.3	30.4±8.7	0.69
TAPSE, mm	17.7±5.2	19±5.2	17.1±5.3	0.29
RV S' velocity (mm/s)	12.48±3.2	13.9±2.8	11±2.8	0.12
Cardiac magnetic resonance imaging findings				
LVEF, %	62.23±10.26	60.44±10.84	64.42±9.9	0.46
LVEDV index (mL/m^2)	62±14.8	65.64±13.91	53±8.47	0.33
LVESV index (mL/m^2)	37.7±8.38	39.31±9.33	34±7.4	0.94
LV CO index (l/min/m^2)	2.82±0.53	3±0.58	2.57±0.5	0.28
LV mass index (g/m^2)	54.2±8.6	50.98±10.92	54.78±8	0.43
Native T1 (ms)	1091±81.6	1102±81.2	1102±78.5	0.89
Native T2 (ms)	50.14±3.9	50.5±3.9	48.93±4.8	0.76
EVF, %	34.92±11.34	34.26±9.8	36.38±14	0.59
RVEF, %	55.9±7.38	53.47±7.87	56.91±7.93	0.30
RVEDV index (mL/m^2)	67.12±13	71.6±13	60.43±10.88	0.25
RVESV index (mL/m^2)	37.42±8.52	38.21±9	34.33±7.77	0.73
RV CO index (L/min/m^2)	2.77±0.55	2.93±0.53	2.6±0.54	0.72
Late gadolinium enhancement findings				
Non-ischemic fibrosis, (n, %)	27 (44)	12 (75)	15 (43)	**0.03**
Ischemic fibrosis, (n, %)	8 (16)	3 (19)	5 (14)	0.48
Myocardial edema, (n, %)	7 (14)	3 (19)	4 (11)	0.38
Pericardial effusion, (n, %)	13 (25)	3 (19)	10 (28)	0.35
RV failure, (n, %)	12 (23)	4 (25)	8 (23)	0.56
Any injury, (n, %)	32 (63)	11 (69)	21 (60)	0.39

cQT: Corrected QT, LVEF: Left ventricular ejection fraction, LVED: Left ventricular end diastolic, LVES: Left ventricular end systolic, RVED: Right ventricular end diastolic, PASP: Pulmonary artery systolic pressure, TAPSE: Tricuspid annular plane systolic excursion, RV: Right ventricle, LVEDV: Left ventricular end diastolic volume, LVESV: Left ventricular end-systolic volume, LV CO: Left ventricle cardiac output, LV: Left ventricle, EVF: Extracellular volume fraction, RVEF: Right ventricular ejection fraction, RVEDV: Right ventricular end diastolic volume, RVESV: Right ventricular end-systolic volume, RV CO: Right ventricle cardiac output

groups. However, 32 patients demonstrated evidence of cardiac injury on CMRI, including at least one of the following findings: myocardial edema (n=7), pericardial effusion (n=13), RV failure (n=12), ischemic (n=8) or non-ischemic fibrosis (n=27) on LGE imaging. CMRI images of various myocardial injury patterns are presented in Supplementary Figure 2. There was a significant difference between patients monitored in group 1 and group 2 for non-ischemic fibrosis [n=12 (75%) vs. n=15 (43%); p=0.03].

The ROC curve demonstrated the predictive value of hs-cTnT for detecting any injury identified on CMRI. The ROC curve for hs-cTnT to predict cardiac injury had an AUC of 0.75; for the optimal cut-off value of 47 ng/L with a sensitivity of 70% and specificity of 70% (95% CI: 0.62-0.88, p=0.003). SII also predicted cardiac injury at a threshold above 936.4, with a sensitivity of 72% and specificity of 69% [AUC=0.72 (95% CI: 592-865), p=0.01]. We did not find a significant association between CMRI-detected cardiac injury and the following biomarkers: NLR [AUC=0.55 (95% CI: 0.37-0.71), p=0.54], D-dimer [AUC=0.60 (95% CI: 0.44-0.76), p=0.22], ferritin [AUC=0.50 (95% CI: 0.33-0.67), p=0.69], CRP [AUC=0.57 (95% CI: 0.40-0.73), p=0.40], fibrinogen [AUC=0.46 (95% CI: 0.29-0.64), p=0.69], or CK-MB [AUC=0.58 (95% CI: 0.41-0.74), p=0.36] (Supplementary Figure 3).

DISCUSSION

Our findings indicate that patients with COVID-19 who required ICU admission exhibited more pronounced inflammatory and immune responses compared to those who did not. Although no significant abnormalities were detected on ECG and TTE, CMRI revealed frequent evidence of cardiac involvement. Hs-cTnT and SII levels at admission were substantially correlated with the need for ICU and recent cardiac injury detected by CMRI in patients with COVID-19.

The inflammatory response is of significant relevance in COVID-19 progression. In a meta-analysis of inflammatory markers and COVID-19 severity, CRP, PCT, IL-6, and the erythrocyte sedimentation rate indicated a significant correlation with disease severity.[14] In COVID-19 patients, the NLR, an inflammatory marker, is linked to a poorer outcome. Consistent with previous studies, our findings showed that CRP, PCT, and NLR were associated with disease severity and ICU admission. In addition to COVID-19, NLR plays a critical role in the prediction of CV disorders. It is linked to increased mortality, particularly in acute coronary syndrome patients, and is a strong predictor of myocardial injury in severe COVID-19 patients.[15,16] Although previous studies have shown an association, our study could not find a statistically significant relationship between NLR and CMRI-detected cardiac damage. However, some studies have reported that these inflammatory markers may not always correlate with cardiac injury, suggesting a more complex relationship that warrants further investigation. For instance, a previous study reported a heterogeneous relationship between inflammatory markers and cardiac involvement, even among patients with elevated troponin levels, which may be attributed to multifactorial underlying mechanisms.[17] This discrepancy highlights the importance of interpreting inflammatory marker levels in a broader clinical context.

In a previous prospective study, CMRI was conducted to determine myocardial involvement in patients who had recently been diagnosed with COVID-19. CMRI was performed on 100 hospitalized or outpatient patients, and cardiac involvement was detected in 78% of cases.[11] Most cases were due to myocardial inflammation, ischemia, and pericardial involvement. Other studies have shown that 26% to 60% of COVID-19 patients exhibit cardiac involvement on CMRI, and these patients experienced worse prognoses and higher mortality rates.[18,19] Our study cohort only included in-hospital patients, and 32 of 51 patients (63%) showed cardiac involvement on CMRI, which is concordant with the findings of previous studies. Therefore, considering COVID-19 as a respiratory system disease may lead to an underestimation of the true extent of patient involvement. Particularly for hospitalized patients, a thorough CV evaluation is necessary.

What we have known so far is that myocarditis is the most prevalent diagnosis in COVID-19 patients, as shown on CMRI.[20] Although most patients demonstrated normal ventricular functions in previous studies, T1-T2 mapping abnormalities, myocardial edema, late gadolinium uptake, pleural effusion, and perfusion deficits provided evidence of cardiac injury in these patients. In a multi-center prospective study of 1.216 hospitalized COVID-19 patients, 3% of the study population was diagnosed with acute myocarditis.[21] However, in a meta-analysis examining CMRI findings of COVID-19 patients, the prevalence of myocarditis was 14%, while that of LGE was 20%.[22] Thus, echocardiography has limited diagnostic utility, whereas CMRI is more valuable in detecting the underlying pathology. In our study, although 32 patients (63%) had fibrosis (either ischemic or non-ischemic) on CMRI, only five exhibited LV dysfunction on echocardiography. This study once again demonstrated that CMRI was superior to echocardiography in identifying cardiac involvement and myocardial damage patterns. We anticipated that ICU patients would have higher levels of cardiac involvement on CMRI; nevertheless, the only significant difference between the two groups was non-ischemic fibrosis. We ascribed this to the typical non-ischemic pattern of LGE in myocarditis. Cardiac involvement and the frequency of non-ischemic fibrosis on CMRI rose in our study cohort as the disease worsened.

The SII has been frequently investigated for its prognostic value in cancer patients. Because it represents the immune response and systemic inflammation, it is a promising marker for understanding the course of disease in COVID-19 patients. Our results are consistent with a recently published study demonstrating the utility of the SII in predicting the in-hospital prognosis and mortality of COVID-19 patients.[23] Our findings indicate that SII is associated with both ICU admission and CMR-detected cardiac injury, supporting its potential broader use as a sensitive and specific biomarker in these contexts.

Studies have demonstrated that myocardial injury is defined by elevated cardiac troponin value, and it is linked to an adverse prognosis. It is known that hospitalized COVID-19 patients with cardiac injury demonstrate elevated high-sensitivity cTnI (hs-cTnI) levels and experience higher hospital mortality than those without injury.[24] A retrospective study confirmed that non-survivors of COVID-19 demonstrated a higher peak level of hs-cTnI.[25] Blood samples were obtained for our study during the first 24 hours after patients' complaints and at the time of hospital admission. A mildly elevated hs-

cTnT below the 99th percentile upper reference limit (>12.48 ng/L) on admission may indicate poor prognosis and be predictive of ICU admission. Our results may provide relevant insights regarding the prognostic utility of admission troponin levels for in-hospital outcomes. Therefore, during the initial admission to the hospital, these patients should be evaluated more carefully and prepared for possible clinical deterioration.

Our data were consistent with the previous studies demonstrating the relationship between higher cTnT release and positive LGE on CMRI.[26] CMRI appointments were scheduled for patients considered to be recovered, typically 4-6 weeks after discharge. A significant elevation of hs-cTnT (>47 ng/L) on admission predicted CMRI-detected cardiac injury shown even after the acute phase of the disease.

Study Limitations

Our study has certain limitations. First, our sample size was small due to the limited availability of CMRI. The small number of patients in the study and the possible unbalanced distribution of comorbidities may have impacted the results. Second, we utilized admission troponin levels because they were part of the criteria for ICU admission; however, peak troponin levels would have provided greater value in demonstrating the relationship with cardiac injury. Third, since the COVID-19 virus and its alpha, beta, and delta variants emerged at the time of the study, we could not evaluate current variant infections, such as omicron. Fourth, opportunistic infections in addition to COVID-19 in the ICU group may have influenced our results. Finally, we could not evaluate the acute effect of COVID-19 using CMRI because of ethical considerations aimed at minimizing exposure risk to healthcare personnel.

CONCLUSION

In summary, COVID-19 induces pronounced inflammatory and immune responses that lead to cardiac injury detectable on CMRI, even in the presence of normal echocardiographic findings. A comprehensive CV examination, including CMRI in selected patients, is necessary, especially in hospitalized patients. Hs-cTnT and SII levels are useful and easily accessible markers that may aid in predicting both ICU admission and cardiac injury.

Ethics Committee Approval: This study was conducted in accordance with the principles of the Declaration of Helsinki and was approved by the Local Ethical Committee of the Ankara Training and Research Hospital, Ankara, Türkiye (approval number: 485/2020, date: 15.01.2021).

Informed Consent: Written informed consent was obtained from each patient after providing detailed information regarding the study.

Authorship Contributions: Concept: M.Y., D.Y.Ö., S.N.M., Design: M.Y., D.Y.Ö., S.N.M., Data Collection or Processing: D.Y.Ö., H.Y., U.B., Analysis or Interpretation: M.Y., H.Y., S.N.M., Literature Search: H.Y., U.B., S.N.M., Writing: M.Y., D.Y.Ö., U.B.

Conflict of Interest: No conflict of interest was declared by the authors.

Financial Disclosure: The authors declared that this study received no financial support.

REFERENCES

1. Guo T, Fan Y, Chen M, et al. Cardiovascular implications of fatal outcomes of patients with coronavirus disease 2019 (COVID-19). *JAMA Cardiol.* 2020;5:811-818.
2. Mehra MR, Desai SS, Kuy S, Henry TD, Patel AN. Cardiovascular disease, drug therapy, and mortality in Covid-19. *N Engl J Med.* 2020;382:e102.
3. Clerkin KJ, Fried JA, Raikhelkar J, et al. COVID-19 and cardiovascular disease. *Circulation.* 2020;141:1648-1655.
4. Hodges G, Pallisgaard J, Olsen AMS, et al. Association between biomarkers and COVID-19 severity and mortality: a nationwide Danish cohort study. *BMJ Open.* 2020;10:e041295.
5. Xue G, Gan X, Wu Z, et al. Novel serological biomarkers for inflammation in predicting disease severity in patients with COVID-19. *Int Immunopharmacol.* 2020;89:107065.
6. Liu Y, Yang Y, Zhang C, et al. Clinical and biochemical indexes from 2019-nCoV infected patients linked to viral loads and lung injury. *Sci China Life Sci.* 2020;63:364-374.
7. Mueller C, Giannitsis E, Jaffe AS, et al. Cardiovascular biomarkers in patients with COVID-19. *Eur Heart J Acute Cardiovasc Care.* 2021;10:310-319.
8. Toraih EA, Elshazli RM, Hussein MH, et al. Association of cardiac biomarkers and comorbidities with increased mortality, severity, and cardiac injury in COVID-19 patients: a meta-regression and decision tree analysis. *J Med Virol.* 2020;92:2473-2488.
9. Alzahrani SH, Al-Rabia MW. Cardiac injury biomarkers and the risk of death in patients with COVID-19: a systematic review and meta-analysis. *Cardiol Res Pract.* 2021:2021;9363569.
10. Huang L, Zhao P, Tang D, et al. Cardiac involvement in patients recovered from COVID-2019 identified using magnetic resonance imaging. *JACC Cardiovasc Imaging.* 2020;13:2330-2339.
11. Puntmann VO, Carerj ML, Wieters I, et al. Outcomes of cardiovascular magnetic resonance imaging in patients recently recovered from coronavirus disease 2019 (COVID-19). *JAMA Cardiol.* 2020;5:1265-1273.
12. Chen BH, Shi NN, Wu CW, et al. Early cardiac involvement in patients with acute COVID-19 infection identified by multiparametric cardiovascular magnetic resonance imaging. *Eur Heart J Cardiovasc Imaging.* 2021;22:844-851.
13. Mitchell C, Rahko PS, Blauwet LA, et al. Guidelines for performing a comprehensive transthoracic echocardiographic examination in adults: Recommendations from the American Society of Echocardiography. *J Am Soc Echocardiogr.* 2019;32:1-64.
14. Zeng F, Huang Y, Guo Y, et al. Association of inflammatory markers with the severity of COVID-19: a meta-analysis. *Int J Infect Dis.* 2020;96:467-474.
15. Haybar H, Pezeshki SMS, Saki N. Evaluation of complete blood count parameters in cardiovascular diseases: an early indicator of prognosis? *Exp Mol Pathol?* 2019;110:104267.
16. Chen Y, Wang K, Luo Y, et al. Predictive value of neutrophil/lymphocyte ratio on myocardial injury in severe COVID-19 patients. *Zhonghua Xin Xue Guan Bing Za Zhi.* 2020;48:572-579.
17. Kotecha T, Knight DS, Razvi Y, et al. Patterns of myocardial injury in recovered troponin-positive COVID-19 patients assessed by cardiovascular magnetic resonance. *Eur Heart J.* 2021;42:1866-1878.
18. Petersen SE, Friedrich MG, Leiner T, et al. Cardiovascular magnetic resonance for patients with COVID-19. *JACC Cardiovasc Imaging.* 2022;15:685-699.
19. Driggin E, Madhavan MV, Bikdeli B, et al. Cardiovascular considerations

for patients, health care workers, and health systems during the COVID-19 pandemic. *J Am Coll Cardiol*. 2020;75:2352-2371.

20. Ojha V, Verma M, Pandey NN, et al. Cardiac magnetic resonance imaging in coronavirus disease 2019 (COVID-19): a systematic review of cardiac magnetic resonance imaging findings in 199 patients. *J Thorac Imaging*. 2021;36:73-83.
21. Dweck MR, Bularga A, Hahn RT, et al. Global evaluation of echocardiography in patients with COVID-19. *Eur Heart J Cardiovasc Imaging*. 2020;21:949-958.
22. Kim JY, Han K, Suh YJ. Prevalence of abnormal cardiovascular magnetic resonance findings in recovered patients from COVID-19: a systematic review and meta-analysis. *J Cardiovasc Magn Reson*. 2021;23:100.
23. Muhammad S, Fischer I, Naderi S, et al. Systemic inflammatory index is a novel predictor of intubation requirement and mortality after SARS-CoV-2 infection. *Pathogens*. 2021;10:58.
24. Shi S, Qin M, Shen B, et al. Association of cardiac injury with mortality in hospitalized patients with COVID-19 in Wuhan, China. *JAMA Cardiol*. 2020;5:802-810.
25. Wang Y, Shu H, Liu H, et al. The peak levels of highly sensitive troponin I predicts in-hospital mortality in COVID-19 patients with cardiac injury: a retrospective study. *Eur Heart J Acute Cardiovasc Care*. 2021;10:6-15.
26. Takashio S, Yamamuro M, Uemura T, et al. Correlation between extent of myocardial fibrosis assessed by cardiac magnetic resonance and cardiac troponin T release in patients with nonischemic heart failure. *Am J Cardiol*. 2014;113:1697-1704.

Supplementary Figures 1-3: https://d2v96fxpocvxx.cloudfront.net/4458d962-0fb2-48a3-a23a-e35265f70f9b/content-images/4bb03e64-8671-42e9-bd62-6fd89f346833.pdf

INTERVENTIONAL CARDIOLOGY PERSPECTIVES

Inter Cardio Pers 2025;1(2):67-71

DOI: 10.4274/intercardiopers.2025.2025-3-3

ORIGINAL ARTICLE

Long-term Follow-up of Patients with Coronary Slow Flow: A Speckle-tracking Echocardiography Study

Mehmet Arslan[1], Özge Özden Kayhan[2], Çağla Akçay Ürkmez[3], Cemre Turgul[4], Kardelen Ohtaroğlu Tokdil[5], Ahmet Barutçu[1]

[1]Department of Cardiology, Çanakkale Onsekiz Mart University Faculty of Medicine, Çanakkale, Türkiye

[2]Clinic of Cardiology, Bahçelievler Memorial Hospital, İstanbul, Türkiye

[3]Clinic of Cardiology, Sakarya Training and Research Hospital, Sakarya, Türkiye

[4]Department of Cardiology, Erciyes University Faculty of Medicine, Kayseri, Türkiye

[5]Department of Cardiology, İstanbul University Cerrahpaşa-Cerrahpaşa Faculty of Medicine, İstanbul, Türkiye

ABSTRACT

Background: While earlier studies have indicated that patients with coronary slow flow (CSF) tend to have favorable outcomes, long-term prospective data remain limited.

Aim: This study aimed to assess the long-term clinical significance of CSF and its effect on cardiac function.

Study Design: A 5-year clinical follow-up was conducted to assess cardiac function in patients with CSF using both conventional and speckle-tracking echocardiography.

Methods: Nineteen patients diagnosed with CSF were included. Echocardiographic and strain parameters were recorded at baseline and re-evaluated after five years. Clinical follow-up was maintained throughout the study period.

Results: No significant changes were observed in echocardiographic or longitudinal strain parameters, all of which remained within normal limits. During the follow-up, there were no cases of mortality, cardiac-related hospitalizations, or acute coronary syndromes.

Conclusion: Patients with CSF demonstrated preserved cardiac function and a favorable long-term prognosis. Ongoing medical treatment likely played a role in maintaining these outcomes.

Keywords: Coronary slow flow, speckle-tracking echocardiography, strain imaging, long-term follow-up

INTRODUCTION

Coronary slow flow (CSF) is identified in approximately 2% of coronary angiographic procedures, yet its clinical relevance and long-term outcomes remain uncertain, and no standardized treatment guidelines have been established.[1-3] Several cross-sectional studies have examined the impact of CSF on cardiac function. Comparative analysis using echocardiographic techniques have found that left ventricular (LV) volumes and function in these patients are generally comparable to those of individuals without CSF.[4-7] Some studies have investigated the effects of pharmacologic therapies and treatment response, typically evaluating coronary flow during short-term follow-up; however, long-term data on ventricular function are limited.[8-10] Additionally, no prospective studies have assessed the extended effects of CSF. The exact pathology of CSF remains poorly defined. Although multiple theories have been proposed and explored, the underlying mechanism is not fully understood. Known secondary causes of CSF include coronary ectasia, coronary spasm, ventricular dysfunction, valvular heart disease, and connective tissue disorders.[2,11-15] Nonetheless, CSF is considered a distinct clinical entity, separate from these conditions. Although CSF has occasionally been associated with ventricular arrhythmias and, in rare cases, sudden cardiac death, it most commonly presents as acute coronary syndrome. While it may contribute to morbidity, a direct link to increased mortality has not been established. Although prior studies indicate that patients with CSF generally have a favorable prognosis, there is a lack of long-term prospective data on this condition.[3,12,16] Speckle-tracking echocardiography (STE) is an advanced imaging technique that allows semiautomatic assessment of LV function, offering greater reproducibility and accuracy than conventional echocardiographic methods. It has been shown to be more effective in evaluating cardiac function and predicting cardiovascular outcomes.[17-19] In this study, we aimed to assess the effect of CSF on

Address for Correspondence: Mehmet Arslan MD, Department of Cardiology, Çanakkale Onsekiz Mart University Faculty of Medicine, Çanakkale, Türkiye

E-mail: mehmet_ma@hotmail.com **ORCID ID:** orcid.org/0000-0001-8785-7944

Cite as: Arslan M, Kayhan ÖÖ, Akçay Ürkmez Ç, et al. Long-term follow-up of patients with coronary slow flow: a speckle-tracking echocardiography study. *Inter Cardio Pers.* 2025;1(2):67-71

Received: 03.03.2025
Accepted: 02.04.2025
Epub: 08.05.2025
Publication Date: 11.08.2025

cardiac function and its clinical relevance by conducting a 5-year clinical follow-up using both conventional echocardiography and STE.

METHODS

Study Population

This study was approved by the Çanakkale Onsekiz Mart University Clinical Research Ethics Committee (approval no: 2011-KAEK-27/2018-E.1800184834, decision date: 16.01.2019) and conducted in accordance with the Declaration of Helsinki. Written informed consent was obtained from all participants. This prospective study excluded patients with secondary causes of CSF, such as coronary ectasia, coronary spasm, ventricular dysfunction, valvular heart disease, and connective tissue disorders. Individuals with structural cardiovascular conditions-including LV dysfunction, LV hypertrophy, cardiomyopathies, or atherosclerotic coronary artery disease-were not included. Additional exclusion criteria were the presence of atrial fibrillation, valvular heart disease, congenital heart defects, pericardial disease, or stage 3-4 hypertension. Patients with bundle branch block on electrocardiography, a history of thoracic surgery, chronic systemic or inflammatory conditions, or malignancy were also excluded. Based on these criteria, 19 patients diagnosed with CSF were enrolled. At baseline, all patients underwent both standard and STE. Clinical follow-up continued for five years, after which echocardiographic assessments were repeated using the same equipment and performed by the same operators to maintain measurement consistency.

TIMI Frame Count and Definition of CSF

The diagnosis of CSF was established using the TIMI frame count method, as described by Gibson et al.[10] A cardiologist blinded to clinical details of the patients performed the frame count analysis. In this method, the initial frame is defined as the point at which contrast dye first enters the ostium of the coronary artery, and the final frame is the one in which the contrast reaches the first bifurcation of the posterior branch of the right coronary artery (RCA) and the distal bifurcations of the circumflex (Cx) and left anterior descending (LAD) arteries. For angiograms recorded at 30 frames per second, normal TIMI frame counts are defined as 20.4±3.0 for the RCA, 22.2±4.1 for the Cx, and 36±2.6 for the LAD. The corrected TIMI frame count for the LAD is obtained by dividing the LAD value by 1.7, with a normal reference value of 21.1±1.5. The average TIMI frame count is calculated from the values of all three major coronary arteries. Patients who showed CSF in at least one of these vessels were classified as having CSF.[20]

Standard Echocardiography

Echocardiographic assessments were performed using a high-resolution imaging system (Vivid 7, GE, USA). Measurements of LV and left atrial (LA) dimensions followed the guidelines of the European Society of Echocardiography.[21] The LA volume index and LV ejection fraction were calculated using the modified biplane Simpson's method. Diastolic function was evaluated by recording early (E) and late (A) diastolic LV filling velocities, along with E-wave deceleration time, using Doppler imaging. Pulsed-wave Doppler of mitral inflow and LV outflow were used to define the timing of mitral and aortic valve opening and closure. Tissue Doppler imaging (TDI) was employed to measure the E' and A' velocities at the lateral wall and septum. The E/E' ratio was calculated manually. Care was taken to optimize image quality by reducing interference from extracardiac structures and ensuring clear visualization of the myocardium.

Speckle-tracking Echocardiography

Speckle-tracking imaging was performed using grayscale B-mode echocardiography at a minimum frame rate of 80 frames per second. The cardiac cycle with the best image quality was selected for analysis, and the LV endocardial borders were traced at end-systole. Speckle-tracking analysis was carried out using an EchoPAC workstation (version 4.2.0, GE Vingmed Ultrasound AS, Horten, Norway). To measure global longitudinal strain (GLS), apical four-chamber, apical long-axis, and two-chamber views were acquired during breath-hold with continuous echocardiography monitoring. The automatic function imaging tool was used to define the regions of interest (ROI) by marking the endocardial surface at the mitral annulus and apex. The software then generated the epicardial surface and constructed the ROI, which was manually adjusted when necessary (Figure 1). Each ROI was segmented into six parts, and the software automatically assessed the tracking quality. A 17-segment LV model was applied to calculate peak systolic strain values, with end-systole identified as the point of aortic valve closure in the apical long-axis view.[22] Final GLS values were presented in a bullseye summary format (Figure 2).

Statistical Analysis

Statistical analyses were performed using Statistical Package for the Social Sciences (SPSS) software, version 21.0 (SPSS Inc., Chicago, IL, USA). Echocardiographic measurements and calculations were independently assessed by two cardiologists. Descriptive statistics were used to summarize the sociodemographic data of the study population. The Wilcoxon signed-rank test was used to compare baseline and follow-up parameters. A p value of <0.05 was considered statistically significant.

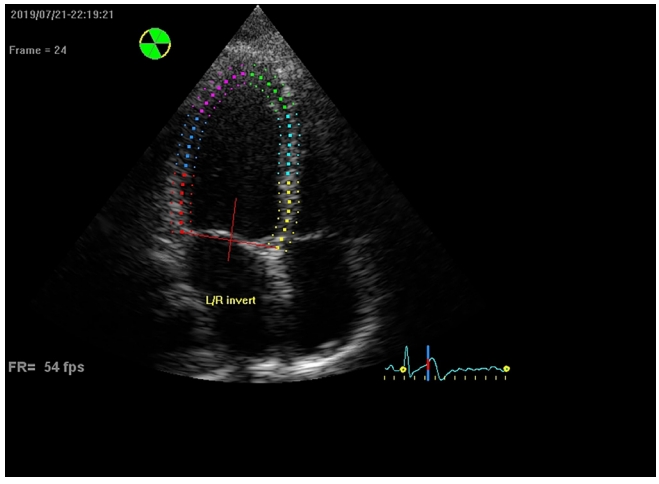

Figure 1. Marking the endocardial borders to define regions of interest

RESULTS

A total of 19 patients were enrolled in the study. Baseline echocardiographic and strain imaging data were collected 5 years earlier, and patients were clinically monitored throughout the follow-up period. At the end of the 5 years, standard echocardiography and strain imaging were repeated using the same echocardiography system. However, repeat imaging could not be performed in the nine patients. For these individuals, clinical status was assessed using national health database records and follow-up phone interviews.

Notably, no deaths occurred during the follow-up period, including among the nine patients who did not undergo repeat imaging. In addition, none of the participants experienced a major acute cardiac event over the 5 years. For the remaining 10 patients who completed follow-up imaging, both standard and STE were conducted. The demographic and clinical profiles of the study population remained consistent, as presented in Table 1.

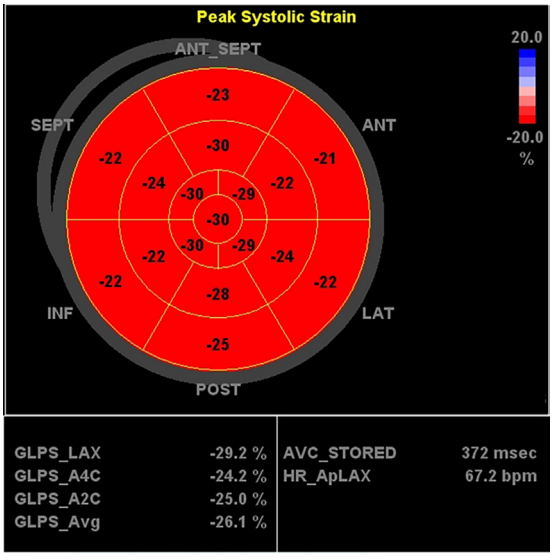

Figure 2. Longitudinal strain bull's-eye plot

Table 1. Demographic characteristics of the study population (n=10)

Variables	
Age (years)	50.60±8.68
Gender/male (%)	8 (80.0%)
BMI (kg/m^2)	29.39±4.81
BSA (m^2)	2.03±0.22
Systolic blood pressure (mmHg)	130.30±11.99
Diastolic blood pressure (mmHg)	79.70±6.62
Heart rate	72.20±7.42
Smoking	60.0% (6)
Alcohol	50.0% (5)
Hypertension	40.0% (4)
Diabetes mellitus	30.0% (3)
Hyperlipidemia	50.0% (5)

BMI: Body mass index, BSA: Body surface area

At 5 years, no statistically significant changes were detected in standard echocardiographic measurements (Table 2). Likewise, longitudinal strain values obtained through STE remained within normal limits and showed no significant differences compared to baseline (Table 3, Figure 3).

DISCUSSION

To our knowledge, this is the first study to provide a 5-year follow-up on patients with CSF. The results show a positive prognosis for all patients, with no reported deaths, cardiac-related hospitalizations, or acute coronary syndromes during the follow-up. Echocardiographic assessments showed no significant decline in LV function or volume over time.

This study used STE, a sensitive imaging technique capable of detecting early myocardial dysfunction even in patients with normal ejection fractions.[17-19] Importantly, strain parameters remained unchanged from baseline to follow-up, reinforcing the idea that CSF does not lead to progressive ventricular dysfunction. Although previous studies have suggested that patients with CSF generally have a good prognosis, long-term data on this condition have been limited.

Previous echocardiographic studies on CSF have mostly been cross-sectional, providing only a snapshot of its effects rather than long-term outcomes. These studies typically found that conventional echocardiographic parameters were similar between CSF patients and controls, but parameters indicating early myocardial dysfunction, such as TDI and strain imaging, were slightly lower in CSF patients.[4-7] However, the lack of longitudinal data leaves uncertainty about the clinical significance of these findings.

Table 2. Echocardiographic parameters of the study population

Parameters	Baseline n=10	Follow-up n=10	p value
Left ventricular diastolic diameter (mm)	48.60±5.44	48.80±4.76	0.959
Left ventricular systolic diameter (mm)	35.70±2.41	35.20±2.39	0.347
Left ventricular ejection fraction (%)	59.09±4.11	58.40±4.45	0.396
Posterior wall thickness (mm)	10.50±1.27	10.50±.0.97	0.943
Interventricular septum thickness (mm)	10.40±1.26	10.60±1.51	0.669
Left atrial diameter (mm)	36.80±5.35	34.70±1.64	0.181
Right ventricular diastolic diameter (mm)	31.10±5.13	31.30±4.19	0.953
Mitral inflow E wave (cm/s)	79.50±19.91	73.13±10.29	0.293
Mitral inflow A wave (cm/s)	74.50±15.69	72.38±18.21	0.674
Medial E' (cm/s)	10.38±2.92	9.88±2.47	0.777
Medial A' (cm/s)	11.13±1.96	11.38±1.30	0.715
Lateral E' (cm/s)	10.63±3.02	10.25±3.20	0.435
Lateral A' (cm/s)	12.14±2.73	10.71±2.69	0.066

E: Early, A: Late

Table 3. Strain parameters of CSF patients at baseline and 5-year follow-up

Variables	Baseline n=12	5-year follow-up n=10	p value
Global longitudinal strain	-20.79±2.24	-21.88±2.75	0.059
4 CH longitudinal strain	-20.48±2.51	-22.34±2.51	0.093
3 CH longitudinal strain	-21.14±2.39	-21.49±1.88	0.507
2 CH longitudinal strain	-20.85±3.08	-22.03±5.18	0.114

CH: Chamber, CSF: Coronary slow flow

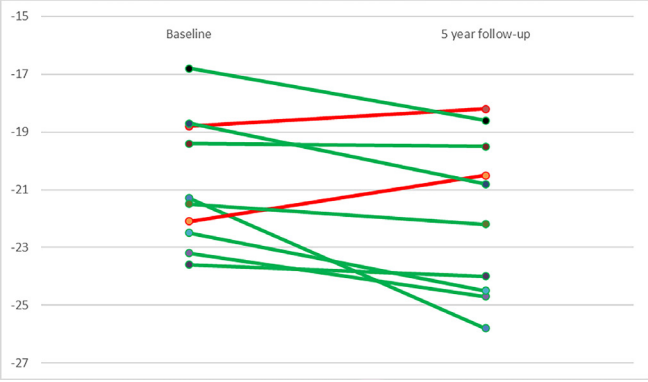

Figure 3. Global longitudinal strain at baseline and 5-year follow-up

Several pharmacological studies have evaluated the short-term effects of various medications on CSF. Some have reported improvements in symptoms and coronary flow following treatment.[8-10] For example, a study on calcium channel blockers showed that anginal symptoms improved in all patients after an average follow-up of 13.6 months.[23] However, long-term evaluations of cardiac function in these patients are missing. A prior study that followed patients with microvascular disease and CSF for an extended period noted persistent symptoms despite a generally favorable prognosis, though cardiac function was not assessed in that study.[24]

Our study offers both long-term clinical follow-up and comprehensive echocardiographic assessment. A recent retrospective observational study examined the link between previous coronary events and long-term outcomes in CSF patients. It found that only those with a history of myocardial infarction had a worse prognosis, while CSF alone was not associated with increased all-cause mortality.[25] In line with these findings, none of the patients in our cohort had a history of myocardial infarction, and all underwent coronary angiography due to anginal symptoms. Our results further support the evidence that patients with CSF, in the absence of prior myocardial infarction, have a favorable long-term prognosis. Additionally, through objective prospective measurements, we showed that their cardiac function remained stable over time.

Although various pharmacological treatments have been explored for tCSF,[8,10,23,26] the clinical trials conducted thus far have been too small to influence clinical guidelines. Currently, there is no standardized treatment protocol for CSF. However, based on expert consensus and previous research, statins and calcium channel blockers are commonly prescribed. In our study, most patients were on these medications. The stability of strain values over the 5-year period suggests that these treatments may have helped preserve cardiac function, although this remains speculative. Previous cross-sectional studies have reported similar medication use among CSF patients, and while not statistically significant, the slight improvements in strain values observed in our study may indicate the potential benefits of long-term medical management.

Study Limitations

This study has several limitations. First, the sample size was relatively small, which may limit the generalizability of the results. A larger cohort would provide more statistical power to detect subtle changes in cardiac function over time. Second, echocardiographic follow-up was not possible for all patients, as nine individuals could not undergo repeat assessments. Although their clinical status was monitored through national health records and phone calls, the lack of follow-up echocardiographic data for these patients may have affected the overall results. Third, while STE is a sensitive tool for assessing myocardial function, its accuracy depends on image quality and operator skill. Despite efforts to ensure high-quality imaging, minor variations in image acquisition and analysis may still exist. Additionally, although most patients were on medical therapy, the study did not systematically assess the impact of different medications on clinical and echocardiographic outcomes. Variations in medication adherence or changes in treatment during follow-up could have influenced the results. Finally, the study did not include a control group of healthy individuals or patients with similar risk factors but without CSF. A comparison with such groups would have provided more insight into whether the observed findings were specific to CSF or influenced by other factors.

Despite these limitations, this study provides valuable long-term data on the prognosis and cardiac function of CSF patients, emphasizing the need for further large-scale prospective studies to validate and expand these findings.

CONCLUSION

Patients with CSF appear to have a favorable long-term prognosis, with cardiac function remaining preserved over time. This suggests that either medical treatment may have a protective effect or CSF does not significantly impair myocardial perfusion to the extent that it affects ventricular function. Large-scale prospective studies are needed to confirm these findings and establish standardized management strategies for CSF.

Ethics Committee Approval: This study was approved by the Çanakkale Onsekiz Mart University Clinical Research Ethics Committee (approval no: 2011-KAEK-27/2018-E.1800184834, decision date: 16.01.2019) and conducted in accordance with the Declaration of Helsinki.

Informed Consent: Written informed consent was obtained from all participants.

Authorship Contributions: Concept: M.A., Ö.Ö.K., Design: M.A., Ö.Ö.K., Data Collection or Processing: M.A., Ö.Ö.K., Analysis or Interpretation: A.B., K.O.T., Literature Search: Ç.A.Ü., C.T., Writing: Ç.A.Ü., C.T.

Conflict of Interest: No conflict of interest was declared by the authors.

Financial Disclosure: The authors declared that this study received no financial support.

REFERENCES

1. Tambe AA, Demany MA, Zimmerman HA, Mascarenhas E. Angina pectoris and slow flow velocity of dye in coronary arteries--a new angiographic finding. *Am Heart J*. 1972;84:66-71.
2. Wang X, Nie SP. The coronary slow flow phenomenon: characteristics, mechanisms and implications. *Cardiovasc Diagn Ther*. 2011;1:37-43.
3. Victor SM, Gnanaraj A, Subban V, Mullasari AS. AS-274: coronary slow flow phenomenon: risk profile. *Am J Cardiol*. 2012;109:132-133.
4. Baykan M, Baykan EC, Turan S, et al. Assessment of left ventricular function and Tei index by tissue Doppler imaging in patients with slow coronary flow. *Echocardiography*. 2009;26:1167-1172.
5. Barutçu A, Bekler A, Temiz A, et al. Left ventricular twist mechanics are ımpaired in patients with coronary slow flow. *Echocardiography*. 2015;32:1647-1654.
6. Gulel O, Akcay M, Soylu K, et al. Left ventricular myocardial deformation parameters are affected by coronary slow flow phenomenon: a study of speckle tracking echocardiography. *Echocardiography*. 2016;33:714-723.
7. Wang Y, Ma C, Zhang Y, et al. Assessment of left and right ventricular diastolic and systolic functions using two-dimensional speckle-tracking echocardiography in patients with coronary slow-flow phenomenon. *PLoS One*. 2015;10:e0117979.
8. Kurtoglu N, Akcay A, Dindar I. Usefulness of oral dipyridamole therapy for angiographic slow coronary artery flow. *Am J Cardiol*. 2001;87:777-779.
9. Cakmak M, Tanriverdi H, Cakmak N, Evrengul H, Cetemen S, Kuru O. Simvastatin may improve myocardial perfusion abnormality in slow coronary flow. *Cardiology*. 2008;110:39-44.
10. Albayrak S, Ordu S, Yuksel H, Ozhan H, Yazgan O, Yazici M. Efficacy of nebivolol on flow-mediated dilation in patients with slow coronary flow. *Int Heart J*. 2009;50:545-553.
11. Beltrame JF, Limaye SB, Horowitz JD. The coronary slow flow phenomenon--a new coronary microvascular disorder. *Cardiology*. 2002;97:197-202.
12. Chesebro JH, Knatterud G, Roberts R, et al. Thrombolysis in myocardial ınfarction (TIMI) Trial, phase ı: a comparison between intravenous tissue plasminogen activator and intravenous streptokinase. Clinical findings through hospital discharge. *Circulation*. 1987;76:142-154.
13. Chatzizisis YS, Coskun AU, Jonas M, Edelman ER, Feldman CL, Stone PH. Role of endothelial shear stress in the natural history of coronary atherosclerosis and vascular remodeling: molecular, cellular, and vascular behavior. *J Am Coll Cardiol*. 2007;49:2379-2393.
14. Gazi E, Barutcu A, Altun B, et al. Intercellular adhesion molecule-1 K469E and angiotensinogen T207M polymorphisms in coronary slow flow. *Med Princ Pract*. 2014;23:346-350.
15. Beltrame JF, Limaye SB, Wuttke RD, Horowitz JD. Coronary hemodynamic and metabolic studies of the coronary slow flow phenomenon. *Am Heart J*. 2003;146:84-90.
16. Alvarez C, Siu H. Coronary slow-flow phenomenon as an underrecognized and treatable source of chest pain: case series and literature review. *J Investig Med High Impact Case Rep*. 2018;6:2324709618789194.
17. Biswas M, Sudhakar S, Nanda NC, et al. Two- and three-dimensional speckle tracking echocardiography: clinical applications and future directions. *Echocardiography*. 2013;30:88-105.
18. Leitman M, Lysyansky P, Sidenko S, et al. Two-dimensional strain-a novel software for real-time quantitative echocardiographic assessment of myocardial function. *J Am Soc Echocardiogr*. 2004;17:1021-1029.
19. Edvardsen T, Helle-Valle T, Smiseth OA. Systolic dysfunction in heart failure with normal ejection fraction: speckle-tracking echocardiography. *Prog Cardiovasc Dis*. 2006;49:207-214.
20. Gibson CM, Cannon CP, Daley WL, et al. TIMI frame count: a quantitative method of assessing coronary artery flow. *Circulation*. 1996;93:879-888.
21. Lang RM, Bierig M, Devereux RB, et al. Recommendations for chamber quantification: a report from the American Society of Echocardiography's Guidelines and Standards Committee and the Chamber Quantification Writing Group, developed in conjunction with the European Association of Echocardiography, a branch of the European Society of Cardiology. *J Am Soc Echocardiogr*. 2005;18:1440-1463.
22. Voigt JU, Pedrizzetti G, Lysyansky P, et al. Definitions for a common standard for 2D speckle tracking echocardiography: consensus document of the EACVI/ASE/Industry Task Force to standardize deformation imaging. *Eur Heart J Cardiovasc Imaging*. 2015;16:1-11.
23. Li L, Gu Y, Liu T, et al. A randomized, single-center double-blinded trial on the effects of diltiazem sustained-release capsules in patients with coronary slow flow phenomenon at 6-month follow-up. *PLoS One*. 2012;7:e38851.
24. Ciavolella M, Avella A, Bellagamba S, Mangieri E, Nigri A, Reale A. Angina and normal epicardial coronary arteries: radionuclide features and pathophysiological implications at long-term follow-up. *Coron Artery Dis*. 1994;5:493-499.
25. Zivanic A, Stankovic I, Ilic I, Putnikovic B, Neskovic AN. Prognosis of patients with previous myocardial infarction, coronary slow flow, and normal coronary angiogram. *Herz*. 2020;45(Suppl 1):88-94.
26. Beltrame JF, Turner SP, Leslie SL, Solomon P, Freedman SB, Horowitz JD. The angiographic and clinical benefits of mibefradil in the coronary slow flow phenomenon. *J Am Coll Cardiol*. 2004;44:57-62.

INTERVENTIONAL CARDIOLOGY PERSPECTIVES

Inter Cardio Pers 2025;1(2):72-74

DOI: 10.4274/intercardiopers.2025.2025-6-4

CASE REPORT

Acute Stent Thrombosis and Myocardial Infarction in a Postsplenectomy Patient with Thrombocytosis

Mustafa Tunahan Öz, Adnan Kaya

Department of Cardiology, Bahçeşehir University Faculty of Medicine, İstanbul, Türkiye

ABSTRACT

We report a case involving acute stent thrombosis in a patient with a history of splenectomy and thrombocytosis. The patient arrived with persistent chest pain and vomiting. The electrocardiogram (ECG) revealed ST-segment elevation in leads D2, D3, AVF, and V4-V6. Primary percutaneous coronary intervention was carried out using a 4.0×23 mm drug-eluting stent following loading doses of 300 mg acetylsalicylic acid and 600 mg clopidogrel. Adequate anticoagulation was ensured with intravenous heparin, monitored by activated clotting time (ACT). An ACT of 258 was achieved within 10 min. The procedure was completed successfully, and the patient was admitted to the intensive care unit. However, a follow-up ECG showed persistent ST-segment elevation, and the patient developed cardiogenic shock with complete atrioventricular block. The patient was returned to the catheterization laboratory, where angiography confirmed stent thrombosis. Balloon angioplasty was performed, and tirofiban was administered along with temporary pacing support. The patient was discharged 3 days after the initial procedure with preserved left ventricular function. This case underscores that acute stent thrombosis can occur despite appropriate intervention and anticoagulation. In patients with splenectomy and thrombocytosis, adequate platelet inhibition and anticoagulation may still be insufficient, increasing the risk of stent thrombosis.

Keywords: Acute stent thrombosis, interventional, myocardial infarction

INTRODUCTION

The causes of thrombocytosis are categorized as either primary or secondary, with secondary (reactive) thrombocytosis being more prevalent than primary.[1]. Secondary thrombocytosis can result from factors such as infections, iron deficiency, splenectomy, medications, malignancies, inflammatory conditions, or hemolysis.[2] Most individuals with secondary thrombocytosis remain asymptomatic and follow a benign course.[3] Nonetheless, in rare instances, it may lead to thrombotic complications including acute myocardial infarction (MI), mesenteric vein thrombosis, or pulmonary embolism. Thrombocytosis following splenectomy accounts for about 1.6% of all cases.[4] MI and other vaso-occlusive events occur in fewer than 5% of patients with secondary thrombocytosis.[5] In our patient, a stroke occurred 1 year after splenectomy, followed by ST-elevation MI 6 years later, and acute stent thrombosis developed just 10 min after a successful percutaneous coronary intervention (PCI). We present this case to illustrate acute stent thrombosis despite an optimized intervention and anticoagulation strategy.

CASE REPORT

Clinical Presentation

A 58-year-old woman presented to the emergency department with persistent chest pain, back pain, and jaw numbness lasting for 2 hours. Her blood pressure was 90/65 mmHg, pulse rate was 52 beats/minute, and oxygen saturation was 98%. The electrocardiogram (ECG) revealed ST-segment elevation in leads V4-V6 and D2-D3, with reciprocal ST-segment depression in V1-V2. Oral loading doses of 300 mg acetylsalicylic acid and 600 mg clopidogrel were given. The patient was then moved to the angiography suite. Coronary angiography identified a 99% subtotal thrombotic occlusion of the right coronary artery (RCA) and 80% stenosis of the circumflex artery (CX), which originates from the right sinus (Figure 1). The left main coronary artery (LMCA) appeared aneurysmal up to the D1 segment, and the left anterior descending (LAD) artery was underdeveloped.

Address for Correspondence: Mustafa Tunahan Öz MD, Department of Cardiology, Bahçeşehir University Faculty of Medicine, İstanbul, Türkiye
E-mail: m.tunahanoz134@gmail.com **ORCID ID:** orcid.org/0009-0003-0674-2523

Cite as: Öz MT, Kaya A. Acute stent thrombosis and myocardial infarction in a postsplenectomy patient with thrombocytosis. *Inter Cardio Pers.* 2025;1(2):72-74

Received: 11.06.2025
Accepted: 07.07.2025
Epub: 14.07.2025
Publication Date: 11.08.2025

Management

Predilatation of the RCA osteal region was done with a 4.0×20 mm non-compliant (NC) balloon. A 4.0×23 mm drug-eluting stent was then deployed, followed by postdilatation with a 4.0×20 mm NC balloon. TIMI 3 flow was achieved and the procedure was completed successfully. The patient was transferred to the intensive care unit; however, her chest pain persisted and worsened 10 min later. Her vital signs showed a pulse of 43 beats/minute and a blood pressure of 70/56 mmHg. A repeat ECG showed continued ST-segment elevation. Due to ongoing ST-elevation in V4-V6, she was taken back to the angiography suite. Temporary pacing was applied to the right ventricle, and control coronary angiography was performed with pacing support. This revealed total stent occlusion at the RCA ostium with thrombus and distal bifurcation embolization. The ostial region was redilated with 4.0×20 mm NC balloon (Figure 2). An intracoronary bolus of 32 µg tirofiban was administered. TIMI 3 flow was restored. After the procedure, her chest pain resolved. A tirofiban (glycoprotein IIb/IIIa inhibitor) infusion at 12 µg for 6 hours was initiated.

Medical History

The patient underwent an appendectomy in 2005. In 2019, she had surgery for a right adnexal mass, which included total abdominal hysterectomy, bilateral salpingo-oophorectomy, omentectomy, and splenectomy. That same year, she received four cycles of chemotherapy with carboplatin and paclitaxel. Coronary angiography performed in 2019 showed a 30% plaque at the CX ostium and an aneurysmatic, rudimentary LAD extending to the LMCA D1 level, for which medical management was recommended. She experienced an ischemic stroke in 2020.

The patient was informed that the procedures would be included in a publication and provided written consent. No artificial intelligence assistance was used in preparing this case report.

Follow-up of the Procedure

Twelve hours after the procedure, echocardiography showed an ejection fraction of 45%, inferior wall hypokinesia, mild mitral regurgitation, mild tricuspid regurgitation, and an enlarged ascending aorta measuring 42 mm. Troponin 1 was 35,342.9 pg/mL (reference 0-15.6 pg/mL), decreasing to 16,914 pg/mL on the second day. Hemoglobin was 11.1 g/dL (reference 12.2-16.2 g/dL), hematocrit 34.7% (reference 37.7-47.9%), white blood cell count 17.52 K/uL (reference 4.23-10.2 K/uL), red blood cell count 4.12 M/uL (reference 4.04-5.48 M/uL), and platelet count 546 K/uL (reference 142-424 K/uL). Prothrombin activity was 83% (reference 70-130%) and the international normalized ratio was 1.14 (reference 0.75-1.2). The patient was discharged on dual antiplatelet therapy, which is considered sufficient to prevent further complications.

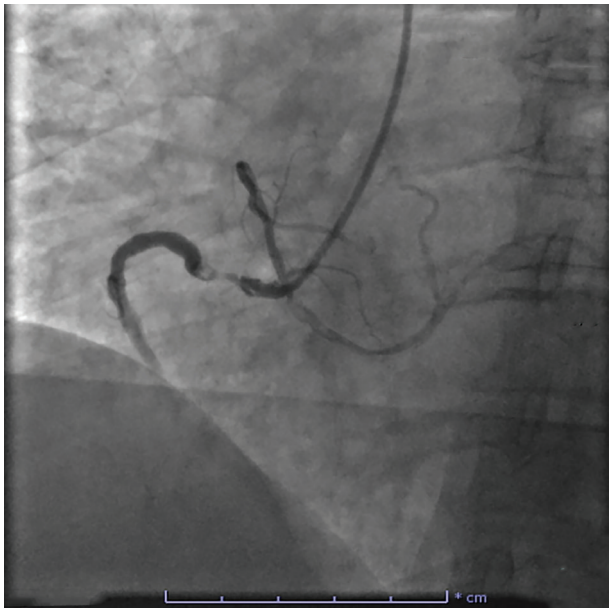

Figure 1. The circumflex artery originates from the right sinus and shows 80% narrowing in its midportion. The right coronary artery is nearly completely occluded with thrombus

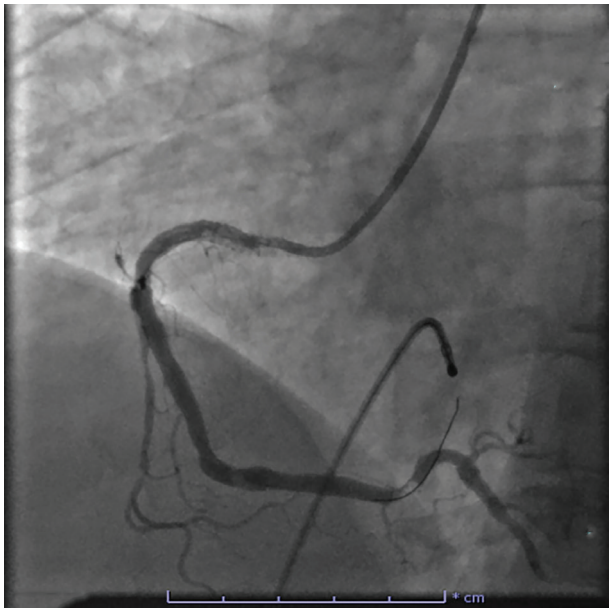

Figure 2. Acute thrombosis following percutaneous coronary intervention. The thrombus resolved after tirofiban administration and balloon inflation within the stent

CONCLUSION

Acute stent thrombosis following PCI is an uncommon occurrence. In this case, it developed in a patient with thrombocytosis secondary to splenectomy. Postsplenectomy thrombocytosis is reported in about 90% of cases due to loss of splenic sequestration.[6] In this patient, a stroke, ST-elevation MI, and acute stent thrombosis occurred after splenectomy. Both predilatation and postdilatation were performed, the stent was appropriately sized, and no residual stenosis was detected. Therefore, the acute stent thrombosis was not procedural in origin. It developed despite activated clotting time (ACT) monitoring. Although periprocedural heparin dosing can vary, the optimal ACT target is 300-350 seconds. The occurrence of acute stent thrombosis after PCI may indicate suboptimal stent patency, and underlying hematologic conditions should be evaluated.

Informed Consent: The patient was informed that the procedures would be included in a publication and provided written consent.

Authorship Contributions: Surgical and Medical Practices: A.K., Concept: A.K., Design: M.T.Ö., Data Collection or Processing: M.T.Ö., Analysis or Interpretation: A.K., Literature Search: M.T.Ö., Writing: M.T.Ö.

Conflict of Interest: No conflict of interest was declared by the authors.

Financial Disclosure: The authors declared that this study received no financial support.

REFERENCES

1. Griesshammer M, Bangerter M, Sauer T, Wennauer R, Bergmann L, Heimpel H. Aetiology and clinical significance of thrombocytosis: analysis of 732 patients with an elevated platelet count. *J Intern Med*. 1999;245:295-300.
2. Rokkam VR, Killeen RB, Kotagiri R. Secondary thrombocytosis. StatPearls [Internet]. Treasure Island (FL): StatPearls Publishing; 2025.
3. Williams B, Morton C. Cerebral vascular accident in a patient with reactive thrombocytosis: a rare cause of stroke. *Am J Med Sci*. 2008;336:279-281.
4. Khan PN, Nair RJ, Olivares J, Tingle LE, Li Z. Postsplenectomy reactive thrombocytosis. *Proc (Bayl Univ Med Cent)*. 2009;22:9-12.
5. Tai YT, Yu YL, Lau CP, Fong PC. Myocardial infarction complicating postsplenectomy thrombocytosis, with early left ventricular mural thrombus formation and cerebral embolism--a case report. *Angiology*. 1993;44:73-77.
6. Chia TL, Chesney TR, Isa D, et al. Thrombocytosis in splenic trauma: in-hospital course and association with venous thromboembolism. *Injury*. 2017;48:142-147.

INTERVENTIONAL CARDIOLOGY PERSPECTIVES

Inter Cardio Pers 2025;1(2):75-81

DOI: 10.4274/intercardiopers.2025.2025-2-11

CASE REPORT

Diagnosis, Management, and Treatment of Coronary Artery Fistulas: Three Case Reports and Literature Review

Damla Yalçınkaya Öner[1], Mikail Yarlıoğlueş[2], Elif Ergün[3], Sani Namık Murat[2]

[1]Clinic of Cardiology, Karaman Training and Research Hospital, Karaman, Türkiye

[2]Clinic of Cardiology, Ankara Training and Research Hospital, Ankara, Türkiye

[3]Clinic of Radiology, Ankara Training and Research Hospital, Ankara, Türkiye

ABSTRACT

Coronary artery fistulas represent a form of congenital coronary arteriovenous malformation. They originate from coronary arteries and most commonly drain into the right atrium and right ventricle, with less frequent drainage into the coronary sinus or pulmonary trunk. Clinical manifestations are influenced by the extent of the left-to-right shunt, which can result in ischemia due to diversion of blood from the nearby myocardium, despite the absence of atherosclerotic coronary artery disease. Coronary angiography continues to be the primary method for diagnosis and enables the interventional closure of these fistulas. Current congenital heart disease guidelines recommend considering both symptoms and fistula size when determining the need for closure. This report represents three patients evaluated in our outpatient clinic who underwent successful treatment with percutaneous coil embolization.

Keywords: Coronary artery fistula, symptomatology, coil embolization

INTRODUCTION

A coronary artery fistula (CAF) is a type of congenital coronary arteriovenous malformation. It represents an uncommon abnormal connection between one or more coronary arteries and a cardiac chamber or a major vessel.[1] The overall incidence in the general population is approximately 0.002%. Among individuals undergoing coronary angiography (CAG), it is identified in about 0.2-0.6% of cases.[2] In nearly 50-60% of instances, CAF originates from the right coronary artery (RCA). The left anterior descending (LAD) coronary artery is the second most common origin, accounting for approximately 25-42% of cases, while the circumflex (Cx) coronary artery is involved in about 18%.[3] These fistulas most frequently drain into the right atrium (RA) and right ventricle (RV), with occasional drainage into the coronary sinus (CS) or pulmonary trunk. Although they are generally asymptomatic and without complications, the likelihood of adverse outcomes increases with age. Clinical manifestations depend on the extent of the left-to-right shunt, which can lead to myocardial ischemia due to diversion of blood away from the surrounding myocardium, despite the absence of atherosclerotic coronary artery disease.[4] In this report, we present three patients diagnosed with this rare congenital anomaly at our outpatient clinic. Through this case series and review, we aim to emphasize that physicians should be vigilant for CAFs when interpreting CAG images in patients with normal or non-obstructive coronary arteries, particularly in those presenting with symptoms, as these anomalies may be easily overlooked.

CASE REPORTS

The first patient was a 53-year-old woman with diabetes who had been experiencing stable angina pectoris for 6 months and was evaluated in our outpatient clinic. Her chest pain was retrosternal, exertional in nature, radiated to the left arm, and associated with dyspnea. During the exercise stress test, significant ST segment depression occurred alongside angina symptoms. CAG demonstrated normal coronary arteries, except for a CAF arising from the LAD artery. Multislice computed tomography (CT) imaging (Figure 1) revealed that the CAF was located between the second diagonal branch of the LAD artery and the main pulmonary artery (PA). Given the presence of typical angina and documented myocardial ischemia, percutaneous coil embolization of the fistula was planned.

The second patient was a 61-year-old woman with hypertension and a family history of cardiovascular disease, who presented with stable angina pectoris of three months' duration. Her chest pain was retrosternal, exertion-induced, and radiated to the neck. She was unable to complete the exercise stress test due to severe dyspnea and fatigue, achieving a maximum of 5 metabolic equivalent of tasks. CAG revealed normal coronary arteries except for two CAFs, originating

Address for Correspondence: Damla Yalçınkaya Öner MD, Clinic of Cardiology, Karaman Training and Research Hospital, Karaman, Türkiye
E-mail: damlaykaya@gmail.com **ORCID ID:** orcid.org/0000-0002-8047-389X

Cite as: Yalçınkaya Öner D, Yarlıoğlueş, M, Ergün E, Murat SN. Diagnosis, management, and treatment of coronary artery fistulas: three case reports and literature review. *Inter Cardio Pers.* 2025;1(2):75-81

Received: 27.02.2025
Accepted: 18.05.2025
Epub: 18.06.2025
Publication Date: 11.08.2025

from both the LAD artery and RCA. Multislice CT imaging (Figure 2) showed that one fistula was between the first septal branch of the LAD artery and the PA, while the other was between the conus branch of the RCA and the PA. Based on the presence of typical angina and confirmed myocardial ischemia, percutaneous coil embolization was planned for both fistulas.

The third patient was a 74-year-old man with diabetes who presented with new-onset angina pectoris and dyspnea that had persisted for 10 days. His symptoms were triggered by prolonged exertion. CAG showed normal coronary arteries except for a CAF originating from the Cx artery. Multislice CT imaging (Figure 3) revealed that the CAF was located between the Cx artery and the entry of the left inferior pulmonary vein (LIPV) into the left atrial cavity. Given the presence of typical symptoms consistent with unstable angina, percutaneous coil embolization of the fistula was scheduled. For all patients, secondary causes of ischemia-such as anemia, thyrotoxicosis, and severe hypertension-were excluded.

After selective catheterization of the coronary ostium using a 6-French guiding catheter, a 260-cm-long, standard 0.014-inch coronary angioplasty guide wire was advanced. Using an external torque device, the wire was navigated to the distal portion of the fistula. A 1.7 F microcatheter (Headway 17 Advanced Microcatheter, Microplex®) was then threaded over the guide wire, through which Microplex 10® platinum endovascular embolization coils were delivered to occlude the fistula. The coils were deployed using a V-grip detachment controller. Coil diameter was selected to be 1.5-2 times the diameter of the narrowest part of the fistula to minimize the risk of migration. The number of coils used depended on the length of the fistula and the need to achieve full cessation of flow. Coils were deployed until complete occlusion was confirmed by angiography, with no contrast passing through the fistula. In the first patient, 2.5 × 4 cm, 2.0 × 4 cm, 3.0 × 4 cm, and 2.0 × 6 cm microcoils were placed. In the second patient, 2.5 × 6 cm, 2.0 × 2 cm, and 3.0 × 6 cm microcoils were placed. In the third patient, 2.5 × 6 cm, 2.0 × 4 cm, 2.0 × 4 cm, 1.5 × 2 cm, and 3.0 × 6 cm microcoils were placed. The procedure was concluded once the fistula tract was completely filled and no residual flow was observed. Follow-up angiography confirmed complete occlusion of the fistulas in all three patients (Figures 4a, 4b, 4c).

Aspirin monotherapy was started in all three patients. At the 1-month follow-up, anginal symptoms had subsided in all cases. The patients were monitored for 1 year without the emergence of new or worsening symptoms.

DISCUSSION

This case report and review article aim to highlight three considerations regarding CAFs. First, CAF should be considered in patients who present with typical cardiac symptoms despite having normal or non-obstructive coronary arteries. Second, both the symptom profile and/or the size of the fistula are important determinants when evaluating the need for closure. Third, percutaneous transcatheter closure (TCC) remains the primary treatment approach for CAFs when not contraindicated.

CAF accounts for up to half of all coronary artery anomalies and is considered the most hemodynamically significant among them.[5] As noted earlier, the most common origin of CAFs is the RCA, followed by the LAD and Cx arteries. While most CAFs involve a single connection, cases with multiple fistulas have also been documented.[6] In our series, the fistulas originated from the LAD and Cx arteries, with one case showing dual origins from both the RCA and LAD artery.

The drainage site of the fistula holds greater clinical significance than its origin, as it is directly related to the severity of symptoms. Approximately 90% of fistulas drain into the low-pressure regions of the cardiovascular system, most commonly the RV in 45% of cases, followed by the RA in 25%, the PA in 15%, and then the superior vena cava and CS, respectively.[7] In our series, two patients had fistulas draining into the

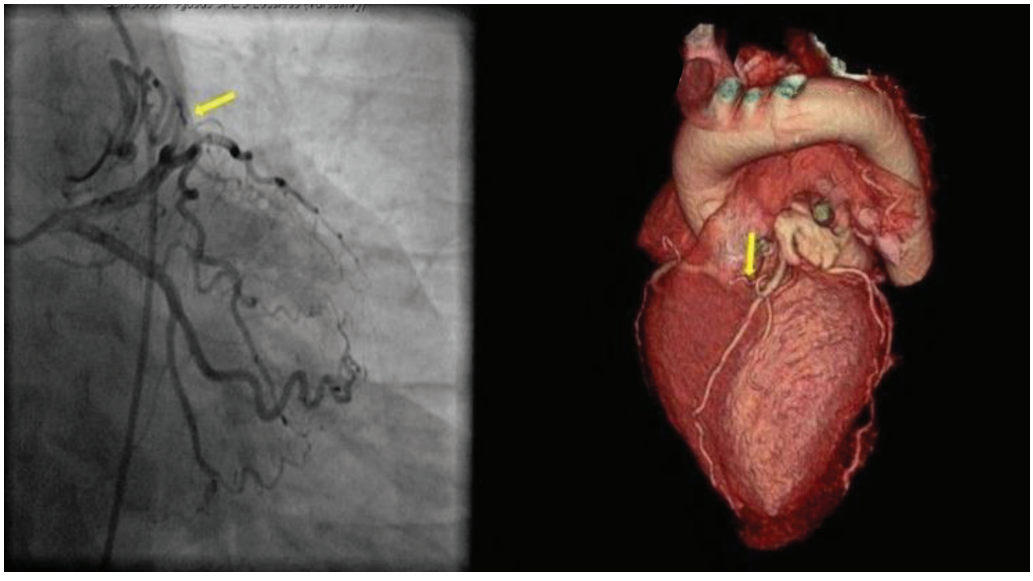

Figure 1. CAG and multislice CT images showing the CAF between the second diagonal branch of the LAD artery and the main PA

CAG: Coronary angiography, CT: Computed tomography, CAF: Coronary artery fistula, LAD: Left anterior descending, PA: Pulmonary artery

PA, and one had a fistula draining into the junction of the LIPV and the RA. The remaining 10% of fistulas drain into the left side of the heart.[8] Additionally, there are reports in the literature describing CAF drainage into the pericardial space.[9] Aside from the drainage site, the shunt volume also shows a strong correlation with clinical presentation. One of our patients exhibited significant exertional dyspnea accompanied by pronounced contrast opacification on CAG. Although we did not perform a direct assessment of shunt volume, based on the symptoms and the presence of myocardial ischemia observed in stress testing, the shunt volume may retrospectively be considered clinically significant in all three patients.

Clinical Presentation

The majority of patients remain asymptomatic. When present, clinical manifestations may include exertional or resting dyspnea, angina pectoris, arrhythmias, thrombosis, embolism, myocardial infarction (MI), and heart failure. In rare instances, pericardial effusion and sudden death may be the initial presentation.[4,10,11] Some cases have reported aneurysm formation and spontaneous rupture of the fistula.[1] Breathlessness and signs of congestive heart failure are typically associated with a large left-to-right shunt, which is an uncommon finding in older individuals.[12] MI can also occur due to reduced blood flow distal to the fistula, even in the absence of coronary atherosclerosis. The mechanism thought to underlie this ischemia is coronary steal,[13] which leads to reduced perfusion of the adjacent myocardium.[14] In our cases, based on clinical symptoms and findings from the stress test, we concluded that myocardial perfusion was impaired and this contributed to MI.

Physical Examination

The primary finding on physical examination is a continuous murmur that is louder during diastole.[15] This murmur has as crescendo-decrescendo pattern. The site where the murmur is loudest can provide clues about the drainage location. If the murmur is loudest

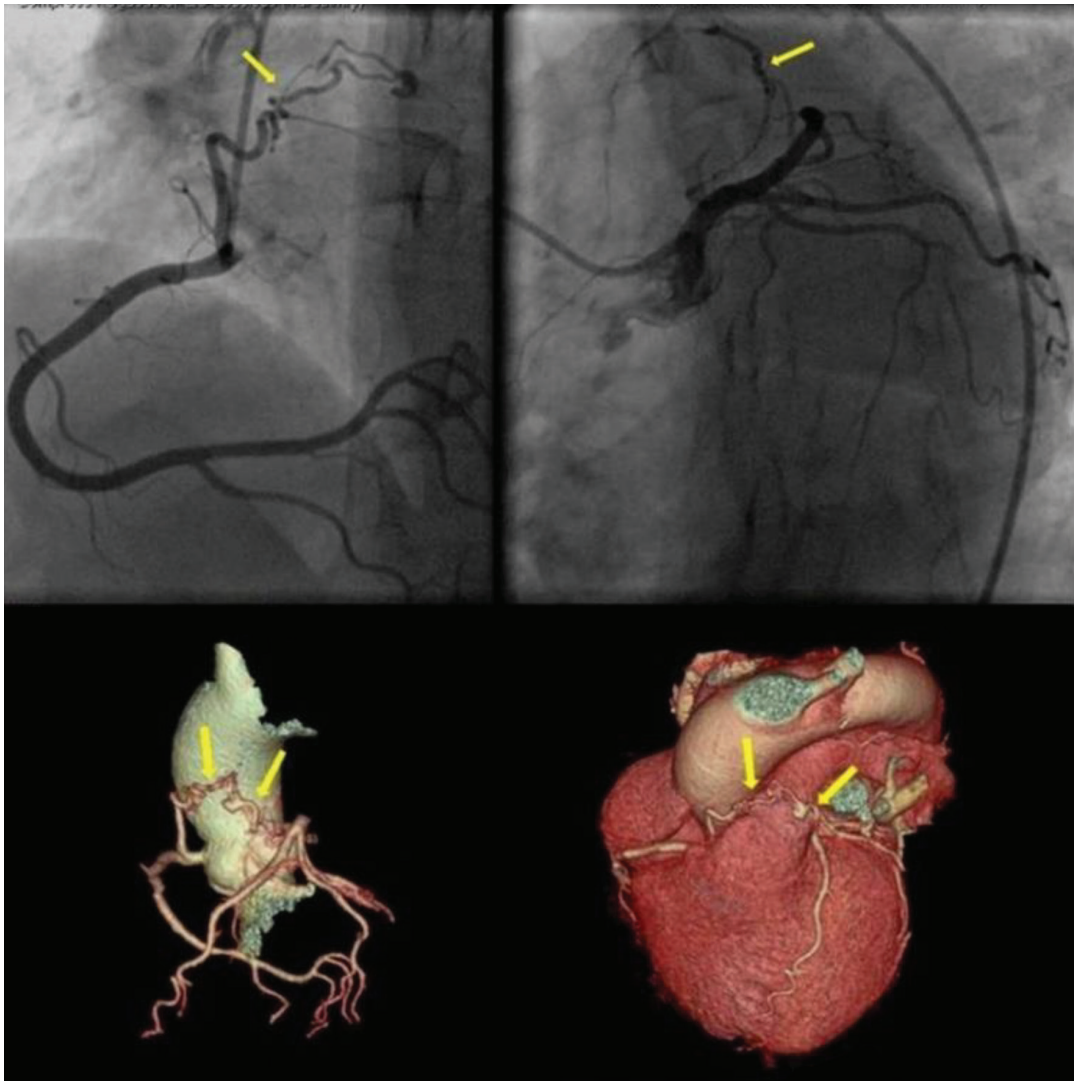

Figure 2. CAG and multislice CT images depicting the CAF between the first septal branch of the LAD artery and the PA; a second CAF between the conus branch of the RCA and the PA

CAG: Coronary angiography, CT: Computed tomography, CAF: Coronary artery fistula, LAD: Left anterior descending, PA: Pulmonary artery, RCA: right coronary artery

at the lower sternal border, the fistula likely drains into the RA. When it is loudest near the left upper sternal border, drainage is into the PA is suggested. If the loudest point is near the apex, drainage into the left ventricle should be considered.[16,17] Additional signs such as an S3 gallop or rales may also be present depending on clinical conditions. Continuous murmurs can also occur in other conditions including patent ductus arteriosus, pulmonary arteriovenous fistula, ruptured sinus of Valsalva aneurysm, and systemic arteriovenous fistula.[18]

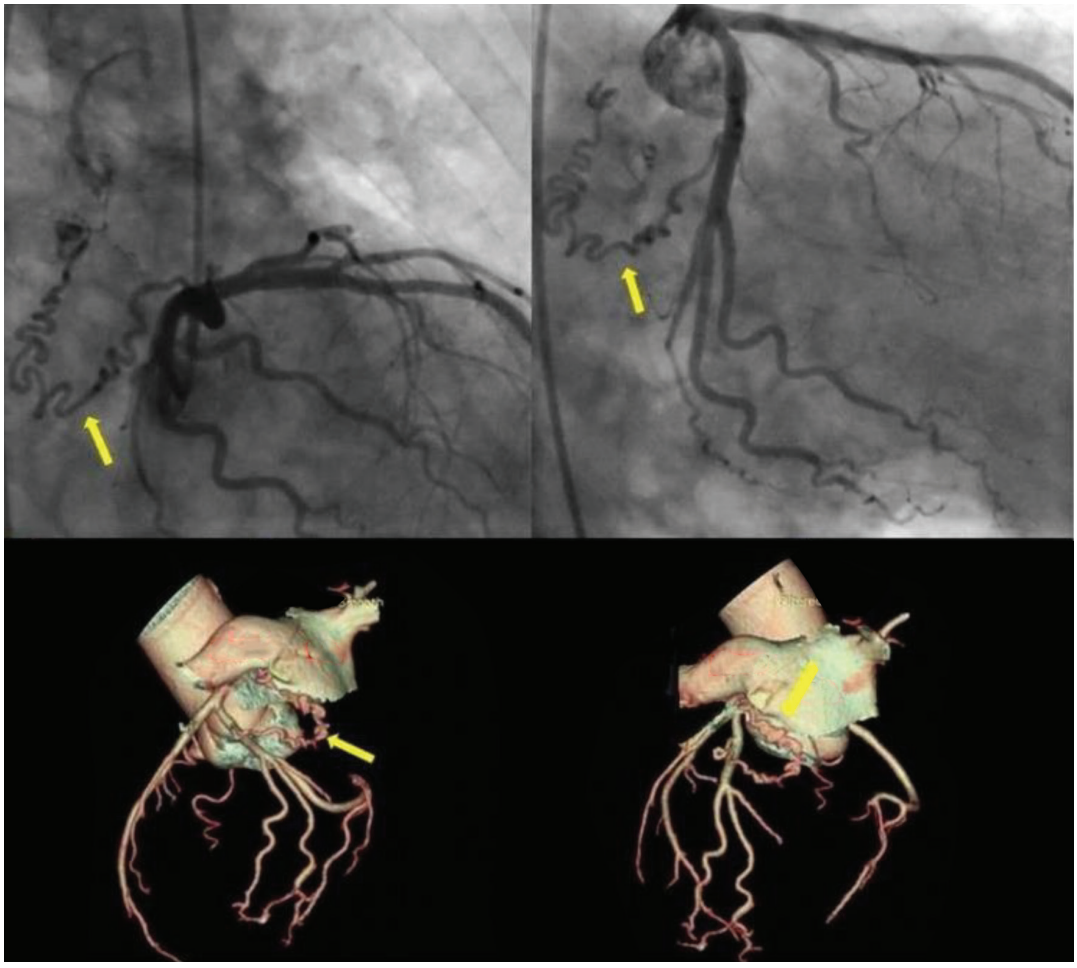

Figure 3. CAG and multislice CT images of the CAF between the Cx artery and the opening of the LIPV into the left atrial cavity

CAG: Coronary angiography, CT: Computed tomography, CAF: Coronary artery fistula, Cx: Circumflex, LIPV: Left inferior pulmonary vein

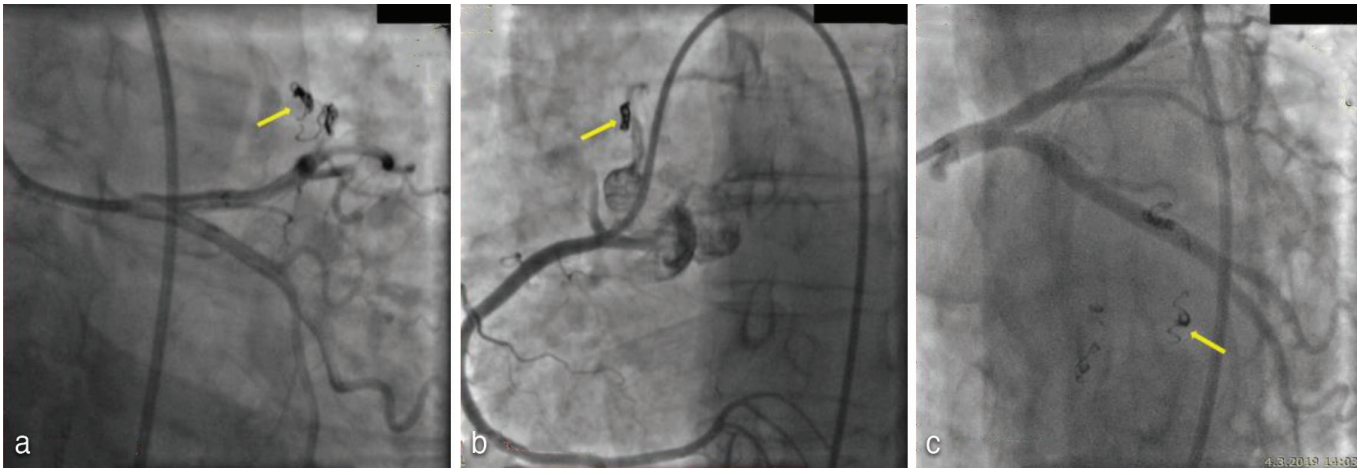

Figure 4. (a, b, c) CAG images following the procedure

CAG: Coronary angiography

Therefore, further evaluation with various cardiac imaging techniques is necessary for differential diagnosis.

Diagnosis

Ischemic changes can be observed on electrocardiography (ECG) due to reduced myocardial perfusion. Although rare, atrial fibrillation and left or right ventricular hypertrophy may also be present. In our cases, no ECG abnormalities were detected at rest; however, significant ST segment depression appeared during the stress test in the first patient.[1,17,19] Echocardiography may show chamber enlargement caused by volume overload or myocardial dysfunction-either regional or global-resulting from ischemia.[17,18,20] In the third patient, echocardiography revealed global hypokinesis in the absence of atherosclerotic coronary artery disease.

Additional cardiac imaging methods include multislice CT and magnetic resonance imaging (MRI).[18] Compared to MRI, CT is more practical to perform, being faster and offering higher resolution. It clearly visualizes the boundaries of the fistulas, and with the latest multislice CT scanners, even smaller coronary branches can be detected. We chose multislice CT to delineate the anatomy. The primary limitation of CT is radiation exposure. MRI can also be used to visualize the anatomy and detect ischemic myocardium through stress thallium studies.[21] Among these options, CAG remains the primary diagnostic method and also enables interventional closure of the fistulas. Figure 5 shows the diagnostic algorithm for CAFs.

Management and Treatment

CAFs can be classified as small (mild), medium (moderate), or large based on their diameter being <1, ≥1-2, or >2 times the largest diameter of the coronary vessel not supplying the CAF, respectively.[22] Since most fistulas are small and hemodynamically insignificant, a follow-up approach may be suitable, especially for small fistulas that are incidentally found and asymptomatic.[19] The 2008 American College of Cardiology and American Heart Association guidelines for managing adults with congenital heart disease (Figure 6) emphasize symptom presence and/or fistula size as key criteria for closure. Proximal CAFs tend to be large, whereas distal fistulas are usually smaller and more tortuous. Large CAFs should be closed regardless of symptoms (class 1, level of evidence, C). Closure is also recommended for mild to moderate fistulas if symptoms are associated with documented MI, arrhythmias, unexplained ventricular dilation or dysfunction, or if complicated by endocarditis (class 1, level of evidence, C). Small, asymptomatic fistulas should not be treated (class 3, level of evidence, C). Clinical monitoring with echocardiography every 3-5 years may be helpful in these patients to detect the onset of symptoms, arrhythmias, or progression in size or chamber enlargement that could affect management (class 2a, level of evidence, C).[23] Because CAFs tend to enlarge with age, early closure is advised in symptomatic patients.[24] The management algorithm for CAFs is presented in Figure 6. Since all three of our patients were symptomatic, we opted for closure of the fistulas.

Treatment options include either surgical intervention or TCC. Due to higher morbidity risk and longer hospital stay associated with open-heart surgery, we selected TCC for our patients. Several contraindications exist for TCC, such as very young age (because of small coronary arteries), a large and wide fistula, aneurysmal formation, the presence of large vascular branches that risk accidental embolization, and the requirement for other concurrent cardiac surgery.[22,25] None of our patients had any contraindications for TCC. Catheter-based closure methods include detachable balloons, stainless steel coils, controlled-release coils, controlled-release patent ductus arteriosus coils, patent ductus arteriosus plugs, regular and covered stents, and various chemicals.[16] We used controlled-release coils and successfully closed the CAFs.

Complications may arise from catheter manipulation, such as coronary artery spasm, dissection, and perforation. Coil migration can occur due to high flow in large CAFs or of coils are undersized. This can be prevented by choosing coils that are 10-20% larger than the fistula diameter.[1] Patients with cardiovascular risk factors-such as hypertension, diabetes mellitus, advanced age, hyperlipidemia, and tobacco use-are more prone to long-term complications after CAF closure, including MI and cardiomyopathy.[22,26] These factors also influence prognosis. MI is a significant complication, occurring in about 10% of patients with large CAFs following closure. Aneurysmal dilation of proximal coronary artery segments that develop in large distal CAFs is at risk of thrombus formation due to stagnant flow after successful closure.[22] In such cases, initiating long-term oral anticoagulation indefinitely may be advisable.

A heparin bolus of 70 IU/kg is recommended during the procedure to maintain an activated clotting time >250 sec and help prevent catheter-related thrombotic complications. However, there is limited data regarding the use of long-term antiplatelet or anticoagulant therapy following coil embolization. Most recommendations are derived from case series and expert opinions. The usual antithrombotic treatment after coil embolization of CAFs involves single antiplatelet therapy with low-dose aspirin.[27] In certain cases, such as patients who have other indications for anticoagulation, therapeutic anticoagulation with vitamin K antagonists or direct oral anticoagulants may be continued. Combining anticoagulation with aspirin might be considered, especially when coil size is small or residual flow persists.[22] For more complex cases, including large fistulas or those with aneurysmal components, dual antiplatelet therapy with aspirin and clopidogrel, or anticoagulation, may be necessary to reduce thrombotic risk. These recommendations aim to balance protection against thrombosis with the risk of ischemic complications, with treatment decisions individualized according to fistula features and patient comorbidities.

Prognosis and Follow-up

Patients who have undergone closure of a CAF generally show a good prognosis regardless of the closure technique used. Prognosis mainly depends on the shunt volume and associated clinical factors such as heart failure, pulmonary hypertension, and the extent of the myocardial ischemia.[28] Recurrence rates after percutaneous closure range from 9% to 19%, while surgical closure has a recurrence rate of about 25%.[29] Echocardiographic follow-up is advised 1 month after either percutaneous or surgical closure. If the patient remains symptom-free, follow-up intervals can be lengthened. Patients should

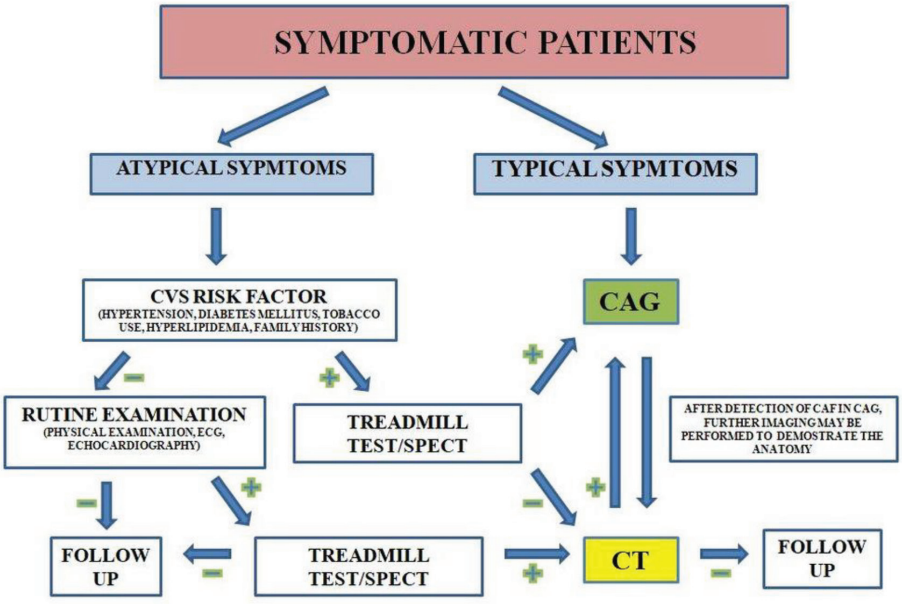

Figure 5. Diagnostic algorithm for CAF

CAF: Coronary artery fistula, CT: Computed tomography, CAG: Coronary angiography, CVS: Cardiovascular, SPECT: Single photon emission computed tomography

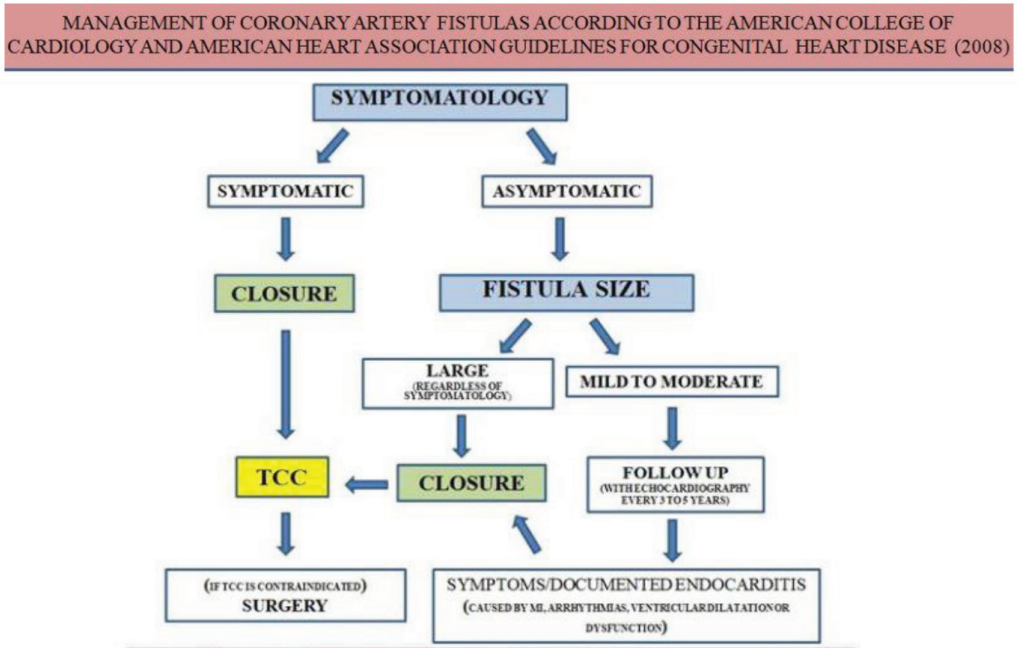

Class[a]	Level[b]	Recommandations
I	C	A large CAVF, regardless of symptomatology, should be closed via either a transcatheter or surgical route after delineation of its course and its potential to fully obliterate the fistula.
I	C	A small to moderate CAVF in the presence of documented myocardial ischemia, arrhythmia, otherwise unexplained ventricular systolic or diastolic dysfunction or enlargement, or endarteritis should be closed via either a transcatheter or surgical approach after delineation of its course and its potential to fully obliterate the fistula.
IIa	C	Clinical follow-up with echocardiography every 3 to 5 years can be useful for patients with small, asymptomatic CAVF to exclude development of symptoms or arrhythmias or progression of size or chamber enlargement that might alter management.
III	C	Patients with small, asymptomatic CAVF should not undergo closure of CAVF.

Figure 6. Management strategy for CAF

[a]Class of recommendation, [b]Level of evidence, CAF: Coronary artery fistula, TCC: Transcatheter closure, MI: Myocardial infarction, CAVF: Coronary arteriovenous fistula

also be monitored for bacterial endocarditis, which has an estimated annual risk of 0.25% per patient.[30]

CONCLUSION

CAF accounts for up to half of all coronary artery anomalies. It should be considered in patients presenting with typical cardiac symptoms despite having normal or non-obstructive coronary arteries. CAG remains the gold standard for diagnosis. A follow-up approach is suitable for managing asymptomatic, small, and hemodynamically insignificant fistulas. The decision to close a fistula depends on symptom presence and/or fistula size. Percutaneous TCC is the preferred intervention unless there are contraindications.

Informed Consent: Consent form was filled out by all participants.

Authorship Contributions: Concept: M.Y., S.N.M., Design: M.Y., S.N.M., Data Collection or Processing: D.Y.Ö., E.E., Literature Search: D.Y.Ö., M.Y., Writing: D.Y.Ö., M.Y.

Conflict of Interest: No conflict of interest was declared by the authors.

Financial Disclosure: The authors declared that this study received no financial support.

REFERENCES

1. Qureshi SA. Coronary arterial fistulas. *Orphanet J Rare Dis*. 2006;1:51.
2. Jama A, Barsoum M, Bjarnason H, Holmes DR Jr, Rihal CS. Percutaneous closure of congenital coronary artery fistulae: results and angiographic follow-up. *JACC Cardiovasc Interv*. 2011;4:814-821.
3. Dodge-Khatami A, Mavroudis C, Backer CL. Congenital heart surgery nomenclature and database project: anomalies of the coronary arteries. *Ann Thorac Surg*. 2000;69(Suppl 4):270-297.
4. Buccheri D, Dendramis G, Piraino D, et al. Coronary artery fistulas as a cause of angina: how to manage these patients? *Cardiovasc Revasc Med*. 2015;16:306-309.
5. Schumacher G, Roithmaier A, Lorenz HP, et al. Congenital coronary artery fistula in infancy and childhood: diagnostic and therapeutic aspects. *Thorac Cardiovasc Surg*. 1997;45:287-294.
6. Sapin P, Frantz E, Jain A, Nichols TC, Dehmer GJ. Coronary artery fistula: an abnormality affecting all age groups. *Medicine (Baltimore)*. 1990;69:101-113.
7. McNamara JJ, Gross RE. Congenital coronary artery fistula. *Surgery*. 1969;65:59-69.
8. Reagan K, Boxt LM, Katz J. Introduction to coronary arteriography. *Radiol Clin North Am*. 1994;32:419-433.
9. Mutlu H, Serdar Küçükoğlu M, Ozhan H, Kansýz E, Oztürk S, Uner S. A case of coronary artery fistula draining into the pericardium causing hematoma. *Cardiovasc Surg*. 2001;9:201-203.
10. Lau G. Sudden death arising from a congenital coronary artery fistula. *Forensic Sci Int*. 1995;73:125-130.
11. Ozeki S, Utsunomiya T, Kishi T, et al. Coronary arteriovenous fistula presenting as chronic pericardial effusion. *Circ J*. 2002;66:779-782.
12. Qureshi SA, Tynan M. Catheter closure of coronary artery fistulas. *J Interv Cardiol*. 2001;14:299-307.
13. Cademartiri F, Malagò R, La Grutta L, et al. Coronary variants and anomalies: methodology of visualisation with 64-slice CT and prevalence in 202 consecutive patients. *Radiol Med*. 2007;112:1117-1131.
14. Kiuchi K, Nejima J, Kikuchi A, Takayama M, Takano T, Hayakawa H. Left coronary artery-left ventricular fistula with acute myocardial infarction, representing the coronary steal phenomenon: a case report. *J Cardiol*. 1999;34:279-284.
15. Ata Y, Turk T, Bicer M, Yalcin M, Ata F, Yavuz S. Coronary arteriovenous fistulas in the adults: natural history and management strategies. *J Cardiothorac Surg*. 2009;4:62
16. Gowda RM, Vasavada BC, Khan IA. Coronary artery fistulas: clinical and therapeutic considerations. *Int J Cardiol*. 2006;107:7-10.
17. Buccheri D, Chirco PR, Geraci S, Caramanno G, Cortese B. Coronary artery fistulae: anatomy, diagnosis and management strategies. *Heart Lung Circ*. 2018;27:940-951.
18. Guray U, Guray Y, Ozbakir C, Yilmaz MB, Sasmaz H, Korkmaz S. Fistulous connection between internal mammary graft and pulmonary vasculature after coronary artery bypass grafting: a rare cause of continuous murmur. *Int J Cardiol*. 2004;96:489-492.
19. Challoumas D, Pericleous A, Dimitrakaki IA, Danelatos C, Dimitrakakis G. Coronary arteriovenous fistulae: a review. *Int J Angiol*. 2014;23:1-10.
20. Angelini P. Coronary artery anomalies--current clinical issues: definitions, classification, incidence, clinical relevance, and treatment guidelines. *Tex Heart Inst J*. 2002;29:271-278
21. Said SA, Hofman MB, Beek AM, van der Werf T, van Rossum AC. Feasibility of cardiovascular magnetic resonance of angiographically diagnosed congenital solitary coronary artery fistulas in adults. *J Cardiovasc Magn Reson*. 2007;9:575-583.
22. Al-Hijji M, El Sabbagh A, El Hajj S, et al. Coronary artery fistulas: indications, techniques, outcomes, and complications of transcatheter fistula closure. *JACC Cardiovasc Interv*. 2021;14:1393-1406.
23. Warnes CA, Williams RG, Bashore TM, et al. ACC/AHA 2008 guidelines for the management of adults with congenital heart disease: a report of the American College of Cardiology/American Heart Association Task Force on Practice Guidelines (Writing Committee to Develop Guidelines on the Management of Adults With Congenital Heart Disease). Developed in collaboration with the American Society of Echocardiography, Heart Rhythm Society, International Society for Adult Congenital Heart Disease, Society for Cardiovascular Angiography and Interventions, and Society of Thoracic Surgeons. *J Am Coll Cardiol*. 2008;52:143-263.
24. Liberthson RR, Sagar K, Berkoben JP, Weintraub RM, Levine FH. Congenital coronary arteriovenous fistula. Report of 13 patients, review of the literature and delineation of management. *Circulation*. 2007;59:849-854.
25. Jung C, Jorns C, Huhta J. Doppler findings in a rare coronary artery fistula. *Cardiovasc Ultrasound*. 2007;5:10.
26. Valente AM, Lock JE, Gauvreau K, et al. Predictors of long-term adverse outcomes in patients with congenital coronary artery fistulae. *Circ Cardiovasc Interv*. 2010;3:134-139.
27. El-Sabawi B, Al-Hijji MA, Eleid MF, et al. Transcatheter closure of coronary artery fistula: a 21-year experience. *Catheter Cardiovasc Interv*. 2020;96:311-319.
28. Armsby LR, Keane JF, Sherwood MC, Forbess JM, Perry SB, Lock JE. Management of coronary artery fistulae. Patient selection and results of transcatheter closure. *J Am CollCardiol*. 2002;39:1026-1032.
29. Said SA, Nijhuis RL, Op den Akker JW, et al. Diagnostic and therapeutic approach of congenital solitary coronary artery fistulas in adults: Dutch case series and review of literature. *Neth Heart J*. 2011;19:183-191.
30. Tirilomis T, Aleksic I, Busch T, Zenker D, Ruschewski W, Dalichau H. Congenital coronary artery fistulas in adults: surgical treatment and outcome. *Int J Cardiol*. 2005;98:57-59.

INTERVENTIONAL CARDIOLOGY PERSPECTIVES

Inter Cardio Pers 2025;1(2):82-84

DOI: 10.4274/intercardiopers.2025.2025-6-5

CLINICAL IMAGE

When Coronary Angiography Fails to Reveal the Culprit: Electrocardiogram as the Decisive Guide

Merve Akbulut Çakır, Fatih Kardaş, Emirhan Çakır, Gizem Ayyıldız

Department of Cardiology, Trakya University Faculty of Medicine, Edirne, Türkiye

Keywords: Acute coronary syndrome, electrocardiography, coronary thrombus, total coronary occlusion

INTRODUCTION

A 43-year-old male patient with a known history of hypertension presented to the emergency department of an external center with chest pain. He was referred to our hospital for coronary angiography with a diagnosis of acute lateral myocardial infarction (MI), based on ST elevation in leads D1, AVL, and V5-6, and reciprocal ST depression in leads D2, D3, and arteriovenous fistulas (AVF) on his electrocardiography (ECG) (Figure 1). Upon arrival at our clinic, the patient was promptly taken to the catheterization laboratory. He reported relief of chest pain, and coronary angiography revealed no lesion in the right coronary artery. No total occlusion was observed in the left anterior descending (LAD) or circumflex (CX) arteries during left coronary system imaging. However, a lesion in the proximal LAD was notable (Figure 2). The patient reported that his chest pain persisted, although less intense. The ECG also showed persistent ST elevation.

Therefore, based on the persistent ischemic findings on ECG, the LAD was wired, and percutaneous transcatheter coronary angioplasty (PTCA) was performed at the proximal lesion. The thrombus at the LAD lesion site had occluded the ostium of the diagonal artery (DG), and PTCA at this site restored flow in the DG. Subsequently, a 3.0 × 26 mm drug-eluting stent with optimal apposition was implanted at the culprit lesion in the LAD. Proximal optimization was performed with a 3.5 × 12 mm non-compliant balloon. LAD-DG kissing PTCA was then carried out, and the LAD stent was further optimized. Control images confirmed restoration of distal flow in both the LAD and the DG (Figure 3). The patient's chest pain resolved, and the procedure was successfully completed.

Lateral MI is diagnosed on ECG by ST elevation in leads D1, AVL, and V5-6, with reciprocal ST depression in leads D2, D3, and AVF. Early revascularization significantly improves clinical outcomes.[1] Moreover, percutaneous intervention has shown better results than fibrinolytic therapy.[3] Hreybe et al. reported an increased risk of ventricular fibrillation in patients presenting with anterior and lateral MI.[2] Lateral MI may result from obstruction of the obtuse marginal artery, DG, or ramus intermedius. In our case, although the DG—completely occluded—was not visible on coronary angiography, it became apparent after LAD PTCA, guided by ECG findings.

In conclusion, in patients presenting with lateral MI who have a high risk of ventricular arrhythmia, if relatively smaller vessels or side branch disease cannot be detected on coronary angiography, ECG findings should be relied upon. The ramus intermedius should be sought, and if a lesion is identified in the LAD or CX, PTCA should be performed in that region to reveal a possible side branch lesion responsible for the ischemia.

Address for Correspondence: Emirhan Çakır MD, Department of Cardiology, Trakya University Faculty of Medicine, Edirne, Türkiye
E-mail: emir.cakir05@gmail.com **ORCID ID:** orcid.org/0000-0002-2231-1526

Cite as: Akbulut Çakır M, Kardaş F, Çakır E, Ayyıldız G. When coronary angiography fails to reveal the culprit: electrocardiogram as the decisive guide. *Inter Cardio Pers.* 2025;1(2):82-84

Received: 16.06.2025
Accepted: 01.08.2025
Publication Date: 11.08.2025

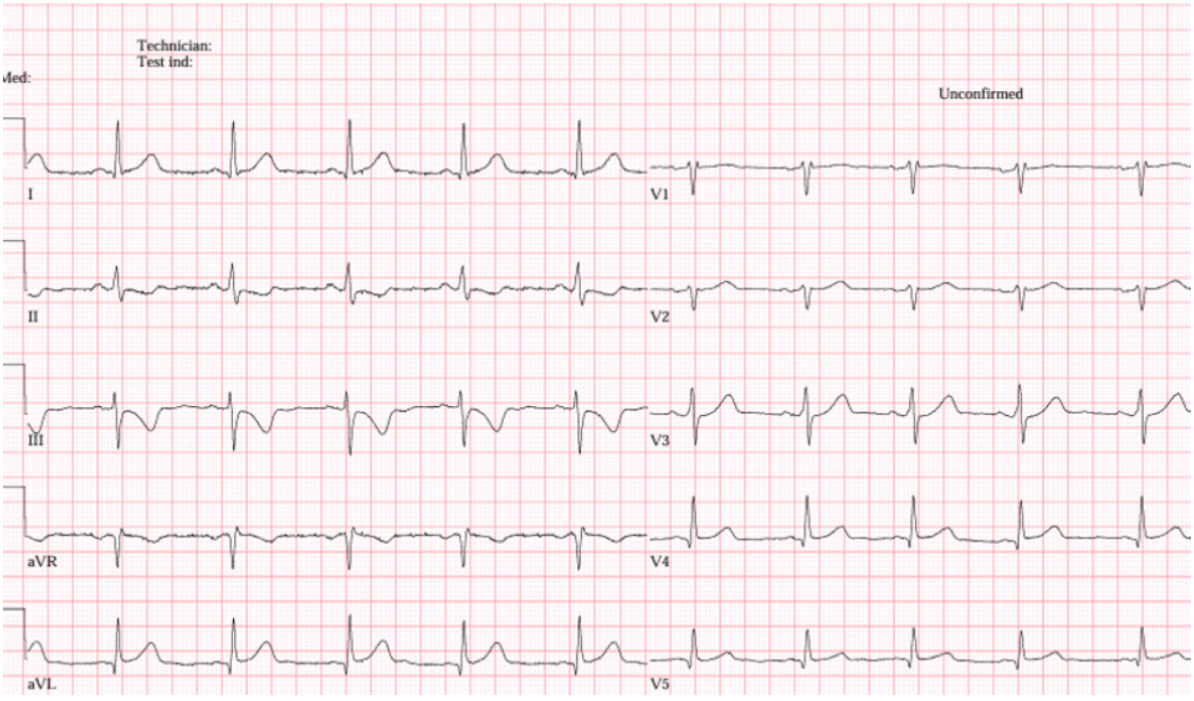

Figure 1. ST elevation in leads D1, AVL, and V5-6, with ST depression in leads D2, D3, and AVF on ECG
ECG: Electrocardiogram

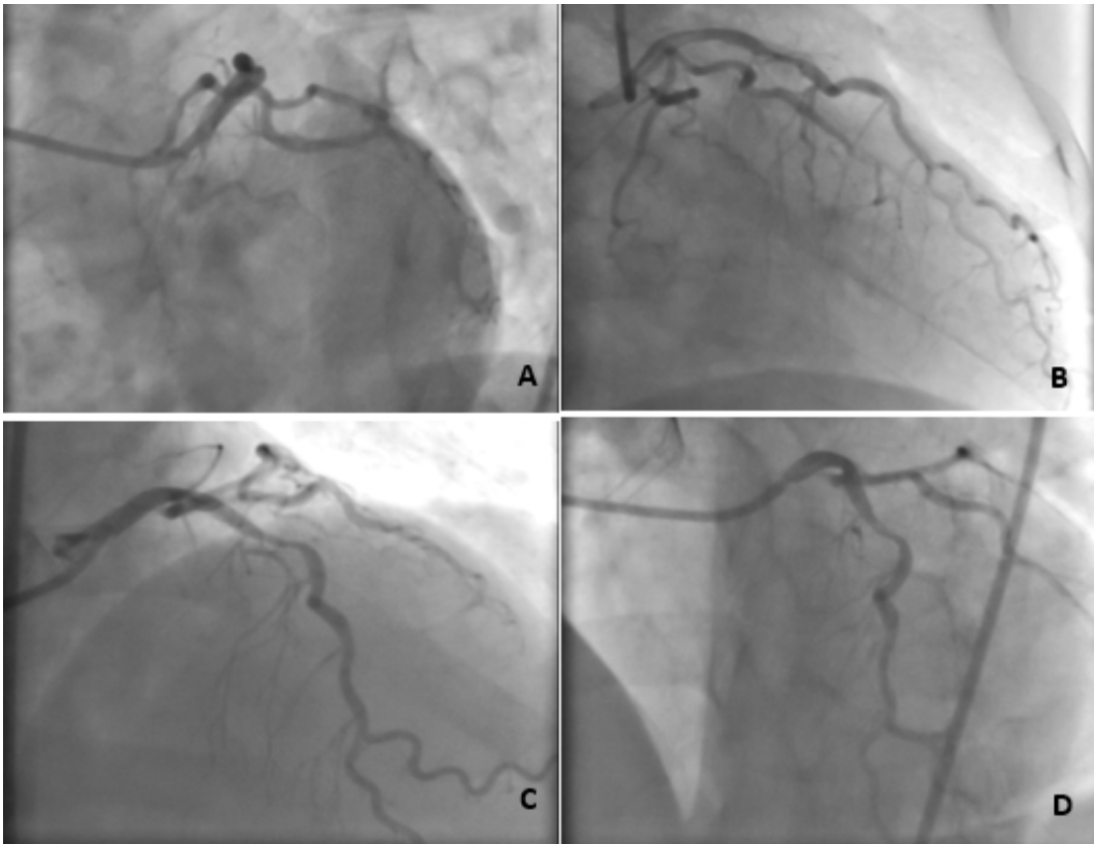

Figure 2. (A) Left caudal view. B) Right caudal view. C) Right cranial view showing a proximal LAD lesion, without total occlusion. D) Left cranial view, showing no totally occluded vessel
LAD: Left anterior descending

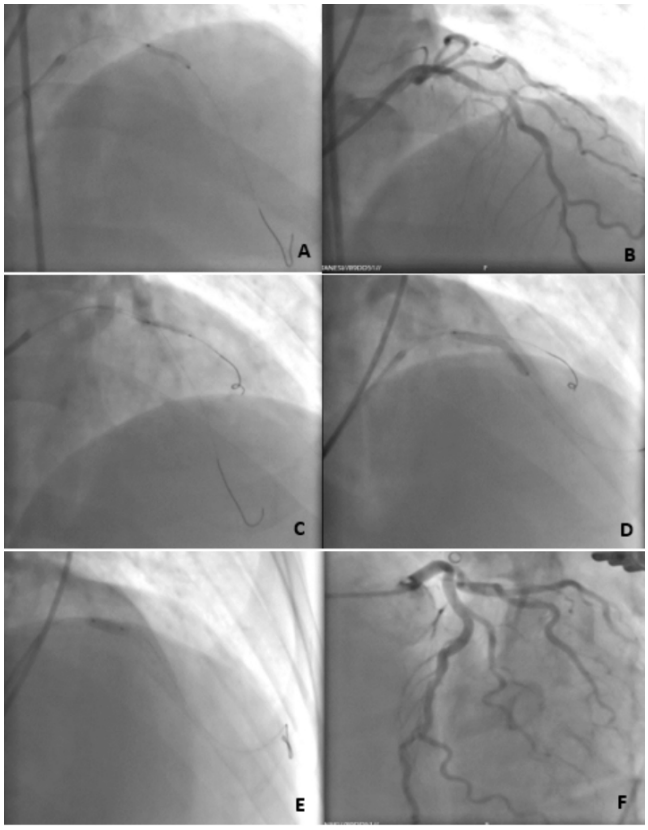

Figure 3. (A) PTCA performed at the proximal LAD lesion site. B) Restoration of flow to the diagonal artery after PTCA. C) PTCA of the diagonal artery. D) Stent implantation at the proximal LAD lesion site. E) POT with an NC balloon in the LAD stent. F) Left cranial view showing restored flow in the LAD and DG
PTCA: Percutaneous transcatheter coronary angioplasty, LAD: Left anterior descending, DG: Diagonal artery

Informed Consent: Written informed consent was obtained from the patient.

Presented in: The study was previously presented as a paper at the 1st Interventional Cardiology Congress 2025.

Authorship Contributions: Surgical and Medial Practices: M.A.Ç., F.K., E.Ç., G.A., Concept: M.A.Ç., F.K., E.Ç., G.A., Design: M.A.Ç., F.K., E.Ç., G.A., Data Collection or Processing: M.A.Ç., F.K., E.Ç., G.A., Analysis or Interpretation: M.A.Ç., F.K., E.Ç., G.A., Literature Search: M.A.Ç., Writing: M.A.Ç., E.Ç.

Conflict of Interest: No conflict of interest was declared by the authors.

Financial Disclosure: The authors declared that this study received no financial support

REFERENCES

1. Anderson JL, Karagounis LA, Califf RM. Metaanalysis of five reported studies on the relation of early coronary patency grades with mortality and outcomes after acute myocardial infarction. *Am J Cardiol.* 1996;78:1-8.
2. Hreybe H, Saba S. Location of acute myocardial infarction and associated arrhythmias and outcome. *Clin Cardiol.* 2009;32:274-277.
3. Thrane PG, Kristensen SD, Olesen KKW, et al. 16-year follow-up of the Danish acute myocardial infarction 2 (DANAMI-2) trial: primary percutaneous coronary intervention vs. fibrinolysis in ST-segment elevation myocardial infarction. *Eur Heart J.* 2020;41:847-854.